

Doctoral Dissertation (Censored)

博士論文 (要約)

**Chemoenzymatic conversion of ribosomally synthesized thioamide to thiazole
and
analysis of the effect of EF-Tu·aminoacyl-tRNA affinities on translation**

(翻訳合成チオアミドからチアゾールへの化学酵素的変換

およびEF-Tu・アミノアシル tRNA 結合力が翻訳に与える影響の解析)

A Dissertation Submitted for the Degree of Doctor of Philosophy

July 2021

令和3年7月 博士(理学) 申請

Department of Chemistry, Graduate School of Science,

The University of Tokyo

東京大学大学院 理学系研究科

化学専攻

Hiroyuki Kimura

木村 寛之

Abstract

The translation system is one of the powerful tools to synthesize peptides and proteins. The translation system has strict substrate specificity and employs only twenty kinds of proteinogenic L- α -amino acids (pAAs). Not only pAAs, bioactive peptidic compounds often contain non-proteinogenic amino acids (npAAs) to enhance their properties, but their installations into peptides are generally not by the translation system because the system has been fine-tuned to utilize twenty pAAs. To overcome this hurdle, genetic code reprogramming technologies have been established, and the installation of npAAs in addition to twenty pAAs has been achieved in the translation system. Such technologies are capable of efficient synthesis of peptides containing npAAs and finally have been applied to *de novo* drug discovery system or creation of proteins with novel function derived from npAAs. However, there remain some building blocks incompatible with the translation system. Therefore, further expanding the repertoire of the substrates in the translation and understanding the mechanism of AA selectivity are required.

In the first part of my Ph.D. course study, I and Dr. Maini aimed to install a thioamide bond in translated peptides. The thioamide is regarded as a useful isostere of the standard amide bond, but the installation has been exclusively carried out by the solid phase peptide synthesis method. Dr. Maini took advantage of the genetic code reprogramming technology to install thioamide bond into the nascent peptides, but the installation of thioamide was always accompanied by the oxoamide-counterpart. Thereby, I first elucidated the origin of the oxoamide-counterpart, which was attributed to the aminoacylation reaction conditions. I also demonstrated the installation of thioamide bonds into macrocyclic scaffolds.

In the second part of my Ph.D. course study, I further derivatize the thioamide on peptides to thiazoline and thiazole. Five-membered heterocycles, such as azoline and azole, exhibit improved protease resistance or structural rigidity, and thus are useful peptidomimetics that substitute the standard amide bond. However, the incorporation of these heterocycles in the translation system has been hardly achieved even with the genetic code reprogramming, because they lay over two amino acid residues and the translation system cannot incorporate such dipeptide motif efficiently during the peptide elongation cycle. In this study, I developed a chemoenzymatic post-translational modification that installs azoline into peptides in the *in vitro* reconstituted translation system. To install these heterocycles a thioamide was utilized. It was previously reported that thioamide has higher reactivity toward nucleophiles, such as ammonia, to form an amidine structure. Based on this study, I hypothesized that this intermolecular nucleophilic attack to the thioamide can be

applied to intramolecular fashion, especially with the downstream Cys or diaminopropionic acid, to form a thiazoline or imidazoline. I first demonstrated that this intramolecular heterocyclization actually took place in a model dipeptide consisting of a thioamide and Cys. Then, I also applied this heterocyclization reaction in the peptides generated by the translation system and the genetic code reprogramming technology. Finally, the thiazoline on the translated peptide was further derivatized to the aromatic thiazole ring, catalyzed by dehydrogenase GodE. Collectively, chemoenzymatic formation of thiazole-containing peptides has been demonstrated. This chemoenzymatic method is compatible with a thioether-linked macrocyclization method, also enabling the formation of macrocyclic peptides containing a thiazole.

In the third part of my Ph.D. course study, I and Dr. Iwane demonstrated the multiple incorporation of *N*-methyl amino acids (^{Me}AAs). Even though ^{Me}AAs confer proteolytic resistance and hydrophobic interaction on peptides, the installation of multiple ^{Me}AAs had suffered from insufficient incorporation efficiency. It has been reported that EF-Tu is responsible for the transport of amino acyl-tRNAs (AA-tRNA) to the ribosome, and Dr. Iwane hypothesized that the cause of the insufficient incorporation is the diminished affinities between ^{Me}AA-tRNAs and EF-Tu. Since EF-Tu recognizes the T-stem region of AA-tRNA, Dr. Iwane expected that the substitution of the T-stem sequence can affect the EF-Tu affinity. To tune the EF-Tu affinities of ^{Me}AA-tRNAs, Dr. Iwane designed three new tRNA T-stem sequences. Indeed, the substituting the T-stem with a designer T-stem sequences, the affinities between ^{Me}AA-tRNAs and EF-Tu can be tuned arbitrarily, and then the incorporation efficiencies of ^{Me}AAs were also improved by selecting the appropriate T-stem sequence. Taking advantage of this affinity-tuning methodology of substituting the T-stem sequence, I demonstrated the ribosomal expression of the model peptides, that contains nine distinct ^{Me}AAs.

In the last part of my Ph.D. course study, I focused on the selectivity of EF-Tu. Previously, the recognition mode of the tRNA T-stem has been extensively studied as described in Chapter 4. Alternatively, the specificity of EF-Tu has been modulated by mutating its binding pocket, resulting in an efficient convey of npAA-tRNA to the ribosome. However, the structure-affinity relationship between EF-Tu residues and the substrate AA-tRNA remains poorly understood. In this study, I newly prepared 33 EF-Tu variants with single-point mutations around the substrate-binding pocket and evaluated their affinities for various npAA-tRNAs. I also conducted the *in vitro* translation experiments with these EF-Tu variants, and I have revealed several residues playing an important role to recognize the amino acid esterified on the tRNA.

In conclusion, I have achieved unique moieties such as thioamide, thiazoline, and thiazole on

translated peptides via genetic code reprogramming, and post-translational modification method. This method would facilitate the production of bioactive peptides containing a proteolytic resistant thiazole moiety. Also, I demonstrated the ribosomal incorporation of multiple ^{Me}AAs into the peptides. These studies have expanded the chemical space of peptides accessible in the translation system. In addition, I have revealed the key residues of EF-Tu which recognizes substrate AA-tRNAs. This research and further understanding of the substrate recognition mechanism at the EF-Tu amino acid-binding pocket would provide a new insight to engineer the pocket to obtain a universally active EF-Tu variant, which eventually leads to further flexible synthesis of peptides.

Table of Contents

| | |
|---|----|
| Abstract..... | 1 |
| Table of contents..... | 4 |
| Abbreviations | 7 |
| Chapter 1. General introduction | 9 |
| 1. 1. The translation system | 10 |
| 1. 1. 1. The translation system synthesizes polypeptides..... | 10 |
| 1. 1. 2. The translation system is an elegantly tuned system synthesizing polypeptides..... | 12 |
| 1. 1. 3. The ternary complex formation | 12 |
| 1. 2. Peptidic bioactive compounds | 16 |
| 1. 2. 1. Bioactive natural peptides often contain non-proteinogenic amino acids..... | 16 |
| 1. 2. 2. RiPPs pathway | 19 |
| 1. 2. 3. NRPS pathway | 21 |
| 1. 2. 4. Oxidation of thiazoline..... | 22 |
| 1. 3. Genetic code reprogramming technologies | 23 |
| 1. 3. 1. The concept of genetic code reprogramming | 23 |
| 1. 3. 2. In vivo reprogramming | 23 |
| 1. 3. 3. In vitro reprogramming | 24 |
| 1. 3. 4. The FIT system | 25 |
| 1. 3. 5. The engineering of EF-Tu/tRNA combination | 26 |
| Chapter 2. Ribosomal formation of thioamide bonds | 29 |
| 2. 1. Introduction..... | 30 |
| 2. 2. Dr. Maini's work | 32 |
| 2. 3. My work | 34 |
| 2. 4. Results and Discussion..... | 34 |
| 2. 4. 1. The elucidation of the origin of S-to-O exchange..... | 34 |
| 2. 4. 2. Suppress the S-to-O exchange during the storage..... | 37 |
| 2. 4. 3. The installation of thioamide in a macrocyclic peptide | 40 |
| 2. 5. Conclusion..... | 42 |
| 2. 6. Experimental details..... | 43 |
| 2. 6. 1. Preparation of nucleotides (DNA template, tRNA, flexizyme) | 43 |
| 2. 6. 2 Preparation of AA-tRNA by flexizyme..... | 45 |
| 2. 6. 3 in vitro translation | 45 |

| | |
|---|----|
| Chapter 3. The chemoenzymatic formation of thiazole-containing peptides via thioamide | 47 |
|---|----|

This chapter is closed for the reason of future publications.

| | |
|---|----|
| Chapter 4. Uniform affinity-tuning of <i>N</i> -methyl-aminoacyl-tRNAs to EF-Tu enhances their multiple incorporation | 49 |
| 4. 1. Introduction | 50 |
| 4. 2. Dr. Iwane's work | 52 |
| 4. 3. My work | 57 |
| 4. 4. Results and Discussion | 57 |
| 4. 4. 1. The expression of a linear peptide containing nine ^{Me} AAs | 57 |
| 4. 4. 2. The expression of a macrocyclic peptide containing nine ^{Me} AAs | 61 |
| 4. 4. Conclusion | 62 |
| 4. 5. Experimental detail | 63 |
| 4. 5. 1 Preparation of nucleotides (DNA template, tRNA, flexizyme) | 63 |
| 4. 5. 3 Preparation of AA-tRNA by flexizyme | 64 |
| 4. 5. 4 In vitro translation | 64 |
| Chapter 5. Analysis of affinity between aminoacyl-tRNA and EF-Tu with a mutated binding pocket | 67 |
| 5. 1. Introduction | 68 |
| 5. 2. Results and discussion | 71 |
| 5. 2. 1 Design and preparation of EF-Tu variants. | 71 |
| 5. 2. 2 Evaluation of ternary complex formation with pAA-tRNAs | 72 |
| 5. 2. 3 Evaluation of ternary complex formation with npAA-tRNAs | 77 |
| 5. 2. 4. Translation using EF-Tu variants | 79 |
| 5. 3. Conclusion | 82 |
| 5. 4. Supplementary results | 83 |
| 5. 5. Experimental details | 84 |
| 5. 5. 1. Introduction of point-mutations by inverse PCR | 84 |
| 5. 5. 2. The sequence of pET-21a-tufA | 87 |
| 5. 5. 3. Purification of EF-Tu | 87 |
| 5. 5. 4. Preparation of nucleotides (DNA template, tRNA, flexizyme) | 89 |
| 5. 5. 5. Preparation of aminoacyl-tRNAs | 89 |
| 5. 5. 6. Reconstitution of EF-Tu/GTP/AA-tRNA | 89 |
| 5. 5. 7. Preparation of DNA, tRNA, and flexizyme | 90 |
| 5. 5. 8. In vitro translation | 90 |

| | |
|-------------------------------------|-----|
| Chapter 6. General conclusion | 91 |
| References | 94 |
| List of achievements | 102 |
| Acknowledgement | 103 |

Abbreviations

| | |
|------------------|---|
| AA-tRNA | Aminoacyl-tRNA |
| Ala ^S | Thionated alanine |
| Amp | Ampicillin |
| ARS | Aminoacyl-tRNA synthetase |
| ATP | Adenosine triphosphate |
| BPB | Bromophenol blue |
| ClAcY | <i>N</i> -chloroacetyl-tyrosine |
| Cm | Chloramphenicol |
| CME | Cyanomethyl ester |
| Dap | Diaminopropionic acid |
| DIEA | <i>N,N</i> -diisopropylethylamine |
| DNB | 3,5-Dinitrobenzyl ester |
| dNTP | Deoxy nucleoside triphosphate |
| DTT | Dithiothreitol |
| <i>E. coli</i> | <i>Escherichia coli</i> |
| EDTA | Ethylenediaminetetraacetic acid |
| EF-Tu | Elongation factor thermo unstable |
| ESI-MS | Electrospray ionization mass spectrometry |
| FIT system | Flexible in vitro translation system |
| FLAG | Asp-Tyr-Lys-Asp-Asp-Asp-Lys |
| fMet, fM | <i>N</i> -formyl methionine |
| FMN | Flavin mononucleotide |
| GDP | Guanosine diphosphate |
| GTP | Guanosine triphosphate |
| HATU | 1-((Dimethylamino)(dimethyliminio)methyl)-1 <i>H</i> -[1,2,3]triazolo [4,5- <i>b</i>]pyridine 3-oxide hexafluorophosphate |
| HEPES | 4-(2-hydroxyethyl)-1-piperazineethanesulfonic acid |
| HOBt | 1 <i>H</i> -Benzo[<i>d</i>][1,2,3]triazol-1-ol |
| HPLC | High performance liquid chromatography |
| HRMS | High resolution mass spectrometry |
| IPTG | Isopropyl-β-D-thiogalactoside |

| | |
|------------------|--|
| LB medium | Luria-Bertani medium |
| LC-MS | Liquid chromatography mass spectrometry |
| LC-MS/MS | Liquid chromatography mass spectrometry/mass spectrometry |
| LP | Leader peptide |
| MALDI-TOF MS | Matrix-Assisted laser desorption ionization-time of flight mass spectrometry |
| ^{Me} AA | <i>N</i> -methyl amino acid |
| mRNA | Messenger RNA |
| NMP | <i>N</i> -methyl pyrrolidone |
| npAA | Non-proteinogenic amino acid |
| npAA-tRNA | Non-proteinogenic aminoacyl-tRNA |
| NRPS | Non-ribosomally synthesized peptides |
| NTP | Nucleoside triphosphate |
| pAA | Proteinogenic amino acid |
| PAGE | Polyacrylamide gel electrophoresis |
| PCR | Polymerase chain reaction |
| PKS | Polyketide synthetase |
| RaPID | Random peptide integrated discovery system |
| RiPPs | Ribosomally synthesized and post-translationally modified peptides |
| SDS | Sodium dodecyl sulfate |
| SPE | Solid phase extraction |
| SPPS | Solid phase peptide synthesis |
| TBAF | Tetra <i>n</i> -butylammonium fluoride |
| TC | Ternary complex |
| TCEP | Tris(2-carboxyethyl)phosphine |
| TFA | Trifluoroacetic acid |
| TIC | Total ion chromatogram |
| Tris | Tris(hydroxymethyl)aminomethane |
| tRNA | Transfer RNA |
| UPLC | Ultra performance liquid chromatography |
| XIC | Extracted ion chromatogram |

Chapter 1.

General introduction

1. 1. The translation system

1. 1. 1. The translation system synthesizes polypeptides

The translation system is one of the essential systems for all living things on Earth. This system synthesizes polypeptides and proteins from twenty kinds of proteinogenic amino acids (pAAs) according to genetic information on a messenger RNA (mRNA), and the resulting peptides and proteins serve indispensable functions, such as metabolisms, mechanical movements, signal transmission. This “translation” of the information on a nucleic acid to the nascent peptide chain sequence takes place at the ribosome by means of adaptor molecules, transfer RNAs (tRNAs). The ribosome accommodates two aminoacyl-tRNA (AA-tRNA) in A-site and P-site at once, and it catalyzes the peptidyl transfer reaction to elongate the nascent peptide chain (Figure 1).

The bacterial translation system derived from *Escherichia coli* is extensively studied from the beginning of molecular biology (1). The translation process is divided into three stages: initiation, elongation, and termination. In the first initiation step, the start codon AUG on the mRNA is recognized by the initiator tRNA (fMet-tRNA^{Ini}), initiation factors, and the ribosome, to form a so-called initiation complex. After the mRNA is correctly placed in the ribosome, the initiation factors are released from the initiation complex. The initiator fMet-tRNA^{Ini} is placed in the P-site, and the codon next to the start codon is decoded by AA-tRNA, which is followed by the elongation stage.

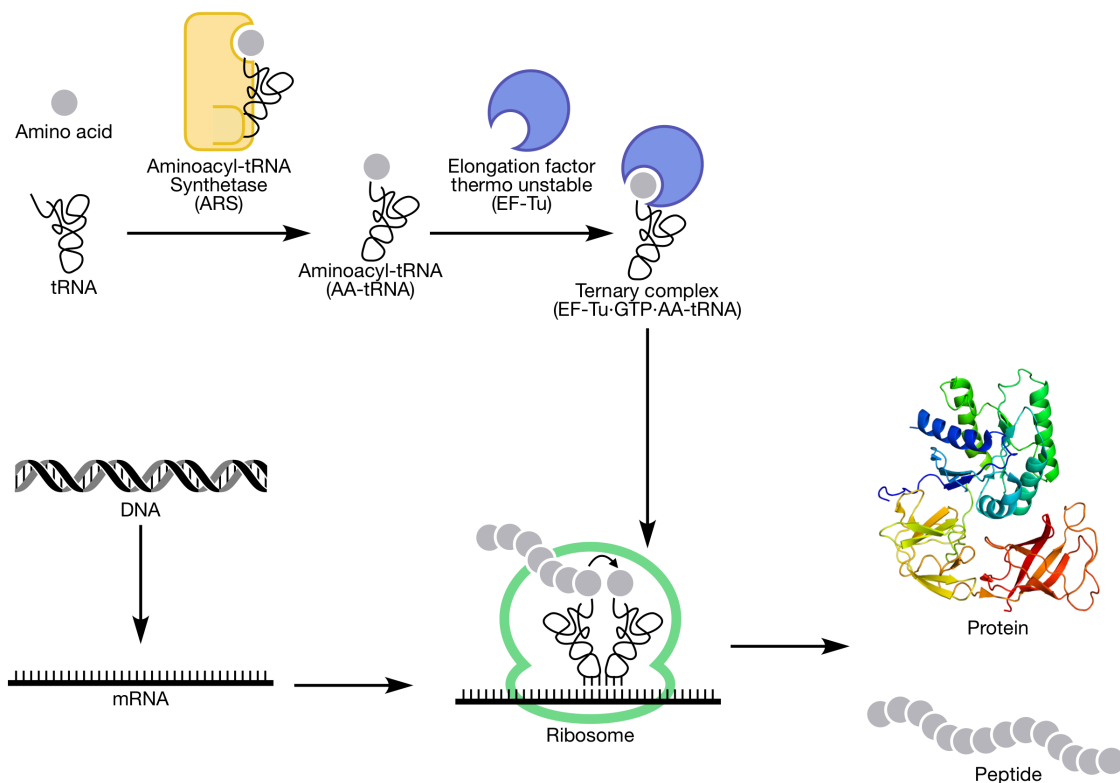


Figure 1 The schematic illustration of the translation system.

| | | 2nd | | | | |
|-----|---|-----|-----|------|-------------|---|
| | | U | C | A | G | |
| 1st | U | Phe | Ser | Tyr | Cys | U |
| | | Leu | | stop | stop Trp | C |
| C | | Leu | Pro | His | Arg | A |
| | | | | Gln | | G |
| A | | Ile | Thr | Asn | Ser | U |
| | | Met | | Lys | Arg | C |
| G | | Val | Ala | Asp | Gly | A |
| | | | | Glu | | G |

Figure 2 The genetic code in the translation system. This table represents the combinations between a codon, a nucleotide triplet on mRNA, and the corresponding proteinogenic amino acids.

During the elongation cycle, each tRNA is aminoacylated with cognate amino acid on the tRNA acceptor stem by each aminoacyl-tRNA synthetase (Figure 1). The resulting aminoacyl-tRNA (AA-tRNA) is captured by an elongation factor thermo unstable, EF-Tu, with GTP, to form the ternary complex (EF-Tu·AA-tRNA·GTP), and then is delivered to the ribosomal A-site. A set of three consecutive nucleotides on an mRNA is a codon, and this codon is recognized by the cognate anticodon of the tRNA, in which a complementary duplex forms between codon and anticodon. Each tRNA has been aminoacylated with cognate amino acid on the tRNA acceptor stem by each aminoacyl-tRNA synthetase, and the ribosome conjugate the amino acids on the A-site tRNA to the P-site tRNA. Afterwards, an elongation factor G (EF-G) is accommodated to the ribosome, conducting the translocation, in which free tRNA at the P-site, which has passed peptidyl chain to the A-site tRNA, is moved to the E-site, and eventually released from the ribosome. Similarly, A-site tRNA which now has an elongated peptidyl chain is moved to the P-site, to make the A-site vacant for the next AA-tRNA. Repeating this cycle, the ribosome elongates the nascent polypeptide chain from amino acids.

In the termination stage, the stop codon of mRNA is recognized by a release factor, instead of AA-tRNA. The release factor hydrolyzes the ester bond between the C-terminal of the peptidyl chain and the P-site tRNA, resulting in the release of the nascent peptide from the translation complex.

The combination of codons and the corresponding amino acids is called the genetic code (Figure

2). This genetic code is common to all living organisms, indicating that this genetic code had been determined as the emergence of life and that it has been inherited from the beginning. In addition, this continuity of the translation system over the history of life indicates that the translation system had been already elegantly constructed to achieve efficient translation without any improvements.

1. 1. 2. The translation system is an elegantly tuned system synthesizing polypeptides

Polypeptides and proteins play important roles in life, and it is required that the polypeptides and proteins are synthesized with extremely high accuracy and efficiency. It is estimated that the ribosome can elongate the nascent peptide with 20–40 amino acids per second, and the error frequency during the translation is estimated no higher than 10^{-4} (2). To achieve this high accuracy the nature has evolved the translation system.

Aminoacyl tRNA synthetases (ARSs) serve a high accuracy during charging amino acids on their cognate tRNAs (3). In addition, some ARSs have proofreading activities as well as acylation efficiency to enhance accuracy. For example, IleRS is in charge of the synthesis of Ile-tRNA^{Ile} but sometimes mischarges Val to tRNA^{Ile} because the binding pocket for Ile is enough large for Val. To prevent the misincorporation, IleRS hydrolyzes Val-tRNA^{Ile} by another catalyzing pocket that can only accept smaller Val (4). In the bacterial translation system, EF-Tu also plays an important role in achieving accurate translation (5). EF-Tu is one of the G-proteins, which binds GTP as a cofactor and utilizes GTP as a molecular switch. Only the GTP-binding form of EF-Tu can bind to AA-tRNA, forming the ternary complex (EF-Tu·AA-tRNA·GTP). The GDP-form of EF-Tu cannot bind to AA-tRNA, thus the hydrolysis of GTP of EF-Tu results in the release of AA-tRNA from the ternary complex. During the ribosomal accommodation of the AA-tRNA, only when the pairing between the codon (on mRNA) and the anticodon (on tRNA) is correct, the ribosome activates the hydrolysis of GTP to release AA-tRNA. This activation energy of the hydrolysis of GTP works as a threshold to discriminate whether the codon is correctly decoded by the AA-tRNA. In addition, the irreversible cleavage of the phosphodiester bond of GTP suppresses the reverse reaction of the translation (i.e., the reformation of the ternary complex by the release of AA-tRNA from the ribosome A-site). Collectively, life paid a cost to synthesize the polypeptide correctly.

1. 1. 3. The ternary complex formation

Furthermore, the formation of the ternary complex between EF-Tu and AA-tRNA has been elegantly tuned. Since EF-Tu delivers all twenty kinds of proteinogenic AA-tRNA to the ribosome, EF-Tu should bind to all AA-tRNA with almost uniform affinities; otherwise, a certain AA-tRNA

with relatively high binding affinity may dominantly bind to EF-Tu, resulting in the disorder of the translation; or a weak AA-tRNA would be competed out in the binding with EF-Tu, also causing the disorder in the translation system.

To achieve these uniform binding affinities between EF-Tu and distinct AA-tRNAs, EF-Tu recognizes two regions of AA-tRNA: the amino acid esterified on the tRNA and the tRNA T-stem sequence (Figure 3A-C). For example, the EF-Tu binding pocket has the weakest affinities for Asp and Glu esterified on the tRNAs, compared to other pAAs. To compensate for these weak affinities, the T-stem regions of their cognate tRNAs (tRNA^{Asp} and tRNA^{Glu}) interact with EF-Tu more strongly than the other tRNAs, and *vice versa*, achieving uniform binding affinities between EF-Tu and pAA-tRNAs (Figure 3D) (6).

The narrow range of near-uniform affinities serves as a threshold to discriminate whether the combination between the amino acid and tRNA is cognate or not. For example, a mischarged Glu-tRNA^{Gln} is synthesized in most archaea and bacteria, and then the side chain carboxylic acid undergoes amidation to generate Gln-tRNA^{Gln} (7). Since the weak affinity originated from Glu cannot be fully compensated by tRNA^{Gln}, Glu-tRNA^{Gln} has an insufficient EF-Tu affinity and is easily competed out during the formation of the ternary complex (8). Similarly, D-Tyr-tRNA has 250-fold less affinity for EF-Tu than L-Tyr tRNA, resulting in the suppression of misincorporation of D-Tyr into the nascent peptide chain (3). Overall, affinities between EF-Tu and AA-tRNA should be one of the important factors determining the incorporation efficiency of the amino acid.

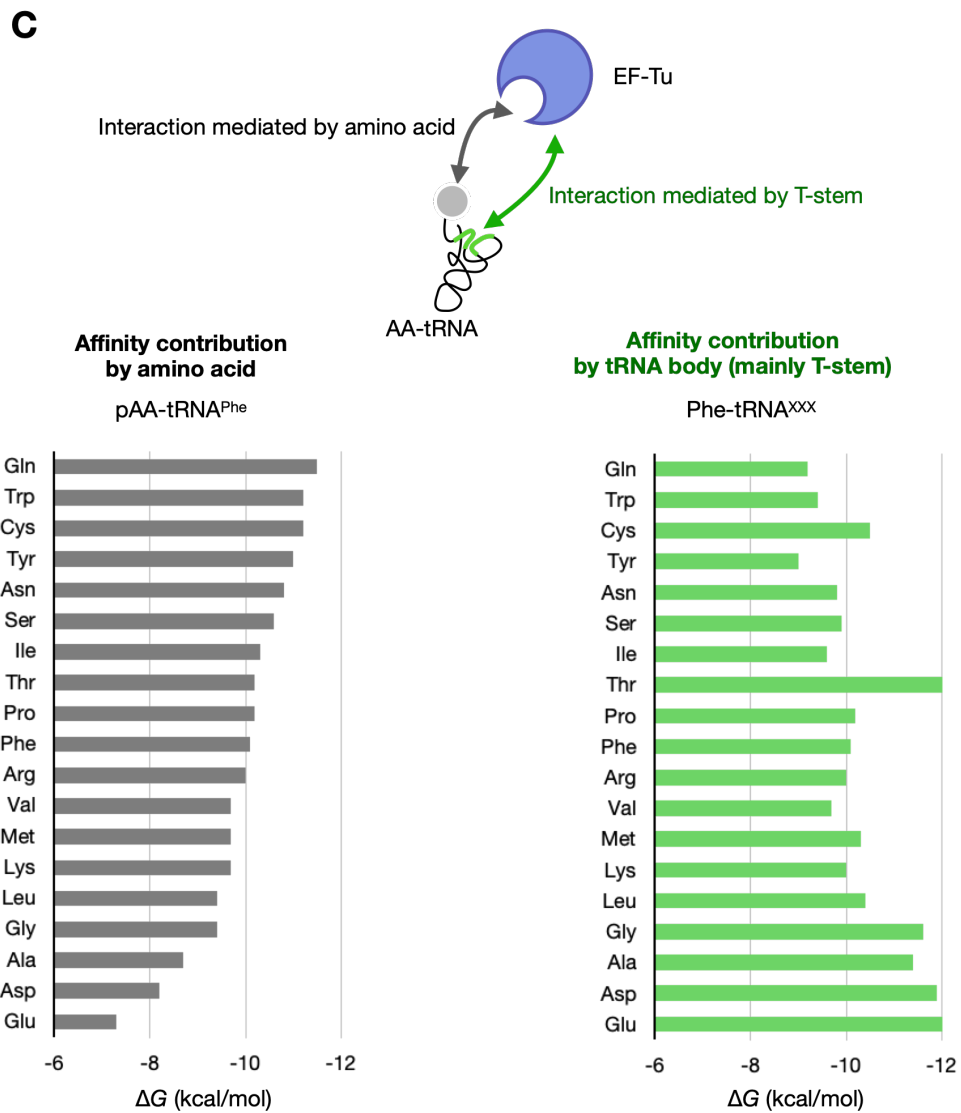
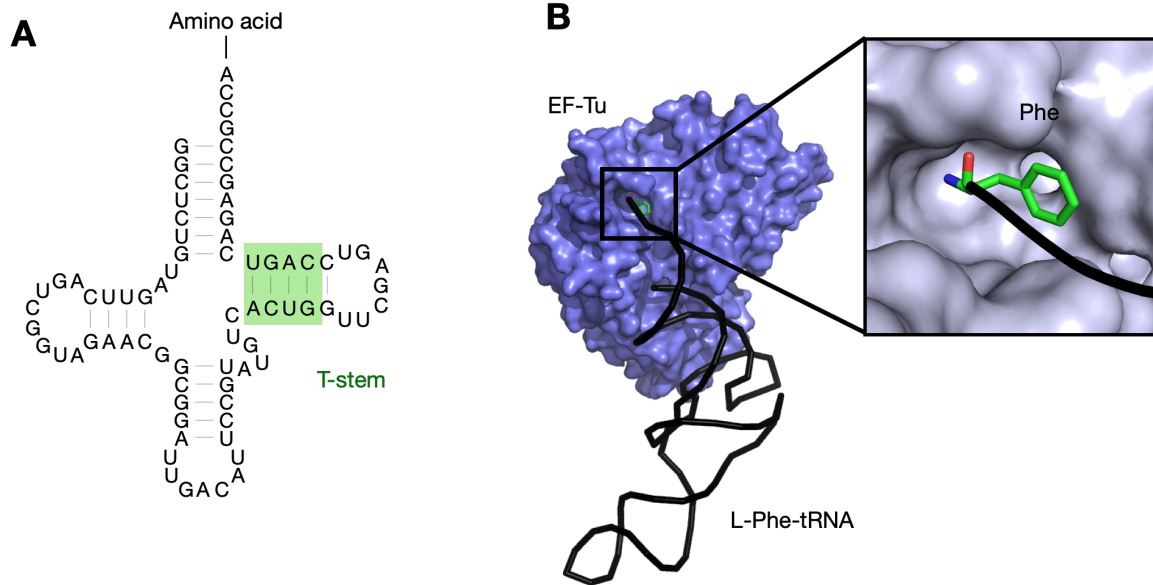


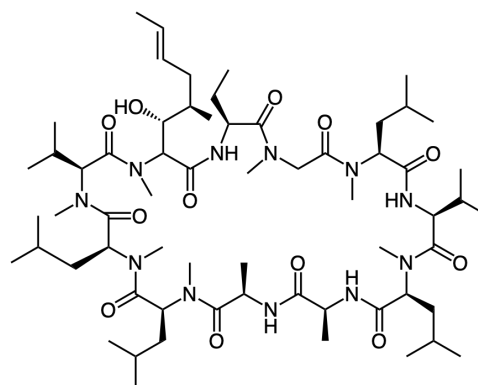
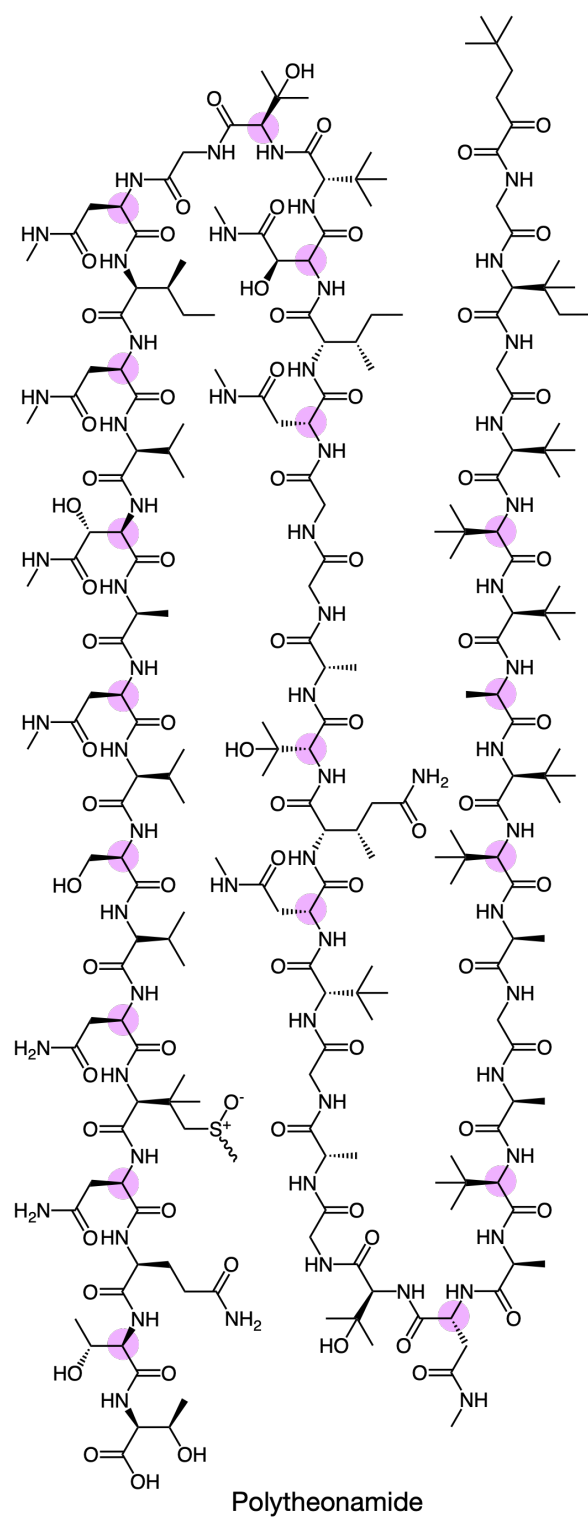
Figure 3 The affinity between EF-Tu and AA-tRNA. (A) The secondary structure of tRNA. The T-stem region is highlighted in green. (B) The co-crystal structure of EF-Tu and L-Phe-tRNA^{Phe}. The esterified amino acid, Phe, is shown in green stick and the magnified view is shown in the right panel. This image was created by using PDB ID: 5AFI. (C) The schematic illustration of the affinity between EF-Tu and AA-tRNA. EF-Tu recognizes two positions of AA-tRNA: amino acid (gray) and T-stem (green). The bottom panels showed the amino acid-mediated affinity (the left panel) and the tRNA body-mediated affinity (the right panel). This bar plots were created by using $\Delta\Delta G$ values reported in reference (6).

1. 2. Peptidic bioactive compounds

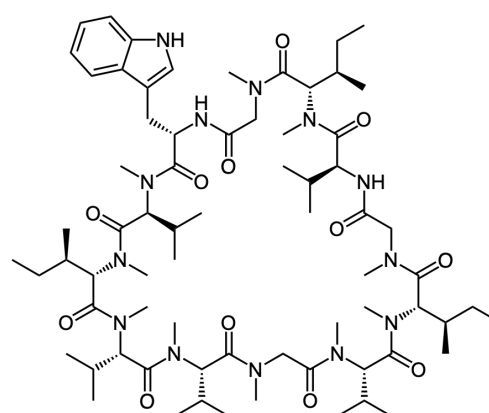
1. 2. 1. Bioactive natural peptides often contain non-proteinogenic amino acids

In nature, there are various kinds of peptidic bioactive compounds consisting of not only twenty kinds of proteinogenic amino acids but also non-proteinogenic amino acids (npAAs). These npAAs confer unique properties on peptides, such as proteolytic resistance or unique conformation. For example, polytheonamide was found from *Theonella swinhoei*, and it contains multiple D-amino acids which are placed alternatively with L-amino acids (Figure 4) (9). This unique alternative configuration probably enables a unique helical folding (10, 11). N-methylations are also frequently found in natural peptides, such as cyclosporin (12) and omphalotin (13). These *N*-methyl-amino acids (^{Me}AAs) install druglike properties to the peptides, *e.g.*, peptidase resistance and cell-permeability (14–18). Thioviridamide, found from *Streptomyces olivoviridis*, contains five thioamide groups and strong cytotoxicity (19). The exact role of thioamides has not been elucidated in thioviridamide, but it has been reported that the substitution of oxoamide with thioamide enhances the structural rigidity and serum stability against protease, and unique hydrogen bonding property (20).

In addition to these single residue-type npAAs, peptide bond isosteres substituting peptide bond which lay over two residues are also founds in peptidic compounds. Petellamide and Telomestatin have azole moieties. Even though the biological function of patellamide itself has not been revealed yet, it has a unique Cu(II) binding affinity owing to its azole structure (21). Telomestatin has an affinity for G-quadruplex (22), which leads to the conformational change of the DNA terminal region. Thiopeptides are one of the classes of natural peptides containing heterocycles. They contain multiple heterocycles such as thiazole and possess strong antibiotic activity against Gram-positive bacteria (23). The significance of heterocycles was investigated in thiocillin, one of the thiopeptides; thiazoles and oxazoles confer the conformational rigidity, and the substitution of these heterocycles with the standard peptide bonds resulted in the decrease of its activity due to the conformational perturbation (24). Collectively, these unique npAAs including backbone-thiazoles are the key factors for bioactivities., and expands the chemical space of peptidic compounds.



Cyclosporin A



Omphalotin A

Figure 4 Examples of the peptidic natural compounds containing npAAs. Polytheonamide contains 18 positions D-amino acids (pink). Cyclosporin and omphalotin are the macrocyclic containing *N*-methylations.

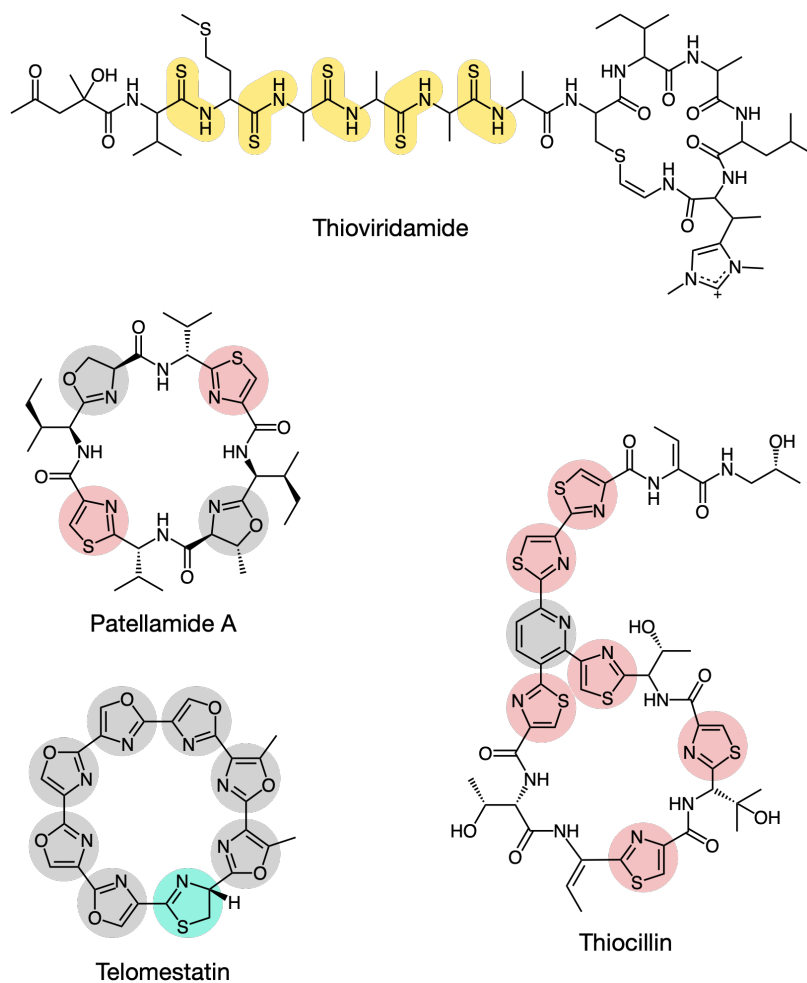


Figure 4 (continued) Examples of the peptidic natural compounds containing npAAs. Thioviridamide contains five thioamide bonds. Patellamide A and telomestatin contain multiple heterocycles. Thiocillin, the class of thiopeptides, contains six thiazole rings and one pyridin core to form the lariat structure.

1. 2. 2. RiPPs pathway

Since the translation system cannot directly access npAA-containing peptides, nature utilizes two pathways to synthesize peptidic compounds: RiPPs (ribosomally synthesized and post-translationally modified peptides) and NRPS (non ribosomally synthesized peptides) pathways. In the RiPPs pathway, at first, a precursor core peptide is synthesized in the translation system and then modified by RiPPs modification enzymes. The precursor peptides generally contain a leader peptide (LP) region, which has an affinity for the cognate modification enzymes and brings the substrate core peptide to the enzymes. Some other types of RiPPs enzymes utilize the “follower peptide” instead of LP (Figure 5A) (25). The modifications introduced by RiPPs enzymes have great diversity. For instance, the D-amino acids in polytheonamide are converted from standard L-configuration pAAs by an epimerase (26). The backbone azoles are also introduced by RiPPs enzymes. In particular, cyclodehydratases, are involved in the formation of thiazoline (27, 28). These cyclodehydratases are a member of the YcaO family and transform Cys residue to thiazoline in an ATP-dependent manner (Figure 5B). First, the enzyme activates the carbonyl group upstream of the Cys residue, by the addition of ATP to increase the leaving ability of the O atom of the carbonyl group. Then it catalyzes an S_N2 attack by the S atom of the thiol group on Cys to the activated carbonyl carbon, resulting in the formation of a thiazoline.

1. 2. 3. NRPS pathway

In the NRPS pathway, a peptidic product is synthesized by a complex of modification enzymes. In this system, one distinct module is required for each substrate amino acid, and thus the overall complex becomes extremely huge (Figure 6A). Since the NRPS pathway does not depend on the translation system, a wider variety of substrates other than amino acids can be incorporated into the products. For example, some NRPS pathways include PKS (polyketide synthetase) domains to synthesize more complicated natural products rather than peptidic compounds.

Cy domain conjugates a Cys amino acid to an elongating peptide chain by deprotonating either thiol or hydroxyl group of Cys, resulting in the formation of the peptide bond (A) or thioester bond (B) (Figure 6B) (28, 29). This is followed by the second reaction in an intramolecular fashion to generate a thiazoline.

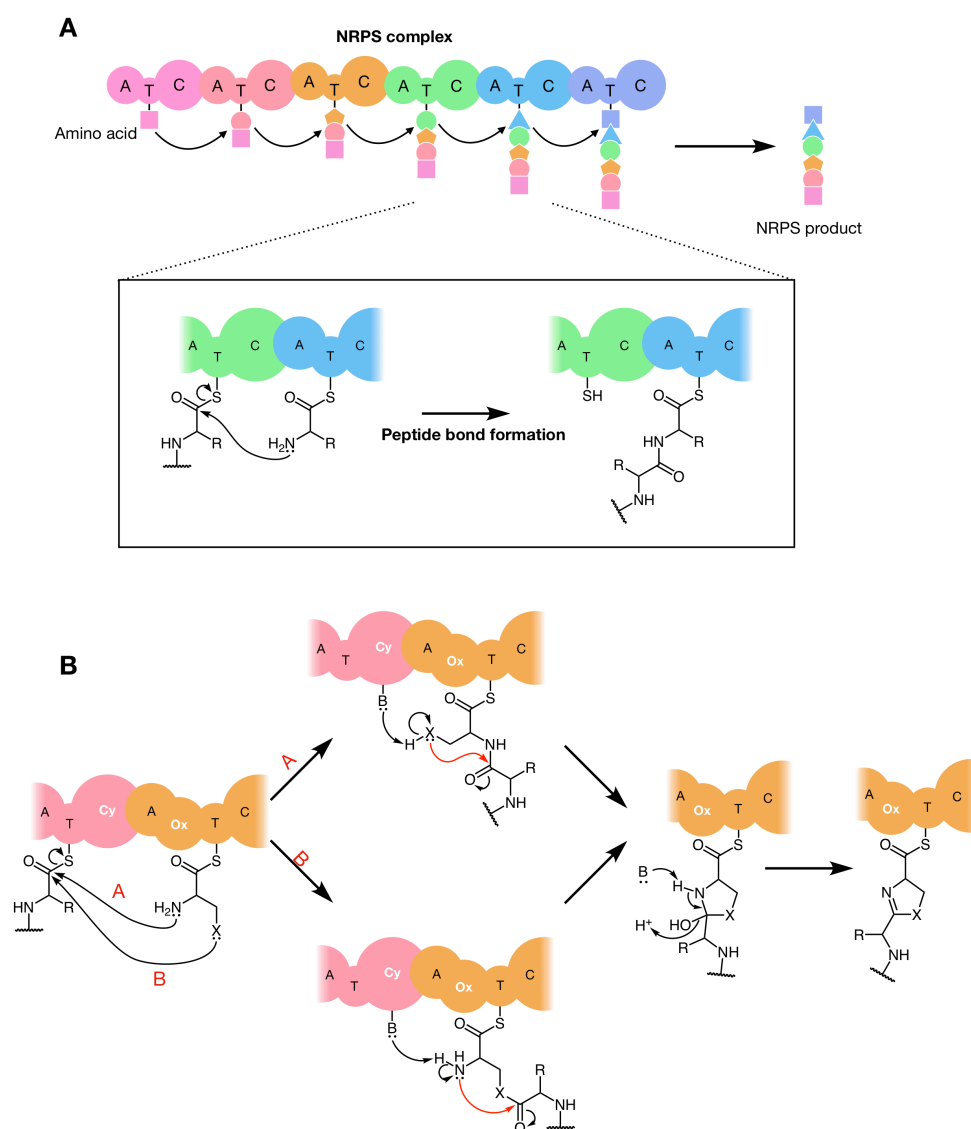


Figure 6 The schematic illustration of NRPS pathway. (A) NRPS complex (B) The installation of thiazoline by Cy domain in the NRPS.

1. 2. 4. Oxidation of thiazoline

Both the RiPPs pathway and NRPS pathway can generate thiazoline moieties as mentioned above, the azoline moiety is easily hydrolyzed by acid/base-catalyzed reaction to reforming the Cys residue. To maintain heterocycle on the peptidic backbone, oxidases convert thiazoline to thiazole. Oxidases involved in both of RiPPs and NRPS pathways, utilize FMN (flavin mononucleotide) as an oxidation cofactor (30, 31). Even though the exact mechanism has not been clearly solved yet, two possible reaction mechanisms are suggested: a hydride transfer, and an electron transfer (radical) mechanisms (Figure 7) (32, 33). The resulting thiazole is much more stable than thiazoline because of its aromaticity.

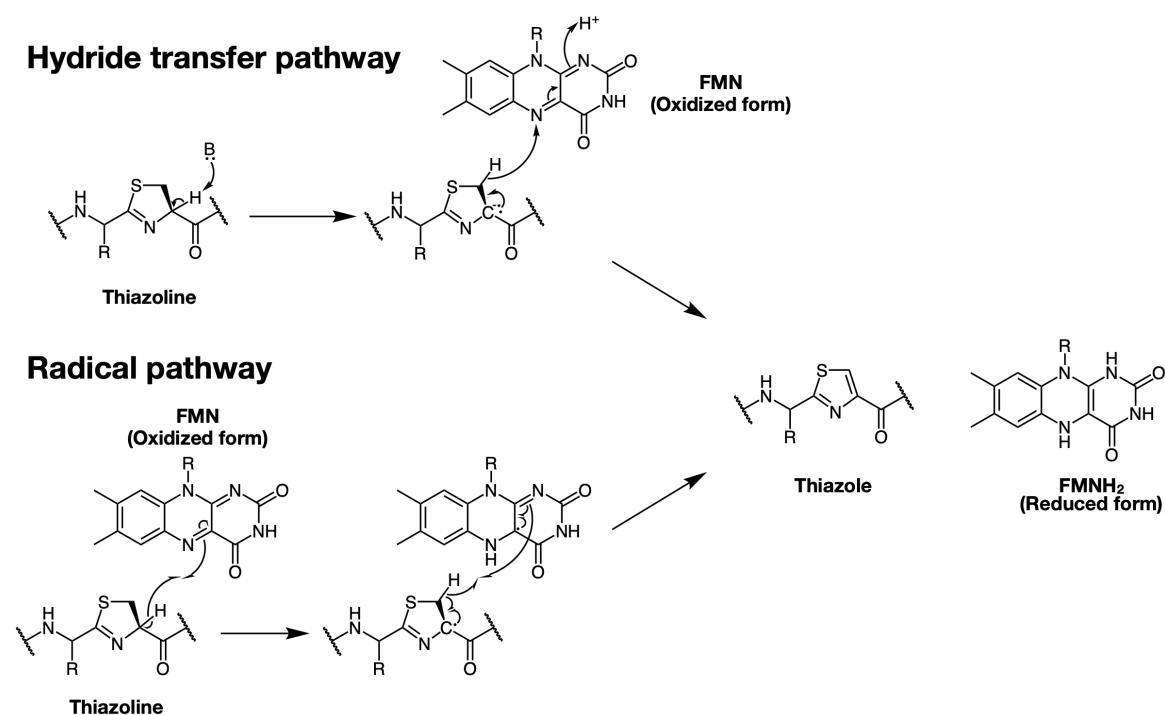


Figure 7 The reaction scheme of FMN-dependent oxidase. Two possible pathways are shown.

1. 3. Genetic code reprogramming technologies

1. 3. 1. The concept of genetic code reprogramming

The natural translation system employs twenty kinds of pAAs to synthesize polypeptides and proteins as previously mentioned. To overcome this hurdle, genetic code reprogramming technologies have been established (34, 35), in which npAA-tRNAs are utilized instead of endogenous pAA-tRNAs to synthesize exotic peptides and proteins containing npAAs. The genetic code reprogramming has been achieved both *in vivo* and *in vitro* and it has advantages over the RiPPs or NRPS pathways, or the SPPS method, owing to an mRNA-templated synthesis.

1. 3. 2. In vivo reprogramming

To date, the *in vivo* genetic code expansion has adopted on orthogonal ARS/tRNA pairs to prepare npAA-tRNAs *in situ* (36). The *in vivo* technology has enabled the synthesis of longer proteins containing npAAs (37, 38). For example, Schultz *et al.*, had evolved *Methanocaldococcus jannaschii* TyrRS/tRNA pair so that *O*-methyl-Tyr could be incorporated into the proteins in *Escherichia coli* (39). In addition, the *in vivo* technology has enabled the directed evolution of proteins with npAAs in *E. coli* (40), which cannot be accessible by other methods. However, the substrate scopes of orthogonal ARSs are limited to amino acids that are similar to the original cognate amino acid (36). Also, npAA of interest is assigned to the amber stop codon (UAG) codon to maintain the endogenous essential protein synthesis; thus, the specialized bacteria strain is required, where whole amber codons are substituted with other two stop codons (41) to achieve a sufficient yield of products.

1. 3. 3. In vitro reprogramming

The *in vitro* reprogramming is generally conducted in the reconstituted cell-free translation system (42), and thus it has much more flexibility in the preparation of npAA-tRNAs, enabling the synthesis of more complicated peptides. From the beginning of the *in vitro* reprogramming research, chemical synthesis of npAA-tRNAs has been utilized, in which npAAs are first conjugated onto deoxy dinucleotide (dCA) and then the esterified dinucleotides are ligated to the precursor of tRNA lacking 3'-dinucleotide (43, 44). The chemical acylation method has provided exotic peptides containing backbone modifications (44). In addition to this chemical synthesis, some promiscuous ARSs have been adopted only when their native substrates are eliminated from the *in vitro* translation system. For example, L-azetidine-2-carboxylic acid (45) and 2-aminoisobutylic acid (46) are charged onto tRNAs by ProRS and ValRS respectively (Figure 8).

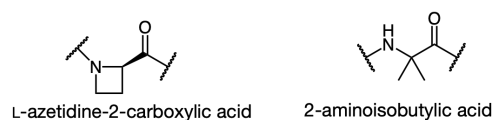


Figure 8 The structure of npAAs introduced by *in vitro* reprogramming using ARS.

1. 3. 4. The FIT system

Among various *in vitro* reprogramming technologies, the FIT (flexible *in vitro* translation) system has been developed by Suga *et al.* (47). The FIT system is the most advanced system, that is employed in many research groups. In the FIT system, npAA-tRNAs are synthesized by flexizyme, which is a ribozyme that originated from the random RNA library (Figure 9A) (48). This flexizyme is capable of the aminoacylation on 3'-CCA end of tRNAs (49) and activated amino acids, and it facilitates the preparation of npAA-tRNAs compared to the chemical acylation method as previously mentioned. In addition, the substrate recognition mode of flexizyme depends on an aromatic ring of the amino acid, almost arbitrary aminoacylation has been achieved (Figure 9B). For example, aliphatic amino acids, such as Leu, can be activated by 3,5-dinitrobenzyl ester as a leaving group. Cyanomethyl ester group is utilized as a non-aromatic leaving group for the amino

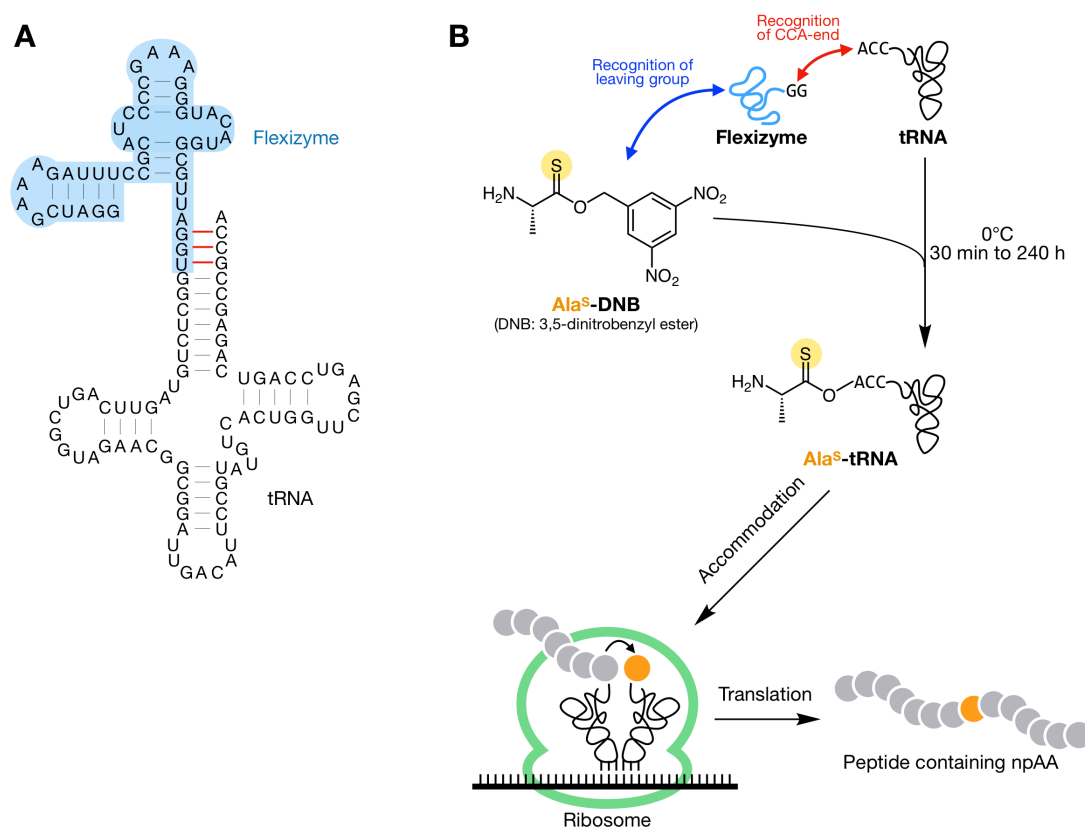


Figure 9 The schematic illustration of the FIT system. (A) The secondary structure of flexizyme and tRNA. (B) The flexizyme-catalyzed aminoacylation reaction using (Ala^S-DNB). The resulting npAA-tRNA can be accommodated to the ribosome, resulting in the formation of peptides containing npAAs.

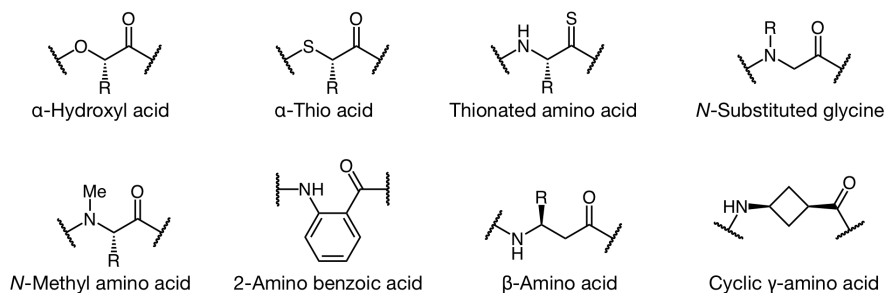


Figure 10 The examples of npAAs installed into peptide by the FIT system.

acids with (an) aromatic ring, such as Phe and its derivatives. (47). The FIT system has been adopted to various npAAs, such as α -hydroxyl acids (50), α -thio acids (51), *N*-methyl amino acids (52), *N*-substituted glycine (53), and β/γ -amino acids (54–57) (Figure. 10).

The FIT system has great compatibility with screening methods based on the mRNA-display technique (58) or mutagenesis analysis of products (59). Furthermore, the construction of a massive library composed of peptides containing npAAs, and the screening method has been established by taking advantage of the FIT system. This screening method has been named the RaPID system (Random Peptide Integrated Discovery) and has been already applied to the discovery of drug-like peptides. Recently, a peptide containing a cyclic β -amino acid, which binds to human serine protease FXIIa, has been discovered via the RaPID system (57). In this peptide, the cyclic β -amino acid induces the unique turn structures to reduce the conformational entropy of the overall peptide; therefore, the binding affinity for the target protein and the serum stability is significantly enhanced by such characteristic backbone structure.

1. 3. 5. The engineering of EF-Tu/tRNA combination

Even though the genetic code reprogramming such as the FIT system, has been one of the most advanced systems to synthesize npAA-containing peptides, there was a hurdle to express arbitrary peptides. For example, the consecutive incorporation of D-amino acids had suffered from the drastically decreased incorporation efficiency (60). Similarly, *N*-methyl amino acids were not fully compatible with the ribosomal peptide synthesis (52). This is likely because each step of npAA incorporation is not as efficient as its natural counterpart in the translation system.

To overcome these limitations, the peptide elongation cycles has been devised. Achenbach *et al.*, have reported that tRNA bodies with enhanced affinities to EF-Tu improved the incorporation of some D-amino acids into peptides in the FIT system (61). Katoh *et al.*, demonstrated that tRNA^{Pro1E2}, a chimera tRNA that has the tRNA^{Pro} body and tRNA^{Glu} T-stem, serves as a good elongator tRNA to incorporate D-amino acids (62). In this chimera structure, the T-stem of tRNA^{Glu}

can bind to EF-Tu stronger than other tRNAs (6) and thus the npAA-tRNA^{Pro1E2} can be efficiently delivered by EF-Tu to the ribosome. The tRNA^{Pro} body (especially the D-arm region) is recognized by elongation factor-P (EF-P), also promoting the peptidyl transfer reaction in the ribosome (63). In addition to the *in vitro* reprogramming, Schultz *et al.*, have conducted a directed evolution of amber suppressor tRNAs from semi-random sequences based on *Methanocaldococcus jannaschii* tRNA^{Tyr} and obtained an evolved tRNA with improved incorporation efficiency of bulky Phe analogs into proteins in *E. coli* (64). They estimated that the evolved tRNA^{Tyr} acquired the enhanced EF-Tu affinity during the directed evolution.

Alternatively, Doi *et al.*, designed EF-Tu mutants bearing an enlarged binding pocket so that improve the affinity for bulky npAA-tRNAs, allowing efficient incorporation of such npAAs into proteins (65). Park *et al.*, conducted the directed evolution of EF-Tu to obtain a positively-charged binding pocket for the amino acid esterified on tRNA. This EF-Tu mutant (EF-Sep) can efficiently incorporate *O*-phosphoserine during the translation (66).

Overall, various kinds of research have focused on the interaction between AA-tRNA and EF-Tu. By reinforcing or tuning the affinities between npAA-tRNAs and EF-Tu, the incorporation efficiencies of npAAs have been enhanced. However, there still remains a hurdle to express designer peptides. For example, D-Pro, which could confer unique conformations on peptides, cannot be efficiently installed into peptides (60). This indicates that the understanding of the interaction between npAA-tRNAs and EF-Tu is not enough.

Chapter 2

Ribosomal formation of thioamide bonds

2. 1. Introduction

A thioamide is the isostere of an oxoamide (67). Even though the difference is only a single atom (oxygen or sulfur), thioamide-containing peptides exhibit unique chemical properties different from oxoamides, such as thermodynamics (68, 69), improved proteolytic stability (70), enhanced conformational rigidity (71), and modified spectroscopic profiles (72, 73). Thioamides are also found in natural peptidic products, such as thioviridamide or thiopeptin (Figure 11), probably enhancing their biological activities (20, 70, 71, 74, 75). Therefore, thioamidation is now regarded as a useful peptidomimetic, and thioamide-containing polypeptides can be regarded as an attractive class of molecules to develop functional peptide derivatives.

The natural products containing thioamides are synthesized by NRPS or RiPPs pathways, in which the thioamide moieties are generated via enzymatic O-to-S conversion after construction of the oxoamide-backbones (76, 77). Even though the reconstitution of RiPPs thioamidation reaction has been *in vitro* reconstituted, the flanking residues of the thioamidation site could not be modified due to the enzymatic preference (78), not allowing for the synthesis of arbitrary sequences. Thus, previously, the synthesis of thioamide-containing peptides mostly depends on the solid-phase peptide synthesis (SPPS) method and its combination with native chemical ligation (79, 80).

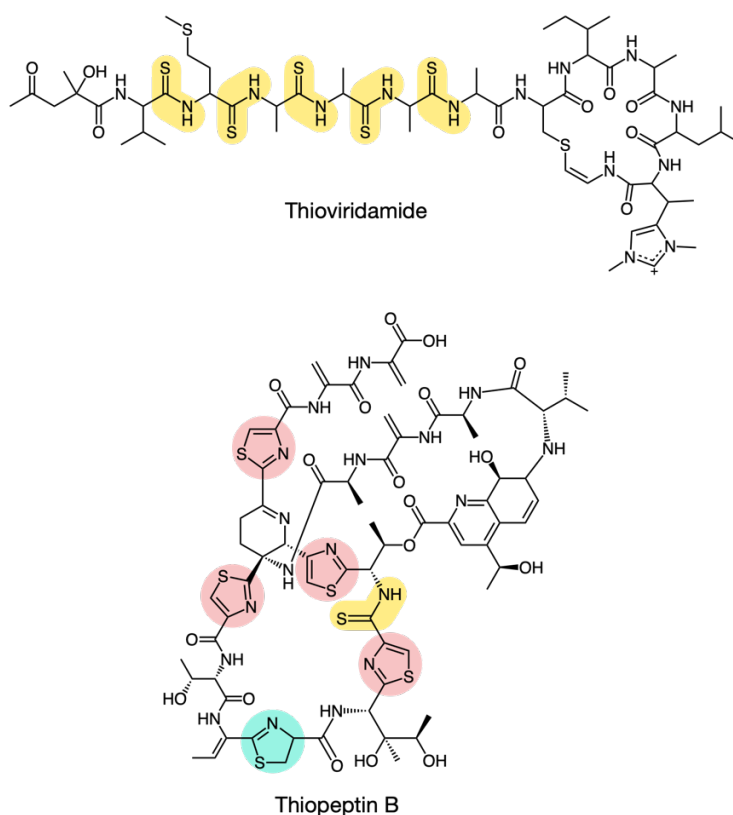


Figure 11 Two natural peptides containing thioamide.

In contrast, the direct incorporation of thioamide in the translation system had been poorly studied. There was only a single report in 1976, in which the ribosomal thioamide bond formation was demonstrated (81); however, this research employed pentanucleotide CACCA as a tRNA-mimic, and thus the reaction did not take place in accordance with the mRNA. Furthermore, the identification of the product depended on the thioamide-specific derivatization (desulfurization) and liquid separation, and thus the direct observation of the formation of the thioamide bond was required.

Here in this research, Dr. Maini and I aimed to install a thioamide in the nascent peptide chain in the ribosomal translation. First, Dr. Maini had hypothesized that the currently widely used method, the genetic code reprogramming can be applied to the installation of a thioamide (82).

Taking the advantage of Dr. Maini's work, I first examined the cause of the S-to-O conversion during thioamide bond formation. I also tested several solvents to suppress the S-to-O conversion during the storage of the thioamide monomer. Then, I aimed to express the macrocyclic peptide containing a thioamide. In addition, I aimed to consecutively incorporate an *N*-methyl amino acid and a thioamide to generate *N*-methyl thioamide linkage in a macrocyclic scaffold.

2. 2. Dr. Maini's work

Dr. Maini had aimed to incorporate a thioamide linkage by taking advantage of flexizyme. To this end, Dr. Maini had synthesized Ala^S-DNB (alanine thiono-3,5-dinitrobenzyl ester) in 5 steps as shown in Figure 12.

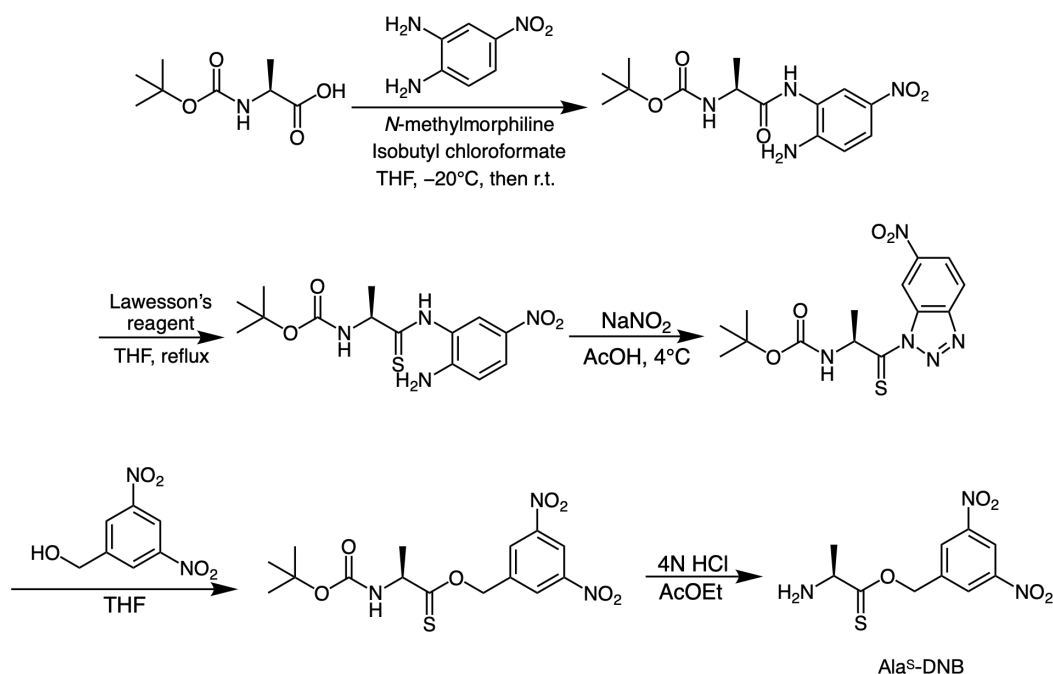


Figure 12 The synthesis scheme of Ala^S-DNB.

Then, Dr. Maini carried out the *in vitro* translation reaction to install Ala^S into the peptide. The template DNA (DNAT1) and the resulting peptide (PepT1) were designed as shown in Figure 13. In template DNAT1, ACC codon (Thr) was reprogrammed by supplementing Ala^S-tRNA^{GluE2_{GGU}} (83) and omitting Thr in the FIT system. After 30 min translation reaction, the peptide product was analyzed by MALDI-TOF MS, and two major peaks were observed (Figure 13). The highest intensity peak was corresponding to the desired peptide containing the thioamide bond (PepT1-thioamide) at 1542.71 *m/z* (calculated 1542.65 *m/z*); however, the second major peak at 1526.73 *m/z* was exactly 16 units less than the [M+H]⁺ ion of PepT1-thioamide, suggesting that it was very likely PepT1-oxoamide. Thus, the PepT1-thioamide and PepT1-oxoamide seemed to be coexpressed by the Ala^S-tRNA in the translation system.

There was a possibility that unexpected misincorporation of Ala instead Ala^S might cause the coexpression of PepT1-thioamide and PepT1-oxoamide; the ACC codon (assigned to Ala^S) could be read by Ala-tRNA^{Ala}, because Ala and Thr are in the same column of the genetic code. To

elucidate this possibility, Dr. Maini changed the codon assignment of Ala^S. In another template, DNAT2 (Figure 13), Ala^S was assigned His (CAC) codon, which is far from Ala codon. The expression of PepT1 was carried out in the FIT system with Ala^S-tRNA^{GluE2}_{GUG} and without His similarly. However, two major ion peaks corresponding to thioamide and oxoamide were observed again, suggesting that the competitive formation of PepT1-oxoamide with PepT1-thioamide was not originated from the Ala misincorporation event during the translation. Therefore, the elucidation of the cause of oxoamide-counterpart was required.

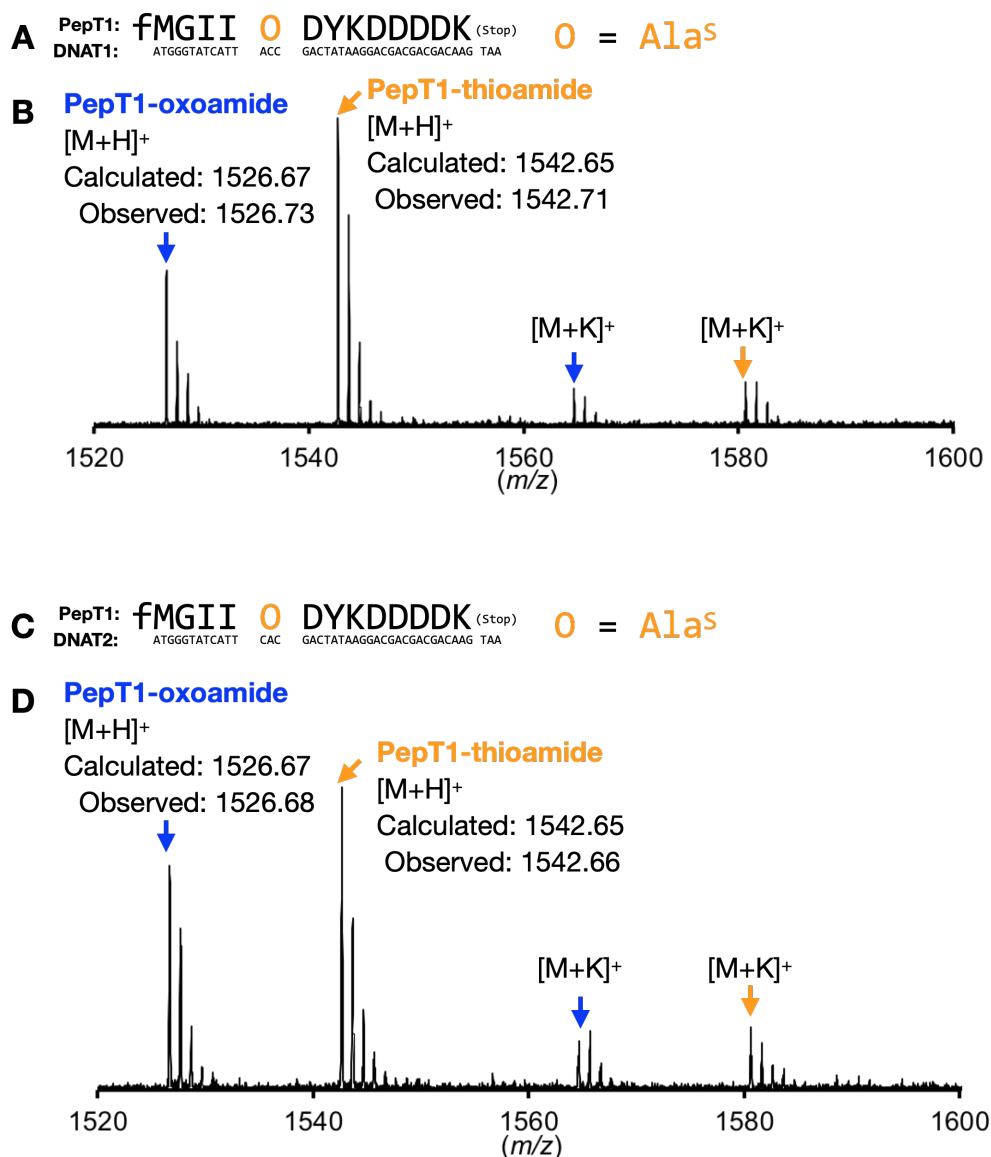


Figure 13 The ribosomal incorporation of a thioamide into model peptide TAP1. (A)(C) The sequence of DNAT1, DNAT2. Both DNAT1 and DNAT2 generate the identical peptide TAP1. (B)(D) MALDI-TOF mass spectra of TAP1. The desired TAP1 were labeled in yellow. The -16 m/z peak which corresponding to the oxoamide counterpart were shown in blue arrows.

2. 3. My work

The first aim of my research is to elucidate the origin of oxoamide-counterpart. In addition, Dr. Maini had successfully demonstrated that the ribosomal formation thioamide linkage, but the example was limited. Thus I decided to express macrocyclic peptide containing a thioamide since macrocyclic scaffolds containing thioamide would have more conformational rigidity (71).

2. 4. Results and Discussion

2. 4. 1. *The elucidation of the origin of S-to-O exchange*

During the peptide synthesis containing a thioamide, the oxoamide-counterpart was always observed regardless of the reprogramming codon (Figure 13). Even though it has been reported that the thioamide bond is fairly stable once it is formed (20), I first hypothesized that the thioamide bond on the translated peptide may undergo the S-to-O exchange. To test this hypothesis, I incubated the thioamide-containing peptide for a prolonged time.

The model peptide (Pep270) (Figure 14) was synthesized in the FIT system, in which the GTC (Val) codon was reprogrammed to Ala^S by supplementing Ala^S-tRNA^{AsnE2#3}_{GAC} (see Chapter 4 for the detailed tRNA^{AsnE2#3} property). The translation reaction was carried out for 30 min, and the reaction mix was divided into three tubes. One sample was subjected to the MALDI-TOF MS right after the translation; two samples were incubated at 37 °C for 2 h or 25 °C for overnight (Figure 14). Even after overnight incubation in the aquatic translation solution, the ratio of the oxoamide-counterpart does not increase, indicating that the S-to-O exchange occurred prior to the translation reaction.

Pep270: fMAGLEAA 0 ALGGYLR^(Stop) 0 = Ala^S
 DNA270: ATGGCGGGTTGGAGGCAGCT GTC GCGCTGGGTGGCTATTACGC TAA

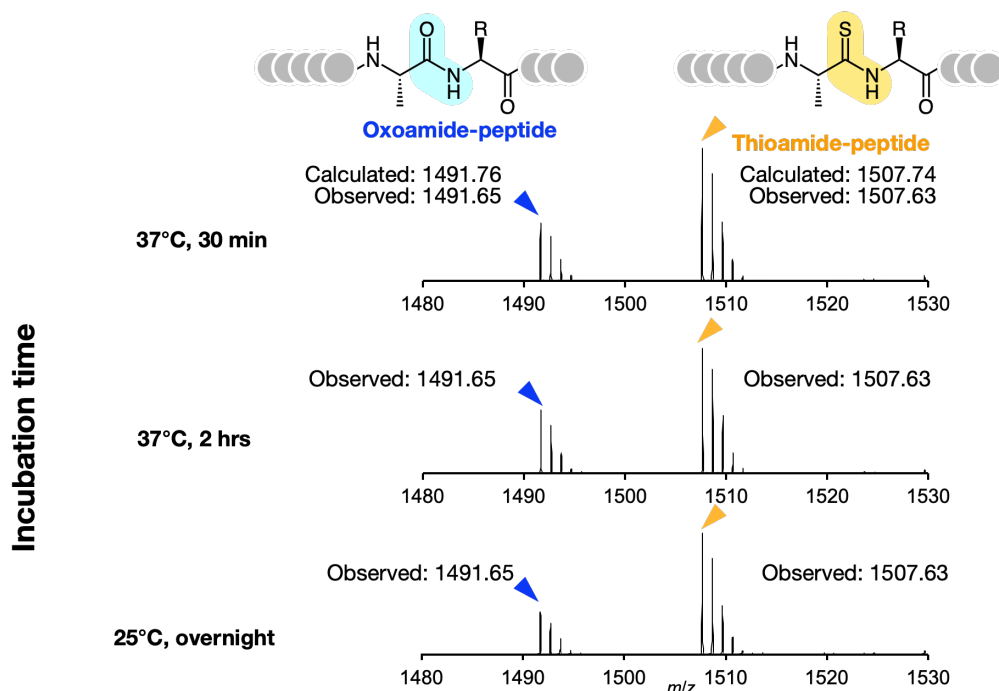


Figure 14 The prolonged incubation of Pep204 containing thioamide.

I next hypothesized that a carbo(S-to-O) exchange occurred during the aminoacylation reaction. To evaluate whether the carbo(S-to-O) exchange in Ala^S-DNB occurred during the aminoacylation reaction, At first, I prepared a fresh Ala^S-DNB in DMSO, and incubated it in 50 mM HEPES-KOH buffer (pH 7.5) to mimic the amino(carbothio)acylation reaction. This monitoring experiment was conducted in the absence of dFx. In addition, I used two types of HEPES buffer prepared with either ¹⁶O-water or ¹⁸O-water. The condition of Ala^S-DNB was monitored by ESI-MS. After 120 min incubation on ice, each sample was diluted with acetonitrile and then subjected to the ESI-MS analysis (Figure 15). The freshly prepared Ala^S-DNB does not contain the oxoamide-counterpart, but after the incubation, the corresponding S-to-O exchanged substrates were observed. Notably, with ¹⁸O-labeled water, Ala^S-DNB showed a – 14 *m/z* shift, implying the S-to-¹⁸O exchange. Thus, the aqueous oxygen was revealed to be the origin of the S-to-O exchange. It is also known that the aminoacyl group rapidly migrates between 2'-OH and 3'-OH on tRNA; thus it is possible that the carbo(S-to-O) exchange on Ala^S-tRNA could also occur during the inter-2'/3'-migration process as soon as Ala^S-tRNA was formed (84). Regardless of the pathway of S-to-O exchange (water attack in aquatic conditions, or migration between 2'-OH and 3'-OH on tRNA), I concluded that the S-to-O exchange is unavoidable.

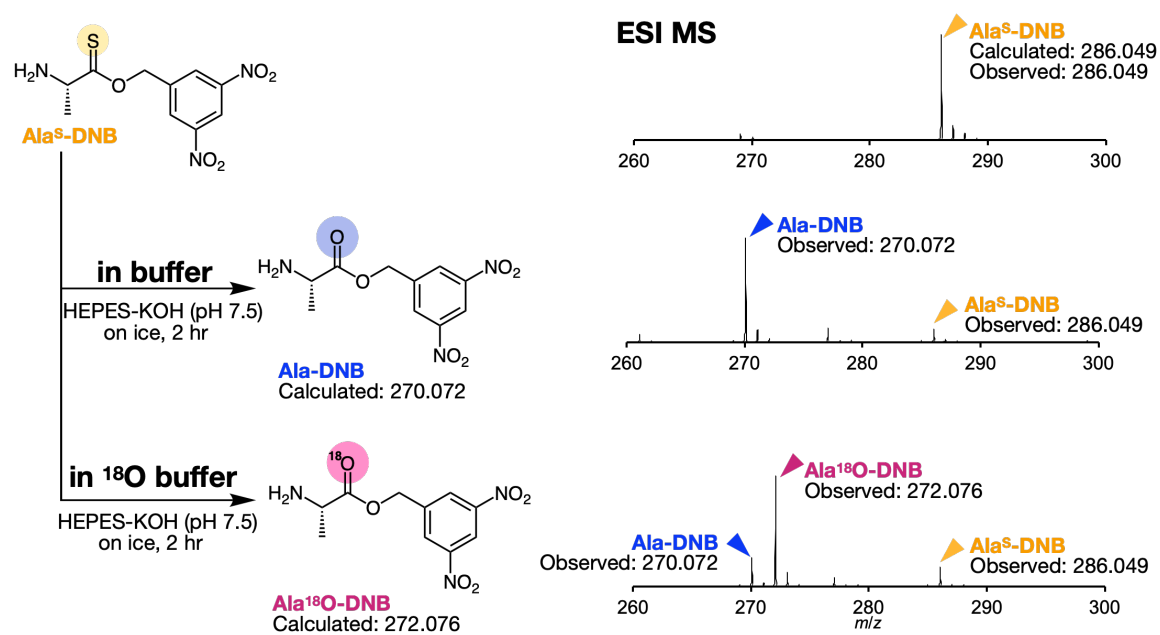


Figure 15 The ESI-MS monitoring of Ala^S-DNB in ¹⁶O or ¹⁸O buffer.

2. 4. 2. Suppress the S-to-O exchange during the storage

Ala^S-DNB was dissolved in 100% DMSO solution for the storage, but I noticed that the S-to-O exchange events occurred even in 100% DMSO solution (Figure 16B). This may be because of the contamination of water, or because the O atom of DMSO attacks the thionoester bond in Ala^S-DNB and the S atom is dissociated, as the O atom of DMSO attacks oxalyl chloride in the Swern oxidation. Since the S-to-O conversion during the storage phase would decrease the convenience of the thioamide installation, I aimed at the suppression of the S-to-O exchange during the storage. I tested seven solvents (acetone, 1,4-dioxane, DMF, acetonitrile, *N*-methyl pyrrolidone (NMP), THF, and water, 100% each) to dissolve Ala^S-DNB and stored them at –80 °C for 10 days, and then measured the mass spectra (Figure 16). Among Ala^S-DNB solutions, surprisingly, Ala^S-DNB remained in six solvents, except for DMSO and water. Especially in NMP, the oxoamide-counterpart was hardly observed. I also conducted the aminoacylation reaction using these Ala^S-DNB solutions and conducted the translation reaction. In all cases, the peptides containing thioamide were successfully observed, suggesting that flexizyme could aminoacylate even with other organic solvents. Note that the aminoacylation reaction was carried out in 80% water and 20% organic solvent solutions containing Ala^S-DNB, or 100% water in the case of Ala^S-DNB was dissolved in water. Since Ala^S-DNB hardly underwent the S-to-O exchange in NMP and the aminoacylation in NMP also generated the Pep204 containing the thioamide correctly, I used Ala^S-DNB dissolved in NMP.

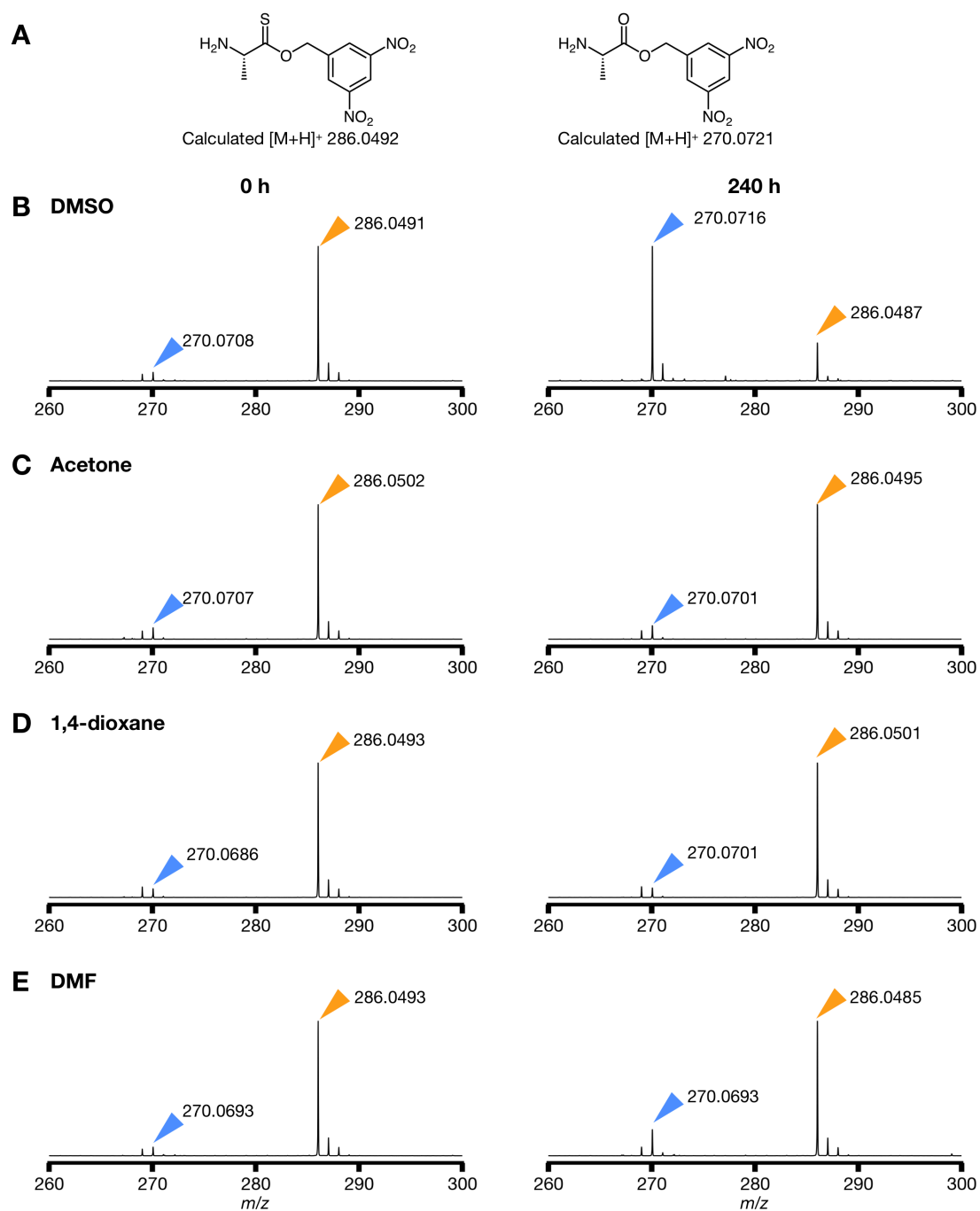


Figure 16 The S-to-O conversion observed in eight kinds of solvents.

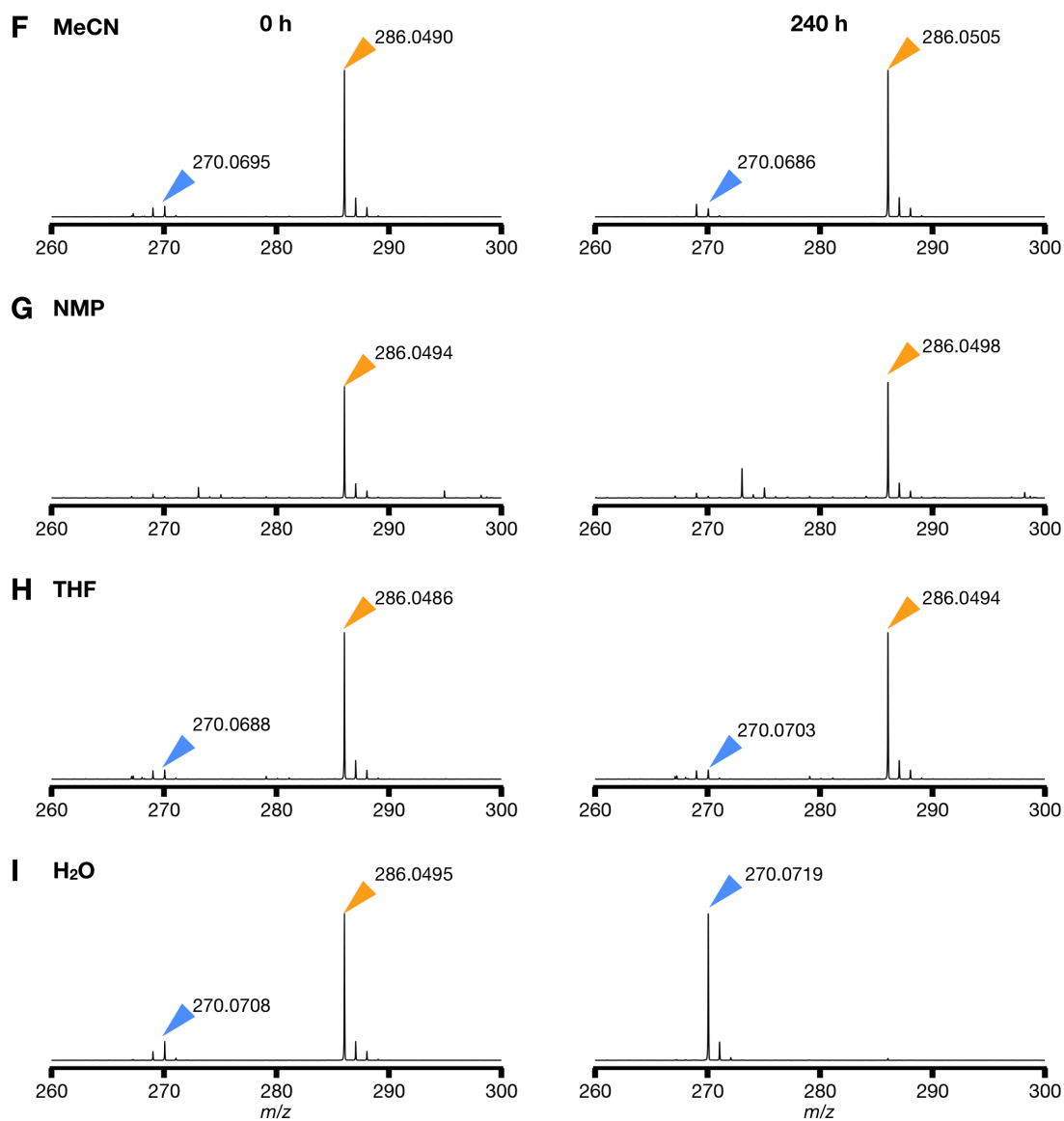


Figure 16 The S-to-O conversion observed in eight kinds of solvents. (continued)

2. 4. 3. The installation of thioamide in a macrocyclic peptide

The thioether-macrocyclic peptide has proven to be a superb peptide scaffold to exhibit certain bioactivity (85). Thereby, I aimed the installation of thioamide into a macrocyclic scaffold. To this end, I utilized the *N*-chloroacetyl-amino acid (^{ClAc}AA) initiator to synthesize a thioether-linked macrocyclic peptide (86). The thioether-macrocyclic peptide containing Ala^S was designed as PepT3. The N-terminal of PepT3 was reprogrammed with *N*-chloroacetyl-tyrosine (^{ClAc}Y) by omitting Met from the FIT system. As expected, the desired peaks of PepT3-thioamide along with the peaks of PepT3-oxoamide were observed in MALDI-TOF analysis (Figure 17). The result was consistent with the thioether-macrocyclic peptide containing the thioamide bond.

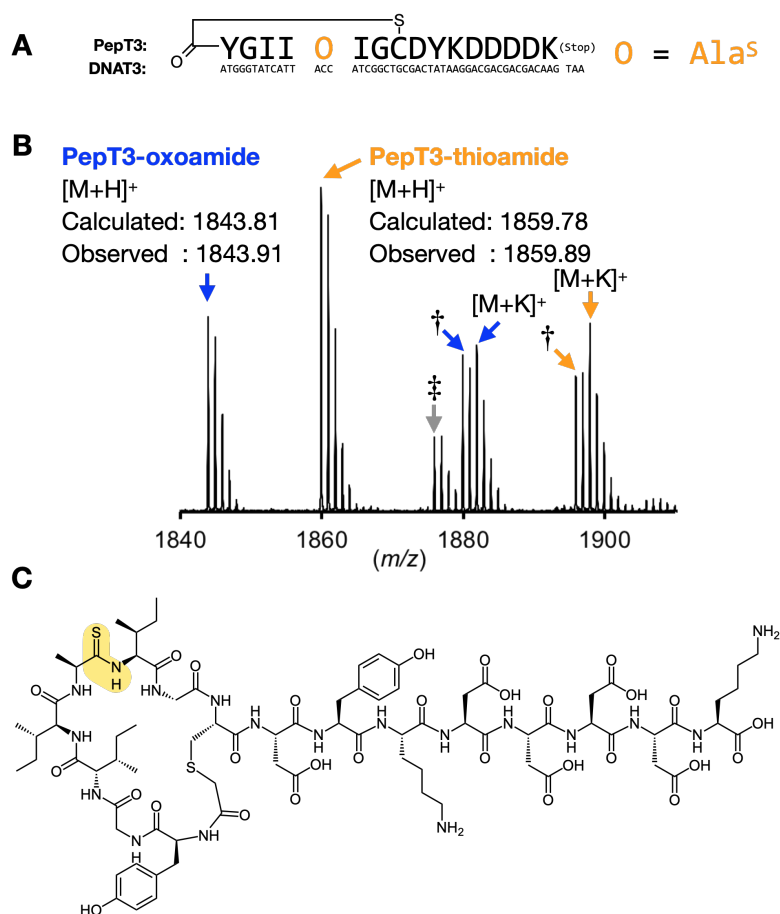


Figure 17 The expression of macrocyclic peptide containing thioamide (TAP3). (A) The sequence of DNAT3 and TAP3. (B) MALDI-TOF mass spectrum. *: potassium adducts, †: linear form that contain intact ClAc group and thiol, ‡: Cys misincorporation into ACC codon. (C) Overall structure of TAP3.

Since the ribosome is known to accept the *N*-methyl-amino group as a nucleophile (86–88), we also investigated if an *N*-methyl-thioamide bond could be generated in the ribosome. We utilized DNAT4 to express a macrocyclic peptide, but this time in addition to Thr ACC codon reassignment to Ala^S, His CAC codon was reassigned to *N*-methyl-phenylalanine (^{Me}F). DNAT4 was translated in the FIT system (lacking Met, Thr, and His) in the presence of ^{Cl}AcY-tRNA^{fMet}_{CAU}, Ala^S-tRNA^{GluE2}_{GGU}, and ^{Me}F-tRNA^{GluE2}_{GUG}. MALDI-TOF analysis suggested that the desired macrocyclic PepT4 containing *N*-methyl-thioamide bond was expressed as expected (Figure 18).

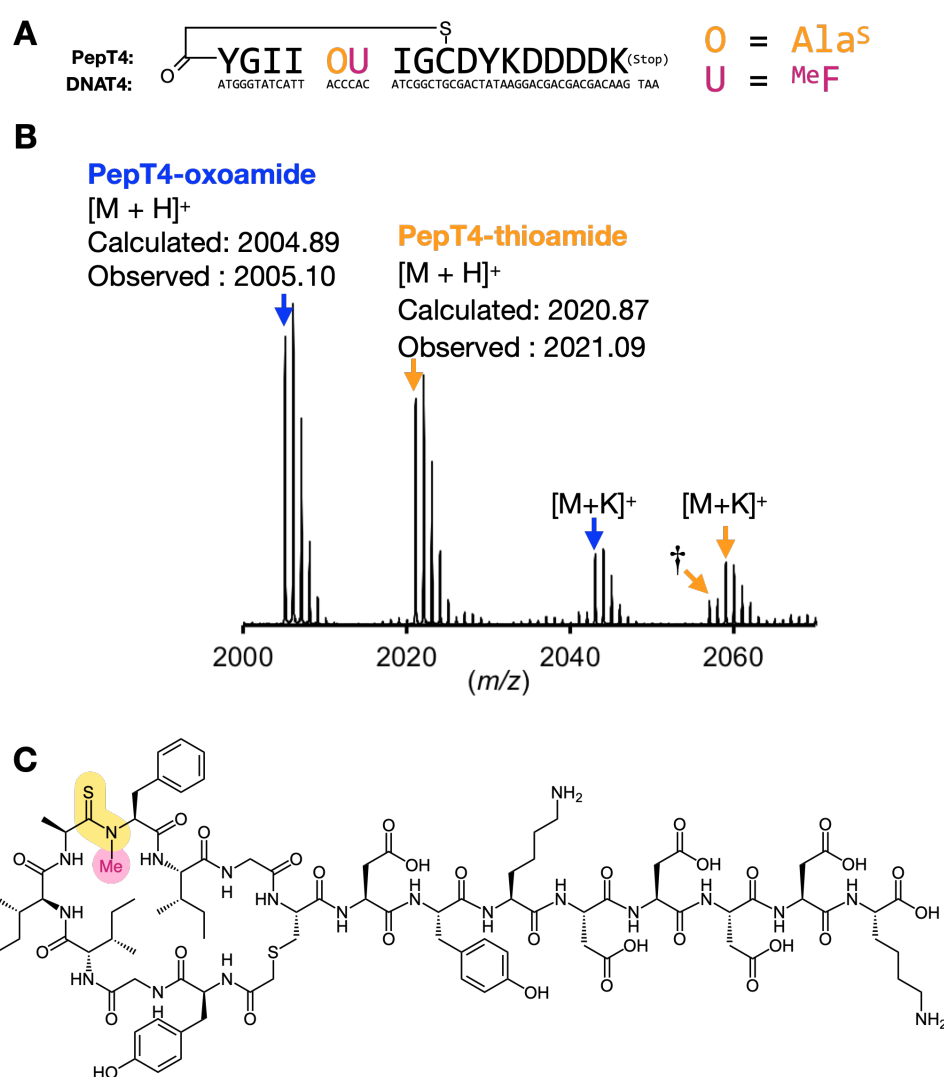


Figure 18 The expression of macrocyclic peptide containing *N*-methyl thioamide (TAP4). (A) The sequence of DNAT4 and TAP4. (B) MALDI-TOF mass spectrum. *: potassium adducts, †: linear form that contain intact ClAc group and thiol. (C) Overall structure of TAP4.

2. 5. Conclusion

Here, Dr. Maini and I demonstrated the ribosomal formation of the thioamide bond. Nearly 50 years ago, the thioamide bond formation in the ribosome had been reported, but the identification of the product was poor, and moreover, it was the mRNA-independent reaction to generate merely dipeptidic moiety. In this study, we have shown the direct identification of the peptide product containing a thioamide in MALDI-TOF MS, indicating that the ribosome is capable of expressing designer peptides containing a thioamide bond in an mRNA-dependent manner using our FIT system. This methodology to incorporate thioamides would facilitate the synthesis of thioamide-containing peptides and proteins which are previously achieved mainly by SPPS and native chemical ligation. Most importantly, our present study has explicitly shown not only the mRNA-dependent expression of thioamide-peptides but also the potential for the ribosomal installation of the thioamide moieties into the libraries of thioether-macrocyclic scaffolds, which can be applicable to their bioactivity screening.

2. 6. Experimental details

2. 6. 1. Preparation of nucleotides (DNA template, tRNA, flexizyme)

DNA templates, tRNAs, eFx, and dFx were prepared using primer extension and PCR reactions using the primer sets listed in Table 1. The combinations of primers were listed in Table 2. The extension and PCR reactions were conducted following the previous report (47). In specifically, the polymerase reaction mixture for both extension and PCR reaction contains was prepared as follows: 10 mM Tris·HCl (pH 9.0), 50 mM KCl, 2.5 mM MgCl₂, 0.25 mM dNTPs, 0.1% (v/v) Triton X-100, and Taq DNA polymerase. In primer extension, appropriate forward and reverse primers (1 μM each) were mixed in the polymerase reaction mixture. The primer extension reaction was performed in a 100 μL scale, by denaturing (95 °C for 1 min), followed by 5 cycles of annealing (50 °C for 1 min) and extension (72 °C for 1 min). The primer extension reaction product was 200-fold diluted and amplified using the appropriate forward and reverse primers (0.5 μM each) in a 1000 μL scale by 12 cycles of denaturing (95 °C for 40 s), annealing (50 °C for 40 s), and extension (72 °C for 40 s). The resulting DNA was purified by phenol/chloroform extraction and ethanol precipitation. The precipitated DNA was washed with 70% ethanol and then dissolved in 100 μL of water. For the *in vitro* transcription/translation in the FIT system, the DNA solution was directly used. For the tRNA and flexizyme, the DNA solution was then subjected to *in vitro* transcription and purification.

Transcription reaction mixture was prepared as follows: 40 mM Tris·HCl (pH 8.0), 1 mM spermidine, 0.01% (v/v) Triton X-100, 10 mM DTT, 30 mM MgCl₂, 5 mM NTPs, 1.5% (v/v) of 2M KOH, 10% (v/v) PCR product and 2% (v/v) T7 RNA polymerase. Stand the reaction mixture at 37 °C overnight. The DNA template was degraded by RQ1 DNase (Promega) following the manufacture's instruction. To the solution, 20% vol. of 500 mM EDTA and 13.5% of 3M NaCl were mixed, and then 120% of isopropanol was added to precipitate the RNA. The precipitated RNA was washed with 70% ethanol and dissolved in 10% vol. of water. The sample was loaded on denaturing polyacrylamide gel [44.5 mM Tris/Tris-borate (pH 8.0), 1 mM EDTA, 8% or 12% (19:1) acrylamide/bis mixed] and the electrophoresis was carried out at 230V for 60 min. The fraction containing tRNA or flexizyme was determined by the UV-absorption. The RNA was extracted to the 0.3 M NaCl and precipitated by ethanol. The precipitated RNA was washed with 70% ethanol and dissolved in water. The concentration was determined by A_{260} .

| Primer | Sequence (5' → 3') |
|----------------|---|
| T7eSD6M.F44 | TAATACGACTCACTATAGGGTTAACTTTAACAAGGAGAAAAACA |
| 1R | CGAAGCTTACTTGTCATCGTCGTCCTTGTAGTCGGTAATGATACCCATGTTTTCTCCTTGTTAAAG |
| 2R | CGAAGCTTACTTGTCATCGTCGTCCTTGTAGTCGTGAATGATACCCATGTTTTCTCCTTGTTAAAG |
| 3R | CGAAGCTTACTTGTCATCGTCGTCCTTGTAGTCGACGCCGATGGTAATGATACCCATGTTTTCTCCTTGTTAAAG |
| 4R | CGAAGCTTACTTGTCATCGTCGTCCTTGTAGTCGTGGTAATGATACCCATGTTTTCTCCTTGTTAAAG |
| T7ex5.F22 | GGCGTAATACGACTCACTATAG |
| flaguua.R18 | CGAAGCTTACTTGTCGTC |
| 210R | AGCTGCCTCCAACCCCGCCATGTTTTCTCCTTGTT |
| 269R | GCGTAAATAGCCACCCAGCGCGACAGCTGCCTCCAACCCCGC |
| 270R | CGAAGCTTAGCGTAAATAGCCACCCAG |
| dFx.R46 | ACCTAACGCCATGTACCCTTTCGGGGATGCGGAAATCTTTCGATCC |
| dFx.R19 | ACCTAACGCCATGTACCCT |
| eFx.R45 | ACCTAACGCTAATCCCCTTTCGGGGCCGCGGAAATCTTTCGATCC |
| eFx.R18 | ACCTAACGCTAATCCCCT |
| Ini-3'.R20 | TG(Me)GTTGCGGGGGCCGGATT |
| Ini-3'.R38 | TGTTGCGGGGGCCGGATTGAACCGACGATCTTCGGG |
| Ini1-1G-5'.F49 | GTAATACGACTCACTATAGGCGGGGTGGAGCAGCTGGTAGCTCGTCGG |
| Ini cat.R44 | GAACCGACGATCTTCGGGTATGAGCCCGACGAGCTACCAAGCT |
| GLU-5.F49 | GTAATACGACTCACTATAGTCCCCTTCGCTAGAGGCCAGGACACCGC |
| GLUGGU.R44 | TCGAACCCCTGTTACCGCCTTACCAAGGCGGTGTCCTGGGCCTC |
| GLUGUG.R44 | TCGAACCCCTGTTACCGCCTTACCAAGGCGGTGTCCTGGGCCTC |
| GLU-3.R37 | TGGCGTCCCCTAGGGGATTTCGAACCCCTGTTACCGCC |
| Glu-3.R20 | TGGCGTCCCCTAGGGGATTTC |

Table 1. The primers used in this study.

| | Primer extension | Primer extension | 1st PCR | 1st PCR | 2nd PCR | 2nd PCR |
|-------------------------------------|------------------|------------------|-----------|-------------|-----------|------------|
| Sequence | Forward | Reverse | Forward | Reverse | Forward | Reverse |
| Pep270 | T7eSD6M.F44 | 210R | T7ex5.F22 | 269R | T7ex5.F22 | 270R |
| DNAT1 | T7eSD6M.F44 | 1R | T7ex5.F22 | flaguua.R18 | | |
| DNAT2 | T7eSD6M.F44 | 2R | T7ex5.F23 | flaguua.R18 | | |
| DNAT3 | T7eSD6M.F44 | 3R | T7ex5.F22 | flaguua.R18 | | |
| DNAT4 | T7eSD6M.F44 | 4R | T7ex5.F22 | flaguua.R18 | | |
| dfx | Fx5'.F36 | dFx.R46 | T7ex5.F22 | dFx.R19 | | |
| efx | Fx5'.F36 | eFx.R45 | T7ex5.F22 | eFx.R18 | | |
| tRNA ^{Ini} _{CAU} | Ini1-1G-5'.F49 | Ini cat.R44 | T7ex5.F22 | Ini-3'.R38 | T7ex5.F22 | Ini-3'.R20 |
| tRNA ^{GLU2} _{GGU} | GLU-5.F49 | GLUGGU.R44 | T7ex5.F22 | GLU-3.R37 | T7ex5.F23 | Glu-3.R20 |
| tRNA ^{GLU2} _{GGG} | GLU-5.F49 | GLUGUG.R44 | T7ex5.F23 | GLU-3.R37 | T7ex5.F24 | Glu-3.R20 |

Table 2. The combination of primers for PCR reaction used in this study.

2. 6. 2 Preparation of AA-tRNA by flexizyme

42 μ M of tRNA and 42 μ M of flexizyme, (dFx for Ala^S) was heated at 95 °C for 2 min in the presence of 83 mM HEPES-KOH buffer (pH 7.5) and gradually cooled at room temperature for 5 min. 33% vol. of 3M MgCl₂ was added to the mixture, and the reaction mixture was incubated at room temperature for 5 min. After cooling the mixture on ice, the 25% vol. of Ala^S-DNB NMP solution was added. The reaction mixture was further incubated on ice for 30 min. After the incubation, the reaction was quenched by the addition of 400% vol. of 0.3 M NaOAc (pH 5.2). After ethanol precipitation in acidic conditions, the pellet was washed twice with 70% ethanol containing 0.1 M NaOAc (pH 5.2) and once with 70% ethanol, and the resulting pellet was dissolved in 1 mM NaOAc just before adding into translation mixture.

2. 6. 3 in vitro translation

The reconstituted cell-free translation system (42) contain all necessary components for translation except for release factor 1 (RF1). Concentrations of the components were optimized in previous studies as follows (47): 50 mM HEPES-KOH (pH 7.6), 100 mM KOAc, 2 mM GTP, 2 mM ATP, 1 mM CTP, 1 mM UTP, 20 mM creatine phosphate, 12 mM Mg(OAc)₂, 2 mM spermidine, 1 mM DTT, 100 μ M 10-formyl-5,6,7,8-tetrahydrofolic acid, 1.2 μ M ribosome, 2.7 μ M initiation factor 1 (IF1), 0.4 μ M IF2, 1.5 μ M IF3, 10 μ M EF-Tu, 10 μ M EF-Ts, 0.26 μ M EF-G, 0.25 μ M RF2, 0.17 μ M RF3, 0.5 μ M ribosome recycling factor (RRF), 0.6 μ M methionyl-tRNA transfolmylase (MTF), 4 μ g/mL creatine kinase, 3 μ g/mL myokinase, 0.1 μ M pyrophosphatase, 0.1 μ M nucleotide diphosphate kinase, 0.1 μ M T7 RNA polymerase, 0.73 μ M Alanyl-tRNA synthetase (AlaRS), 0.03 μ M ArgRS, 0.38 μ M AsnRS, 0.13 μ M AspRS, 0.02 μ M CysRS, 0.06 μ M GlnRS, 0.23 μ M GluRS, 0.09 μ M GlyRS, 0.02 μ M HisRS, 0.4 μ M IleRS, 0.04 μ M LeuRS, 0.11 μ M LysRS, 0.03 μ M MetRS, 0.68 μ M PheRS, 0.16 μ M ProRS, 0.04 μ M SerRS, 0.09 μ M ThrRS, 0.03 μ M TrpRS, 0.02 μ M TyrRS, 0.02 μ M ValRS, 1.5 mg/mL native *E. coli* tRNA mixture (Roche), 500 μ M each pAAs.

The translation products were analyzed by MALDI-TOF MS or ESI-LC-MS. For the MALDI-TOF MS analysis, the peptide expressed in 2.5 μ L of the translation reaction was desalted by SPE C-tip (Nikkys Technos) twice with SPE-wash solution (aqueous solution containing 4% acetonitrile and 0.5% acetic acid) and then eluted with SPE-elute solution [aqueous solution containing 80% acetonitrile, 0.5% acetic acid, and half-saturated (*R*)-cyano-4-hydroxycinnamic acid]. MALDI-TOF MS measurements were performed using ultrafleXtreme (Bruker Daltonics) under reflect/positive mode and externally calibrated with peptide calibration standard II (Bruker Daltonics).

Chapter 3.

The chemoenzymatic formation of thiazole-containing peptides via thioamide

This chapter is closed for the reason of future publications.

This chapter is closed for the reason of future publications.

Chapter 4.

Uniform affinity-tuning of *N*-methyl-aminoacyl-tRNAs to EF-Tu enhances their multiple incorporation

4. 1. Introduction

EF-Tu is one of the most abundant proteins in the cell and often occupy 6% of the total protein in bacteria (89). EF-Tu binds to AA-tRNA and GTP to form the ternary complex. The complex is accommodated to the ribosome, and then AA-tRNA is placed into the ribosomal A-site. Uhlenbeck *et al.*, have measured these binding affinities (ΔG values) between twenty pAA-tRNAs and EF-Tu, and have revealed that the affinities converge to the near-uniform values (-9.5 to -10.5 kcal/mol) regardless of the species of AA-tRNA (90). This narrow range of affinities works as a threshold in discriminating non-cognately paired AA-tRNAs, such as Glu-tRNA^{Gln}. These uniform affinities are achieved by a compensatory relationship between the two binding regions: the amino acid moiety and the T-stem region of the tRNA (91–93). For example, the EF-Tu binding pocket has the weakest affinities for negatively charged amino acids, such as Asp and Glu at the 3'-end tRNAs. On the other hand, the T-stem regions of their cognate tRNAs (tRNA^{Asp} and tRNA^{Glu}) have stronger EF-Tu affinities compared to other tRNAs to compensate for the weak affinities derived from Asp and Glu (6).

As the genetic code reprogramming rises, numerous kinds of npAA have been installed into the peptides and proteins (34, 35); however, the incorporation efficiency of npAAs often drops compared to the pAA incorporation. Researchers have estimated that the cause of the diminished incorporation of npAAs could be attributed to the insufficient affinities between EF-Tu and npAA-tRNAs (3), and thus they have enhanced them to improve npAA incorporations as described in Chapter 1 (61, 64–66, 94, 95). Particularly, Katoh *et al.*, have reported that substituting the tRNA^{Pro} T-stem with that of tRNA^{Glu} is effective to improve the EF-Tu affinities, resulting in the enhanced incorporation efficiencies of D-, β -, or γ -amino acids (54–57, 62, 96).

Besides the above npAAs, *N*-methyl amino acids (^{Me}AAs) are a useful motif in the peptide products, but they remained as incompatible substrates for the translation system. The incorporation efficiencies of ten ^{Me}AAs (^{Me}V, ^{Me}L, ^{Me}I, ^{Me}N, ^{Me}D, ^{Me}E, ^{Me}R, ^{Me}K, ^{Me}Q, and ^{Me}W) dropped less than 12% compared to their pAA controls, while other nine ^{Me}AAs (^{Me}G, ^{Me}A, ^{Me}S, ^{Me}T, ^{Me}C, ^{Me}M, ^{Me}F, ^{Me}Y, and ^{Me}H) showed moderate or comparable yields (>20% relative to each pAA control) (52). When the multiple ^{Me}AA residues appear in the nascent peptide chain sequence, the yield and fidelity decreased. In addition, the consecutive incorporation of ^{Me}AAs is further less efficient. Thus, there remains an important challenge to incorporate not only a greater number of distinct ^{Me}AAs but also consecutively into the peptide chain.

Here in this research, Dr. Iwane and I aimed to improve the incorporation efficiencies of ^{Me}AAs by tuning the affinity between ^{Me}AA-tRNA and EF-Tu. Dr. Iwane estimated that the interaction

between ^{Me}AA-tRNAs and EF-Tu could be hampered by the *N*-methyl modification. Dr. Iwane also hypothesized that these insufficient affinities between EF-Tu and ^{Me}AA-tRNAs could cause the reduced incorporation efficiency of ^{Me}AA (Figure 51). To enhance EF-Tu affinities of ^{Me}AA-tRNAs, Dr. Iwane designed three new T-stem sequences. Indeed, Dr. Iwane demonstrated that the incorporation efficiencies of ^{Me}AAs could be improved by substituting the T-stem with the designer one. Taking the advantage of Dr. Iwane's work, I aimed to express the exotic peptides containing multiple ^{Me}AAs in a single sequence. I demonstrated that the incorporation of nine ^{Me}AAs into both linear and macrocyclic scaffold peptides.

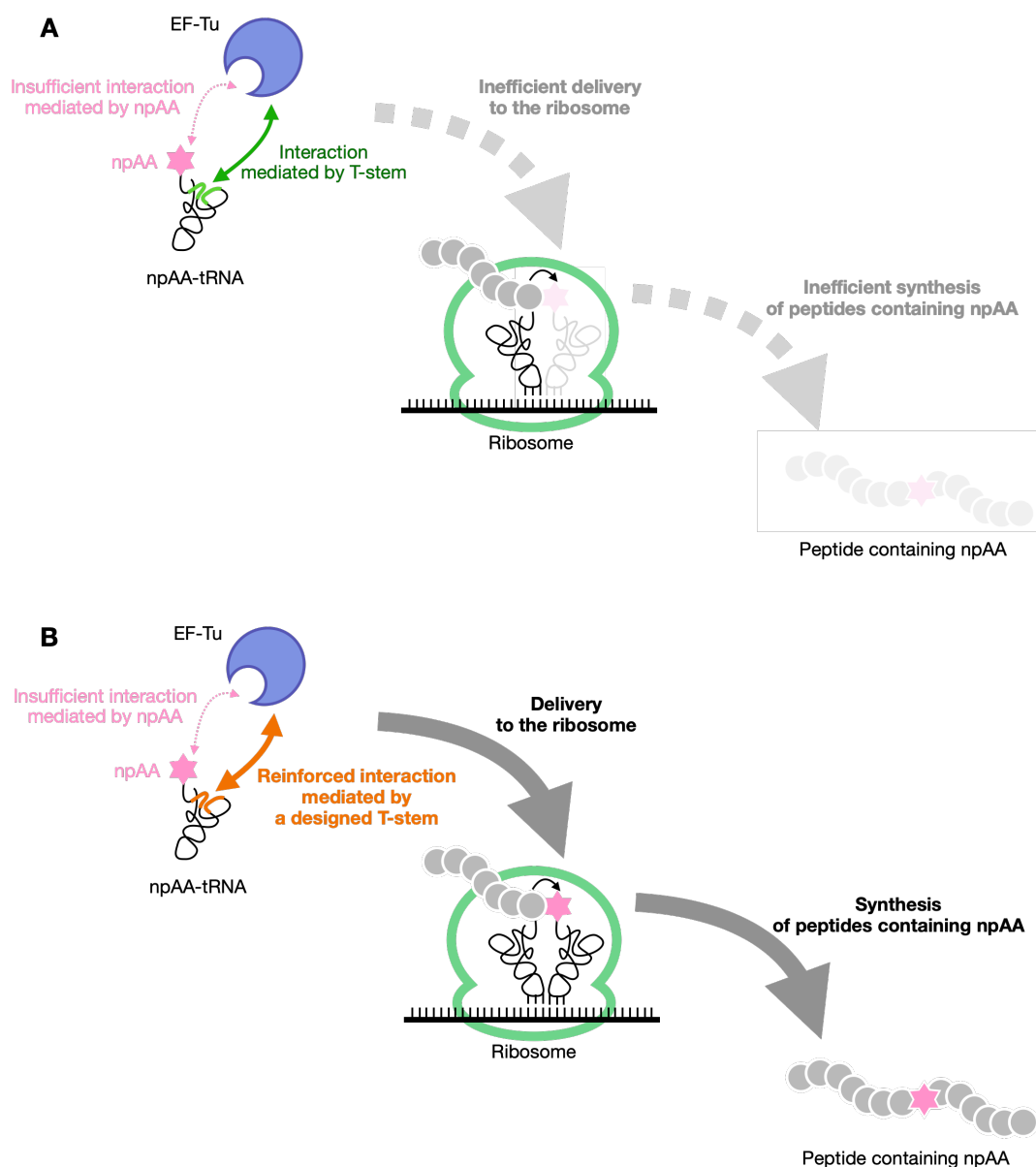


Figure 51. Schematic illustration of this study. (A) Insufficient affinity caused by nonstandard structure of npAA would cause the diminished delivery and translation. (B) Engineered T-stem would reinforce the affinity between npAA-tRNA and EF-Tu, resulting in the recovery of translation incorporating npAA.

4. 2. Dr. Iwane's work

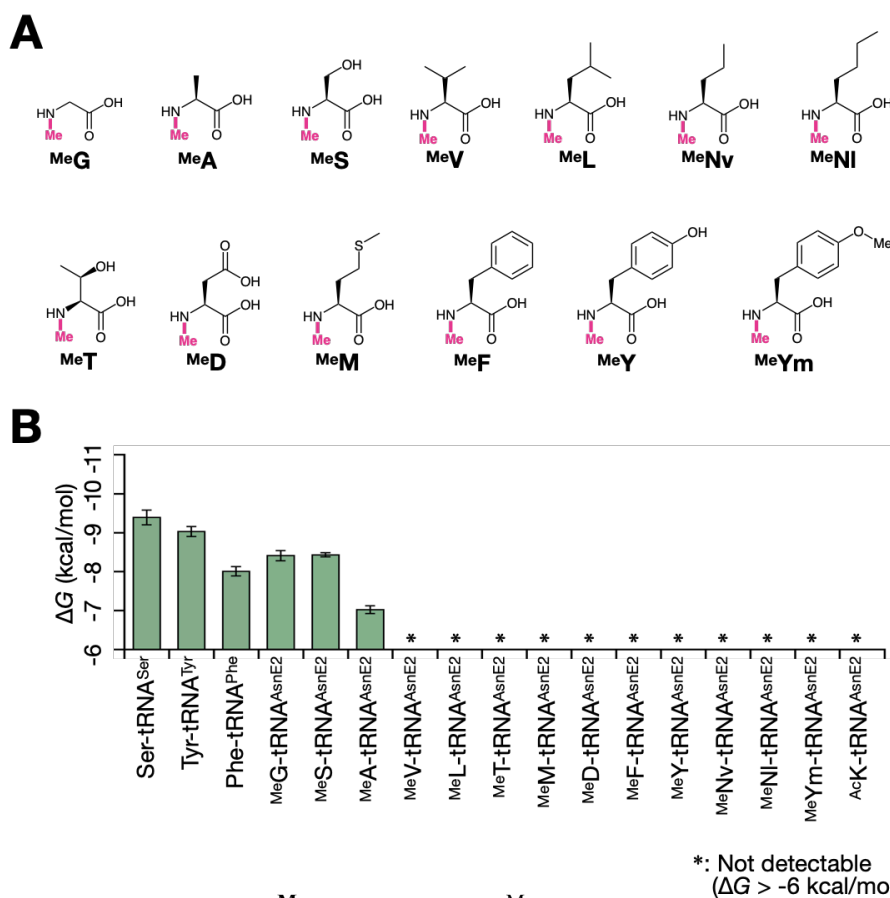


Figure 52. EF-Tu affinities of ^{Me}AA-tRNA. (A) ^{Me}AAs used in this study. (B) EF-Tu affinities of pAA-tRNA and ^{Me}AA-tRNAs. Reprinted with permission from "Uniform affinity-tuning of *N*-methyl-aminoacyl-tRNAs to EF-Tu enhances their multiple incorporation" *Nucleic Acids Res.* <https://doi.org/10.1093/nar/gkab288> Copyright: Oxford University Press.

The affinities between D-Tyr-tRNA and EF-Tu has been reported and indeed it is 250-fold weaker than L-Tyr control (3), but the affinities between EF-Tu and ^{Me}AA-tRNAs had not been reported. Thus, at first, Dr. Iwane measured the affinities between EF-Tu and various kinds of ^{Me}AA-RNAs by RNase A protection assay (97). In this assay, tRNA^{AsnE2}_{GAC} was used because that tRNA has been conventionally used in the Suga group (47). Thirteen kinds of ^{Me}AA used in this study [^{Me}G, ^{Me}A, ^{Me}S, ^{Me}T, ^{Me}F, ^{Me}Y, ^{Me}V, ^{Me}L, ^{Me}M, ^{Me}D, ^{Me}Nv (*N*-methylnorvaline), ^{Me}NI (*N*-methylnorleucine), and ^{Me}Ym (*N*-methyl-*p*-methoxyphenylalanine), Figure 52A] were esterified on tRNA^{AsnE2}_{GAC} by flexizyme (47). As the reference of the EF-Tu affinities, three canonical pAA-tRNAs (Phe-tRNA^{Phe}_{GAA}, Tyr-tRNA^{Tyr}_{GUA}, and Ser-tRNA^{Ser}_{CGA}) were used, and they exhibited certain EF-Tu affinities, ranging from -8.0 to -9.4 kcal/mol. On the other hand, most ^{Me}AA-tRNAs showed undetectable EF-Tu affinities (ΔG > -6 kcal/mol) (Figure 52B), suggesting that the *N*-methylation could hamper the interaction against EF-Tu. This can be explained by the cocrystal structure of the ternary complex (*Thermus aquaticus* EF-Tu·*E coli* Phe-tRNA^{Phe}·GTP, PDB: 5AFI).

The amino group of Phe at 3'-end of tRNA is stabilized by a hydrogen bond with Asn285 of EF-Tu (91). This hydrogen bond seems to define the orientation of Phe in the binding pocket. The amino group of Phe is tightly surrounded by the pocket allowing no space for additional methylation. (Figure 53) Therefore, a steric clash between the EF-Tu pocket and an additional *N*-methylation could occur and disrupt the hydrogen bond formation, decreasing the affinities in ^{Me}AA-tRNA^{AsnE2}_{GAC}. Among thirteen ^{Me}AA-tRNAs, three exceptions, ^{Me}G-tRNA^{AsnE2}_{GAC} (−8.4 kcal/mol), ^{Me}S-tRNA^{AsnE2}_{GAC} (−8.4 kcal/mol), and ^{Me}A-tRNA^{AsnE2}_{GAC} (−7.0 kcal/mol) showed EF-Tu affinities, probably because their relatively small sidechain may alleviate a steric clash against the EF-Tu pocket.

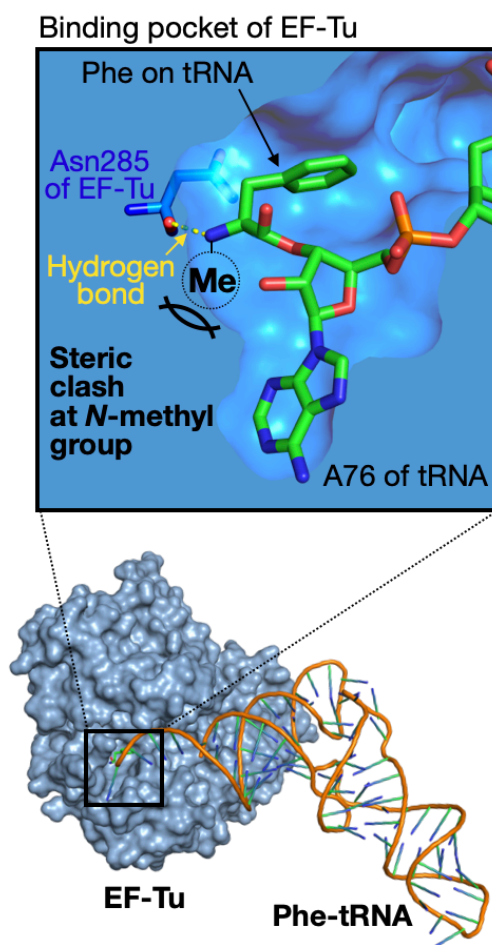


Figure 53. Cocrystal structure of the ternary complex. Reprinted with permission from "Uniform affinity-tuning of *N*-methyl-aminoacyl-tRNAs to EF-Tu enhances their multiple incorporation" *Nucleic Acids Res.* <https://doi.org/10.1093/nar/gkab288> Copyright: Oxford University Press.

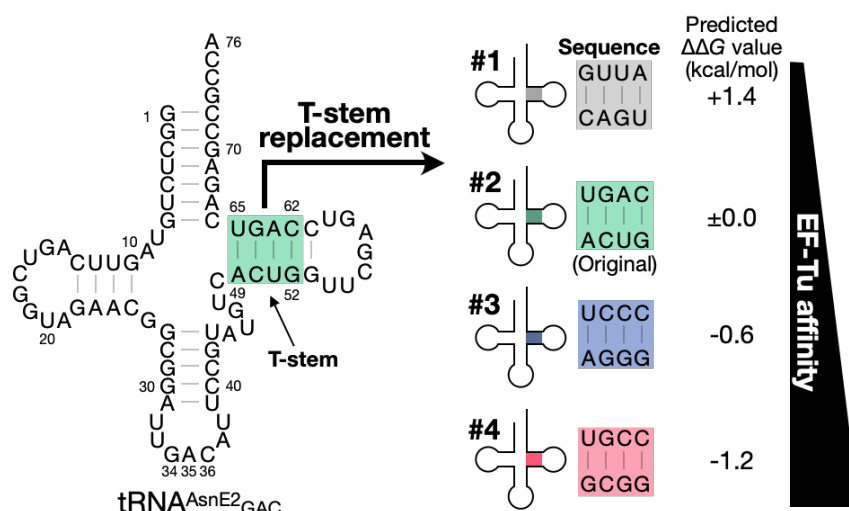


Figure 54. Secondary structure of tRNA and designed T-stem sequences. Reprinted with permission from "Uniform affinity-tuning of *N*-methyl-aminoacyl-tRNAs to EF-Tu enhances their multiple incorporation" *Nucleic Acids Res.* <https://doi.org/10.1093/nar/gkab288> Copyright: Oxford University Press.

To improve these affinities between EF-Tu and various ^{Me}AA-tRNAs, Dr. Iwane decided to substitute the T-stem sequence of tRNA. To this end, Dr. Iwane utilized the research conducted by Uhlenbeck. The Uhlenbeck group had intensively investigated the effect of a single base-pair substitution at the tRNA T-stem region (residues at 49–52 and 62–65, Figure 54) and had revealed that each base pair at the T-stem contributes the whole EF-Tu affinity independently (98). For example, when the A49-U65 base pair of the original tRNA^{AsnE2} is substituted with the C49-G65 base pair, the $\Delta\Delta G$ value (relative ΔG value compared to the original tRNA^{AsnE2}) is predicted to be +0.5 kcal/mol weaker according to this Uhlenbeck's report. Based on this knowledge, Dr. Iwane designed three new T-stem sequences (Figure 54), whose EF-Tu affinities were expected to increase as the T-stem number increases. In this order, the original T-stem of tRNA^{AsnE2} was renamed as #2. The T-stem #1 should have a weaker binding affinity ($\Delta\Delta G$: +0.6 kcal/mol compared to #2), while #3 and #4 are designed to have stronger affinities ($\Delta\Delta G$: -0.6 and -1.2 kcal/mol respectively). The tRNA whose T-stem was substituted with #X T-stem is denoted as tRNA#X hereafter.

The feasibility of these designed T-stem was evaluated using ^{Me}G-tRNA_{GAC}#1–4. The affinity of ^{Me}G-tRNA_{GAC}#2 (the original sequence) was $\Delta G = -8.4$ kcal/mol, and the substitution with #3 or #4 T-stem reinforced the affinities ($\Delta G = -9.3$ kcal/mol for #3, and -9.7 kcal/mol for #4). Not only the reinforcement, but the #1 T-stem also showed the weakened affinity ($\Delta G = -7.0$ kcal/mol).

Next, Dr. Iwane tested four kinds of $^{\text{Me}}$ AA-tRNA^{AsnE2}_{GACS} ($^{\text{Me}}$ G, $^{\text{Me}}$ S, $^{\text{Me}}$ A, and $^{\text{Me}}$ L) in the *in vitro* translation using the FIT system to elucidate the relationship between the EF-Tu affinities of $^{\text{Me}}$ AA-tRNAs and their incorporation efficiencies in the translation system. The model peptide P1 containing a single $^{\text{Me}}$ AAAs was expressed by a genetic code reprogramming technology, the FIT system. In P1, GUC (Val) codon was reprogrammed to $^{\text{Me}}$ AAAs supplementing one of the $^{\text{Me}}$ AA-tRNA^{AsnE2}_{GAC} molecules. The synthesized P1 was analyzed by MALDI-TOF MS to determine the incorporation fidelity.

The model peptides P1 containing one of $^{\text{Me}}$ AAAs ($^{\text{Me}}$ G, $^{\text{Me}}$ S, $^{\text{Me}}$ A, and $^{\text{Me}}$ L) were expressed in the FIT system containing the corresponding $^{\text{Me}}$ AA-tRNA^{AsnE2}_{GAC} with a series of T-stem (#1–4). Dr. Iwane observed the desired peptide P1- $^{\text{Me}}$ AA as the sole product only when $^{\text{Me}}$ AA-tRNAs have

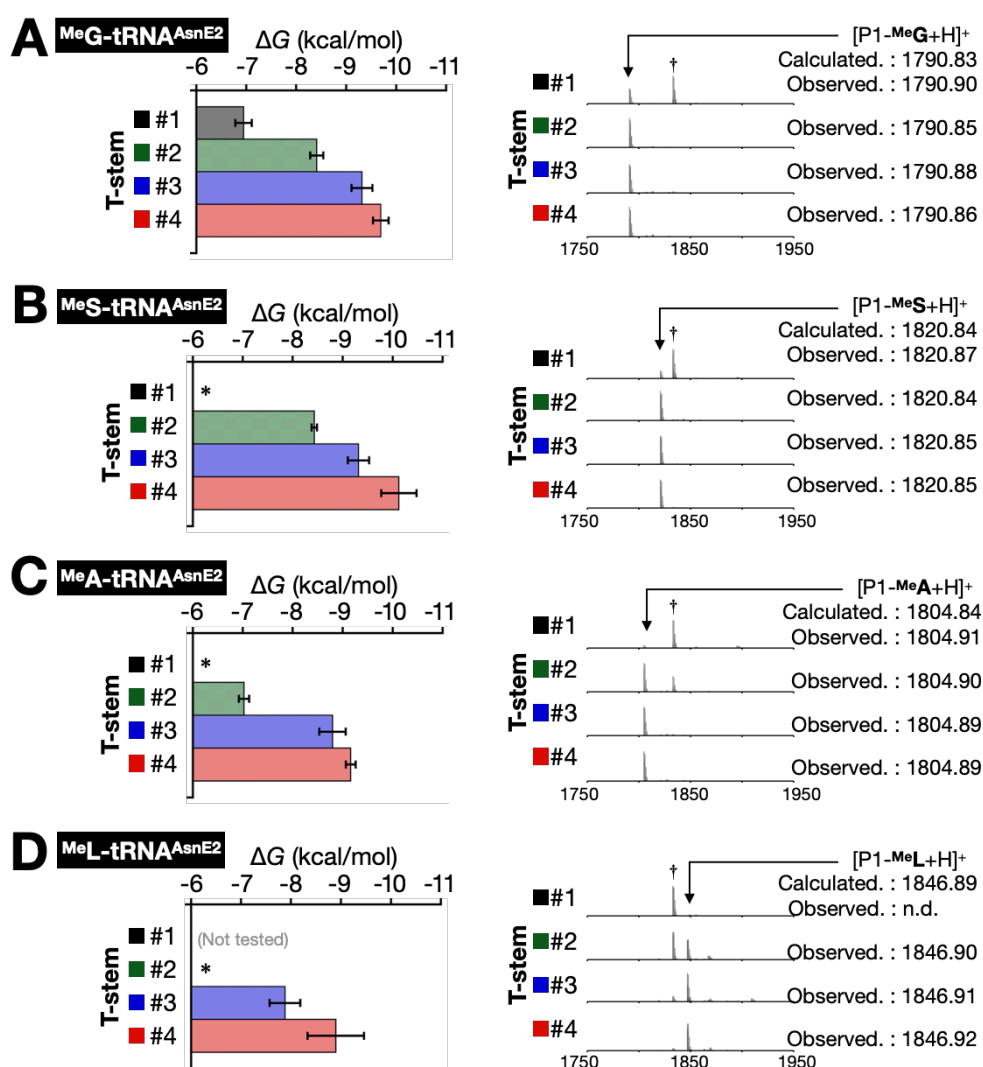


Figure 55. The EF-Tu affinities and translation accuracy determined by MALDI-TOF MS. Left panels show the affinities with a series of T-stem sequences. Right panels are MALDI-TOF mass spectra corresponding to P1- $^{\text{Me}}$ AA. †: Ile-misincorporation at Val codon instead of $^{\text{Me}}$ AA. Reprinted with permission from "Uniform affinity-tuning of *N*-methyl-aminoacyl-tRNAs to EF-Tu enhances their multiple incorporation" *Nucleic Acids Res.* <https://doi.org/10.1093/nar/gkab288> Copyright: Oxford University Press.

sufficient affinities for EF-Tu (Figure 55 A #2–4, B #2–4, C #3–4, and D #4). In contrast, when the affinity of ^{Me}AA-tRNA for EF-Tu was insufficient or undetectable, the expression fidelity of the desired P1-^{Me}AA was poor, giving a peak of P1-Ile (Figure 55A #1, B #1, C #1–2, and D #1–3). It should be noted that ^{Me}L was reported as a very poor substrate (52), but P1-^{Me}L was cleanly expressed by using ^{Me}L-tRNA_{GAC}#4 (Figure 55 D #4). Collectively, the above results clearly demonstrated that the reprogramming fidelity can be significantly improved by reinforcing the affinity of ^{Me}AA-tRNA to EF-Tu. In addition, Dr. Iwane measured nine ^{Me}AA-tRNAs with T-stem variant. The measured ΔG value is summarized in Figure 56.

| | #1 | #2 | #3 | #4 |
|-------|----------------------|--------------------------------------|--------------------------------------|--------------------------------------|
| MeG | -6.95 (± 0.16) | -8.41 (± 0.13) | -9.32 (± 0.21) | -9.69 (± 0.16) |
| MeS | * | -8.43 (± 0.05) | -9.32 (± 0.21) | -10.12 (± 0.35) |
| MeA | * | -7.03 (± 0.10) | -8.80 (± 0.26) | -9.16 (± 0.10) |
| MeF | - | * | -7.90 (± 0.02) | -9.01 (± 0.15) |
| MeY | - | * | -8.11 (± 0.04) | -9.37 (± 0.15) |
| MeNva | - | * | -8.26 (± 0.06) | -8.55 (± 0.08) |
| MeV | - | * | -7.42 (± 0.10) | -8.39 (± 0.09) |
| MeNle | - | * | -7.79 (± 0.10) | -8.58 (± 0.08) |
| MeYme | - | * | -7.72 (± 0.09) | -8.64 (± 0.11) |

Figure 56. The EF-Tu affinities of ^{Me}AA-tRNA with T-stem variants. The bold fonts indicate that the combination between the T-stem and ^{Me}AA is selected as uniform set in the next experiment.

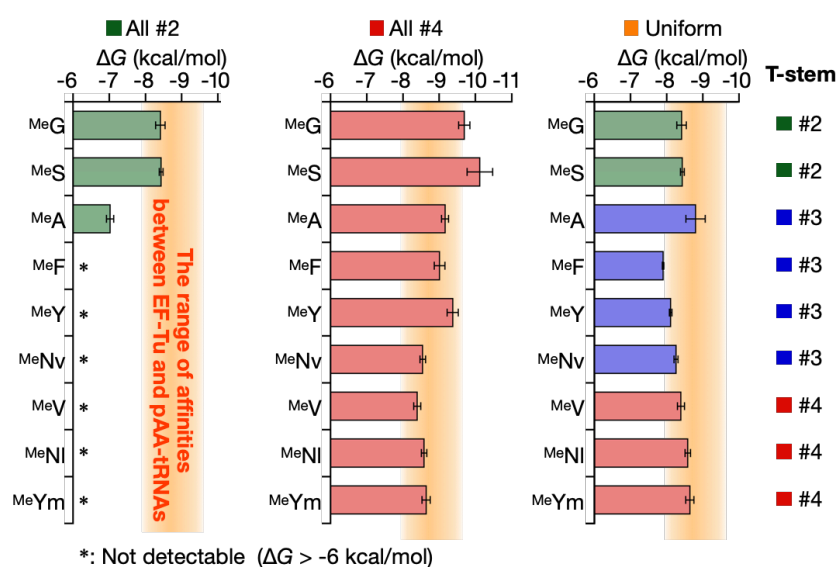
4. 3. My work

Here, in my PhD thesis, I conducted the multiple incorporation of ^{Me}AAs into linear and macrocyclic scaffolds by employing the T-stem set devised by Dr. Iwane. In addition, I carried out the expression of a macrocyclic peptide containing nine ^{Me}AAs.

4. 4. Results and Discussion

4. 4. 1. The expression of a linear peptide containing nine ^{Me}AAs

To express a linear peptide containing nine ^{Me}AAs the genetic code was reprogrammed with nine ^{Me}AAs as shown in Figure 57. In this genetic code, five pAAs (Phe, Leu, Ile, Val, and Ala) were excluded, and the vacant codon boxes were artificially divided into nine codon boxes in the FIT system (99). The reprogramming was carried out by supplementing ^{Me}G-tRNA_{CAA}#X, ^{Me}S-tRNA_{GAG}#X, ^{Me}A-tRNA_{CGC}#X, ^{Me}Nv-tRNA_{CAC}#X, ^{Me}Y-tRNA_{GAU}#X, ^{Me}F-tRNA_{GGC}#X, ^{Me}Ym-tRNA_{UAA}#X, ^{Me}Ni-tRNA_{UAG}#X, and ^{Me}Ym-tRNA_{UGA}#X.



| | | 2nd | | | |
|-----|---|------|-----|------|-----|
| | | U | C | A | G |
| 1st | U | MeYm | Ser | Tyr | Cys |
| | | MeG | | Stop | Trp |
| | C | MeS | Pro | His | Arg |
| | | MeNi | | Gln | |
| | A | MeY | Thr | Asn | Ser |
| | | Met | | Lys | Arg |
| | G | MeV | MeF | Asp | Gly |
| | | MeNv | MeA | Glu | |

Figure 57. The EF-Tu affinities of selected T-stem set. Reprinted with permission from "Uniform affinity-tuning of *N*-methyl-aminoacyl-tRNAs to EF-Tu enhances their multiple incorporation" *Nucleic Acids Res.* <https://doi.org/10.1093/nar/gkab288> Copyright: Oxford University Press.

tRNA_{GAA}#X, ^{Me}Nl-tRNA_{CAG}#X, and ^{Me}V-tRNA_{GAC}#X and excluding Phe, Leu, Ile, Val, and Ala from the FIT system. For the T-stem sequence, I prepared three sets of T-stem combinations: all-#2, all-#4, and the uniform set (Figure 57). In the all-#2 set, all ^{Me}AAs were charged on tRNA#2 whose T-stems were not engineered, and thus most of their EF-Tu affinities were supposed to be not sufficient. In the all-#4 set, all nine ^{Me}AA-tRNAs have the strongest #4 T-stem to simply maximize their EF-Tu affinities. On the other hand, the uniform set employs the best T-stem based on the affinities. By using this T-stem set, the EF-Tu affinities of ^{Me}AA-tRNAs should fall into -7.9 to -8.8 kcal/mol, which is comparable with those of pAA-tRNAs (-8.0 to -9.4 kcal/mol, Figure 52B). In addition, the concentrations of each AA-tRNA were adjusted to 10 μ M considering the aminoacylation efficiency.

The model peptide P2, which contains nine ^{Me}AAs and fifteen pAAs, was designed and expressed in the FIT system supplemented with a tRNA set (all-#2, all-#4, or uniform set) (Figure 58). The synthesized P2 was conventionally purified by anti-FLAG M2 affinity agarose gel through its C-terminal FLAG tag (Asp-Tyr-Lys-Asp-Asp-Asp-Asp-Lys) and analyzed by MALDI-TOF MS to determine their incorporation fidelity by the genetic code reprogramming (Figure 58). The use of the all-#2 set generated the desired P2 along with byproducts that have -28 and -14 m/z . In contrast, the all-#4 set did not generate a peak corresponding to P2, and instead P2* with +2 m/z value compared to the desired P2. In addition, byproduct series with -14, +14, or +16 m/z difference relative to P2* were also observed. Not only these byproducts but also several unidentified peptide byproducts were observed in around $m/z = 2500$ region, probably generated by unintended truncation during the translation with the all-#2 or all-#4 set (Figure 58). In contrast, when the uniform set was tested, the desired peptide P2 was correctly synthesized as a nearly sole product. Even though a very small -14 m/z byproduct was observed along with P2, its intensity was drastically reduced compared to other T-stem sets. The wider m/z mass spectrum showed that the truncation also seemed to be suppressed. This successful synthesis using the uniform T-stem set indicates that appropriately tuning to the uniform affinities is effective for the accurate synthesis of the *N*-methyl-peptide.

All-#2 (green bar):

- Unidentified byproduct (truncation)
- $[P2+H]^+$ Calculated.: 4019.97, Observed.: 4019.91

All-#4 (red bar):

- Unidentified byproduct (truncation)
- $[P2^*+H]^+$ Observed.: 4021.97
- $[P2+H]^+$ Calculated.: 4019.97, Observed.: 4019.89

Uniform (orange bar):

- $[P2+H]^+$ Calculated.: 4019.97, Observed.: 4019.89

PAA-control (black bar):

- $[P2-pAA+2H]^+$
- $[P2-pAA+H]^+$ Calculated.: 3819.92, Observed.: 3819.89

Zoomed-in regions (3760-4100 m/z):

- All-#2:** $[P2+H]^+$ Calculated.: 4019.97, Observed.: 4019.91; P2-14, P2-28
- All-#4:** $[P2^*+H]^+$ Observed.: 4021.97; $P2^*+14$ to $P2^*+16$, $P2^*+28$ to $P2^*+30$, $P2^*+44$ to $P2^*+46$, $P2^*+60$ or more
- Uniform:** $[P2+H]^+$ Calculated.: 4019.97, Observed.: 4019.89
- PAA-control:** $[P2-pAA+H]^+$ Calculated.: 3819.92, Observed.: 3819.89

59

These translation failures observed in the all-#2 set or all-#4 set could be attributed to the imbalanced EF-Tu affinities. For instance, -14 series for the all-#2 set and -14, +14, or +16 series for the all-#4 set might be generated by the misincorporation events during the translation. For example, there could be a possibility that ^{Me}Nl-tRNA_{CAG}#2 has relatively weaker EF-Tu affinities than others in the all-#2 set. Thereby, the CUG codon, which is originally assigned to ^{Me}Nl, might be inefficiently decoded by ^{Me}Nl-tRNA_{CAG}#2, and then it might cause the misincorporation by ^{Me}Nv-tRNA_{CAC}#2 because two nucleotides are identical in their anticodons (CAG and CAC). This misincorporation of ^{Me}Nv instead of ^{Me}Nl could result in a -14 *m/z* difference. Conversely, a misincorporation of ^{Me}Nl instead of ^{Me}Nv could result in a +14 *m/z* difference. The +16 *m/z* difference misincorporation of Thr (ACG codon) instead of ^{Me}A (assigned to CGG codon) could result in +16 *m/z* difference, and P2* itself with +2 *m/z* difference from P2 could be attributed to the combination of -14 and +16 *m/z*.

These translation failures when using the all-#2 set can be attributed to the insufficient affinities of the ^{Me}AA-tRNAs decreasing the fidelity of the multiple ^{Me}AA incorporation, as is the case with the single incorporation. On the other hand, the inaccurate translation observed for the all-#4 set suggests that unnecessary reinforcements of ^{Me}AA-tRNA affinity to EF-Tu can cause a disorder in the translation. This can be explained by the slow release of AA-tRNA from EF-Tu to the ribosomal A site as previously reported (100).

Besides these byproducts, the truncation event observed in the all-#2 and #4 sets was also attributed to the inefficient delivery of ^{Me}AA-tRNAs or inefficient release of ^{Me}AA-tRNAs from the ternary complex. The uniform tuning methodology could successfully suppress these translation failures.

I also quantified the expression level of P2 by means of radioactive isotope ¹⁴C. The peptide was expressed in the FIT system contains 50 μM of [¹⁴C]-Asp instead of non-labeled Asp. After 30 min translation reaction, the reaction mixture was subjected to tricine-SDS-PAGE to separate free [¹⁴C]-Asp and the expressed peptide that contains [¹⁴C]-Asp in the C-terminal FLAG tag (Asp-Tyr-Lys-Asp-Asp-Asp-Lys). The expression level of the peptide was determined by autoradiography.

In the case of the all-#2 or all-#4 set, only one band was observed in the tricine-SDS-PAGE. Judging from the MALDI-TOF MS, these translation reactions generated various kinds of peptides including the desired P2 and its byproducts, and thus the quantification of P2 was not available. On the contrary, in the case of the uniform set, almost a single peak was observed in the MALDI-TOF MS, and the expression level of P2 turned out to be 0.48 μM. This amount of peptide is enough for

practical application such as the RaPID system since it was possible to discover *de novo* macrocyclic peptide binders containing cyclic β -amino acids, one of whose expression level was about 0.7 μM (57).

4. 4. 2. The expression of a macrocyclic peptide containing nine ^{Me}AAs

As the highlight to demonstrate the potential of this methodology, a macrocyclic peptide containing multiple ^{Me}AAs was expressed. The model macrocyclic peptide P3 was designed as shown in Figure 59, which was composed of 9 kinds of ^{Me}AAs, 13 kinds of pAAs, and *N*-chloroacetyl-L-tyrosine (^{ClAc}Y) at the N-terminal position enabling spontaneous thioether-linked macrocyclization with a downstream Cys (101). The N-terminal ^{ClAc}Y was installed into the peptide by omitting Met and supplementing ^{ClAc}Y-tRNA^{Ini}. Nine ^{Me}AAs were assigned in the genetic code as previously described with the uniform T-stem set. In total, six codon boxes (Phe, Leu, Ile, Met, Val, and Ala) were reprogrammed to npAAs in this experiment.

The expressed macrocyclic P3 was analyzed by MALDI-TOF MS (Figure 59) and tricine-SDS-PAGE similarly to P2. P3 was accurately expressed with an expression level of 0.37 μM (1.5 ng/ μL).

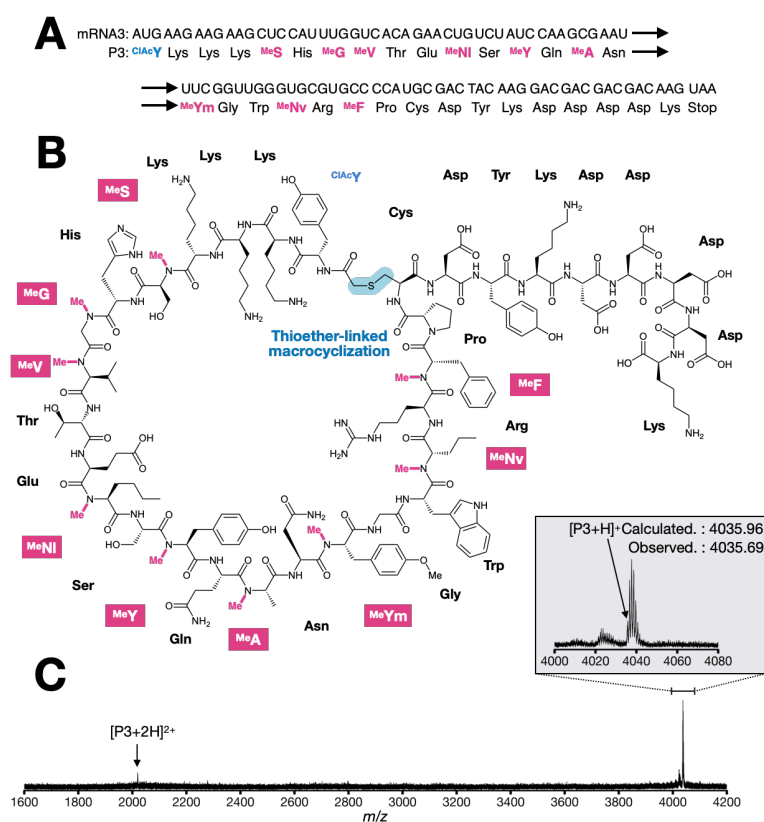


Figure 59. The expression of P3 and MALDI-TOF mass spectra. Reprinted with permission from "Uniform affinity-tuning of *N*-methyl-aminoacyl-tRNAs to EF-Tu enhances their multiple incorporation" *Nucleic Acids Res.* <https://doi.org/10.1093/nar/gkab288> Copyright: Oxford University Press.

4. 4. Conclusion

Here, Dr. Iwane and I have demonstrated a new methodology to achieve the ribosomal synthesis of nonstandard peptides containing a rich variety of ^{Me}AAs. This study attributed the previously observed inefficient incorporation of ^{Me}AAs to the impaired EF-Tu-mediated accommodation of the ^{Me}AA-tRNAs. Dr. Iwane's demonstration clearly showed that most ^{Me}AA-tRNAs have weaker EF-Tu affinities than pAA-tRNAs, and these insufficient affinities resulted in the failure of the *in vitro* translation with the genetic code reprogramming using ^{Me}AAs. In addition, Dr. Iwane designed three T-stem sequences, that serve as a substitution candidate to tune the EF-Tu affinities. Following this concept, I demonstrated that the tRNA set, whose EF-Tu affinities were uniformly tuned, was effective to express a peptide containing multiple ^{Me}AAs. This affinity-tuning strategy dramatically improves the expression of peptides containing multiple ^{Me}AAs with high fidelity and expression level, even though some ^{Me}AAs are consecutively and/or alternately placed in a single sequence. Overall, 24 distinct building blocks, fifteen pAAs and nine ^{Me}AAs (linear P2), or fourteen pAAs, nine ^{Me}AAs, and ^{ClAc}Y (macrocylic P3) were available for expressing *N*-methyl-peptides consisting of these amino acids.

The present data have exceeded the previous record of the genetic code reprogramming achieved to place 23 building blocks consisting of 20 pAAs and 3 npAAs (99, 102). The knowledge established in this work enables us to further expand the utility of exotic amino acids to the translation chemistry world. Particularly when the knowledge is integrated with the RaPID system, it will allow us to rapid and high-throughput screening of binding peptides to target proteins of interest using a massive library of randomized macrocylic peptides, yielding therapeutically valuable peptides with improved pharmacological properties.

4. 5. Experimental detail

4. 5. 1 Preparation of nucleotides (DNA template, tRNA, flexizyme)

DNA templates, tRNAs, eFx, and dFx were prepared following section 2. 6. 1.

The primers and their combinations are listed in Table 5, 6, and 7.

| Name | Sequence |
|-----------|--|
| Primer-1 | 5' - TAATACGACTCACTATAGCCCGATAGCTCAGTCGGTAGAGCAGGGGACTGAAATCCCGTGTCC - 3' |
| Primer-2 | 5' - GTGCCCCGACTCGGAATCGAACCAAGGACACGGGGATTTC - 3' |
| Primer-3 | 5' - GCGTAATACGACTCACTATAG - 3' |
| Primer-4 | 5' - GG(Me)TGCCCGGACTCGG - 3' |
| Primer-5 | 5' - TG(Me)GTGCCCCGACTCGG - 3' |
| Primer-6 | 5' - GCGTAATACGACTCACTATAGGTGGGTTCCCGAGCGGCCAAGGGAGCAGACTGTAATCTGCCG - 3' |
| Primer-7 | 5' - GGTGGTGGGGGAAGGATTCGAACCTTCGAAGTCTGTGACGGCAGATTACAGTCTG - 3' |
| Primer-8 | 5' - GG(Me)TGGTGGGGGAAGGAT - 3' |
| Primer-9 | 5' - TG(Me)GTGGTGGGGGAAGGAT - 3' |
| Primer-10 | 5' - GCGTAATACGACTCACTATAGGAGAGATGCCCGAGCGGCTGAACGGACCGGTCTCGAAACCCGGAG - 3' |
| Primer-11 | 5' - GCGGAGAGAGGGGATTTGAACCCCGGTAGAGTTGCCCTACTCCGGTTTTCGAGACC - 3' |
| Primer-12 | 5' - GG(Me)CGGAGAGAGGGGGA - 3' |
| Primer-13 | 5' - TG(Me)GCGGAGAGAGGGGGA - 3' |
| Primer-14 | 5' - GTAATACGACTCACTATAGGCTCTGTAGTTCACTCGGTAGAACGGCGG - 3' |
| Primer-15 | 5' - GCGGCTCTGCAATGACTCGAACACTGGACATACGGAATGTCAATCCGCCGTTCTACCG - 3' |
| Primer-16 | 5' - GG(Me)CGGCTCTGCAATG - 3' |
| Primer-17 | 5' - GCGGCTCTGACTGGACTCGAACAGTGACATACGGAATGTCAATCCGCCGTTCTACCG - 3' |
| Primer-18 | 5' - GG(Me)CGGCTCTGACTGG - 3' |
| Primer-19 | 5' - GCGGCTCTGAGGGGACTCGAACCCCTGACATACGGAATGTCAATCCGCCGTTCTACCG - 3' |
| Primer-20 | 5' - GG(Me)CGGCTCTGAGGGG - 3' |
| Primer-21 | 5' - GCGGCTCTGACGGGACTCGAACCCGCGACATACGGAATGTCAATCCGCCGTTCTACCG - 3' |
| Primer-22 | 5' - GG(Me)CGGCTCTGACGGG - 3' |
| Primer-23 | 5' - TG(Me)GCGGCTCTGCAATG - 3' |
| Primer-24 | 5' - TG(Me)GCGGCTCTGACTGG - 3' |
| Primer-25 | 5' - TG(Me)GCGGCTCTGAGGGG - 3' |
| Primer-26 | 5' - TG(Me)GCGGCTCTGACGGG - 3' |
| Primer-27 | 5' - GTAATACGACTCACTATAGGCTCTGTAGTTCACTCGGAAGAACGGCGG - 3' |
| Primer-28 | 5' - GCGGCTCTGACTGGACTCGAACAGTGACATACGGATTTTCAGTCCGCCGTTCTTCCG - 3' |
| Primer-29 | 5' - GCGGCTCTGAGGGGACTCGAACCCCTGACATACGGATTTTCAGTCCGCCGTTCTTCCG - 3' |
| Primer-30 | 5' - GCGGCTCTGACGGGACTCGAACCCGCGACATACGGATTTTCAGTCCGCCGTTCTTCCG - 3' |
| Primer-31 | 5' - GCGGCTCTGACTGGACTCGAACAGTGACATACGGATTTTCAGTCCGCCGTTCTTCCG - 3' |
| Primer-32 | 5' - GCGGCTCTGACGGGACTCGAACCCGCGACATACGGATTTTCAGTCCGCCGTTCTTCCG - 3' |
| Primer-33 | 5' - GCGGCTCTGACTGGACTCGAACAGTGACATACGGAACTCAATCCGCCGTTCTTCCG - 3' |
| Primer-34 | 5' - GCGGCTCTGACGGGACTCGAACCCGCGACATACGGAACTCAATCCGCCGTTCTTCCG - 3' |
| Primer-35 | 5' - GCGGCTCTGACTGGACTCGAACAGTGACATACGGAACTCAATCCGCCGTTCTTCCG - 3' |
| Primer-36 | 5' - GCGGCTCTGACGGGACTCGAACCCGCGACATACGGAACTCAATCCGCCGTTCTTCCG - 3' |
| Primer-37 | 5' - GCGGCTCTGACTGGACTCGAACAGTGACATACGGATTATCAGTCCGCCGTTCTTCCG - 3' |
| Primer-38 | 5' - GCGGCTCTGAGGGGACTCGAACCCCTGACATACGGATTATCAGTCCGCCGTTCTTCCG - 3' |
| Primer-39 | 5' - GCGGCTCTGACGGGACTCGAACCCGCGACATACGGATTATCAGTCCGCCGTTCTTCCG - 3' |
| Primer-40 | 5' - GCGGCTCTGACTGGACTCGAACAGTGACATACGGAGTGTGAGTCCGCCGTTCTTCCG - 3' |
| Primer-41 | 5' - GCGGCTCTGAGGGGACTCGAACCCCTGACATACGGAGTGTGAGTCCGCCGTTCTTCCG - 3' |
| Primer-42 | 5' - GCGGCTCTGACGGGACTCGAACCCGCGACATACGGAGTGTGAGTCCGCCGTTCTTCCG - 3' |
| Primer-43 | 5' - GCGGCTCTGACTGGACTCGAACAGTGACATACGGACTGCCAGTCCGCCGTTCTTCCG - 3' |
| Primer-44 | 5' - GCGGCTCTGAGGGGACTCGAACCCCTGACATACGGACTGCCAGTCCGCCGTTCTTCCG - 3' |
| Primer-45 | 5' - GCGGCTCTGACGGGACTCGAACCCGCGACATACGGACTGCCAGTCCGCCGTTCTTCCG - 3' |
| Primer-46 | 5' - GCGGCTCTGACTGGACTCGAACAGTGACATACGGATTGCGAATCCGCCGTTCTTCCG - 3' |
| Primer-47 | 5' - GCGGCTCTGAGGGGACTCGAACCCCTGACATACGGATTGCGAATCCGCCGTTCTTCCG - 3' |
| Primer-48 | 5' - GCGGCTCTGACGGGACTCGAACCCGCGACATACGGATTGCGAATCCGCCGTTCTTCCG - 3' |
| Primer-49 | 5' - TAATACGACTCACTATAGGGTTAACTTTAACAAGGAGAAAAACATGAAGAAGAAG - 3' |
| Primer-50 | 5' - CGAAGCTTACTTGTCTGCTGCTCTTGTAGTCGTAGACCTTCTTCTCATTTTTCTC - 3' |
| Primer-51 | 5' - CGAAGCTTACTTGTCTGTC - 3' |
| Primer-52 | 5' - GAGAAAAACATGAAGAAGAAGCTCCATATGTTGGTCACAGAAGTGTCTATCGCGCAAAA - 3' |
| Primer-53 | 5' - GTCGTCTTGTAGTCTGGGGCAGCACCAACCAACCAAAATTTGCGGATAGACAGT - 3' |
| Primer-54 | 5' - CGAAGCTTACTTGTCTGCTGCTCTTGTAGTC - 3' |
| Primer-55 | 5' - GAGAAAAACATGAAGAAGAAGCTCCATTTGGTCACAGAAGTGTCTATCCAAGCGAATTT - 3' |
| Primer-56 | 5' - GTCGTCTGCTCTTGTAGTCGATGGGGCAGCACCAACCAACCAAAATTCGCTTGGATAGACAGT - 3' |

Table 5.

| tRNA | Anticodon | T-stem | Extension | | PCR | |
|--------------------|-----------|--------|----------------|----------------|----------------|----------------|
| | | | Forward primer | Reverse primer | Forward primer | Reverse primer |
| Phe without 3'-A | GAA | - | Primer-1 | Primer-2 | Primer-3 | Primer-4 |
| Phe | GAA | - | Primer-1 | Primer-2 | Primer-3 | Primer-5 |
| Tyr without 3'-A | GUA | - | Primer-6 | Primer-7 | Primer-3 | Primer-8 |
| Tyr | GUA | - | Primer-6 | Primer-7 | Primer-3 | Primer-9 |
| Ser without 3'-A | CGA | - | Primer-10 | Primer-11 | Primer-3 | Primer-12 |
| Ser | CGA | - | Primer-10 | Primer-11 | Primer-3 | Primer-13 |
| AsnE2 without 3'-A | GAC | #1 | Primer-14 | Primer-15 | Primer-3 | Primer-16 |
| AsnE2 without 3'-A | GAC | #2 | Primer-14 | Primer-17 | Primer-3 | Primer-18 |
| AsnE2 without 3'-A | GAC | #3 | Primer-14 | Primer-19 | Primer-3 | Primer-20 |
| AsnE2 without 3'-A | GAC | #4 | Primer-14 | Primer-21 | Primer-3 | Primer-22 |
| AsnE2 | GAC | #1 | Primer-14 | Primer-15 | Primer-3 | Primer-23 |
| AsnE2 | GAC | #2 | Primer-14 | Primer-17 | Primer-3 | Primer-24 |
| AsnE2 | GAC | #3 | Primer-14 | Primer-19 | Primer-3 | Primer-25 |
| AsnE2 | GAC | #4 | Primer-14 | Primer-21 | Primer-3 | Primer-26 |
| AsnE2 | GAA | #2 | Primer-27 | Primer-28 | Primer-3 | Primer-24 |
| AsnE2 | GAA | #3 | Primer-27 | Primer-29 | Primer-3 | Primer-25 |
| AsnE2 | GAA | #4 | Primer-27 | Primer-30 | Primer-3 | Primer-26 |
| AsnE2 | CAA | #2 | Primer-14 | Primer-31 | Primer-3 | Primer-24 |
| AsnE2 | CAA | #4 | Primer-14 | Primer-32 | Primer-3 | Primer-26 |
| AsnE2 | GAG | #2 | Primer-14 | Primer-33 | Primer-3 | Primer-24 |
| AsnE2 | GAG | #4 | Primer-14 | Primer-34 | Primer-3 | Primer-26 |
| AsnE2 | CAG | #2 | Primer-14 | Primer-35 | Primer-3 | Primer-24 |
| AsnE2 | CAG | #4 | Primer-14 | Primer-36 | Primer-3 | Primer-26 |
| AsnE2 | GAU | #2 | Primer-14 | Primer-37 | Primer-3 | Primer-24 |
| AsnE2 | GAU | #3 | Primer-14 | Primer-38 | Primer-3 | Primer-25 |
| AsnE2 | GAU | #4 | Primer-14 | Primer-39 | Primer-3 | Primer-26 |
| AsnE2 | CAC | #2 | Primer-14 | Primer-40 | Primer-3 | Primer-24 |
| AsnE2 | CAC | #3 | Primer-14 | Primer-41 | Primer-3 | Primer-25 |
| AsnE2 | CAC | #4 | Primer-14 | Primer-42 | Primer-3 | Primer-26 |
| AsnE2 | GGC | #2 | Primer-14 | Primer-43 | Primer-3 | Primer-24 |
| AsnE2 | GGC | #3 | Primer-14 | Primer-44 | Primer-3 | Primer-25 |
| AsnE2 | GGC | #4 | Primer-14 | Primer-45 | Primer-3 | Primer-26 |
| AsnE2 | CGC | #2 | Primer-14 | Primer-46 | Primer-3 | Primer-24 |
| AsnE2 | CGC | #3 | Primer-14 | Primer-47 | Primer-3 | Primer-25 |
| AsnE2 | CGC | #4 | Primer-14 | Primer-48 | Primer-3 | Primer-26 |

Table 6.

| Name | Corresponding mDNA | Extension | | 1st PCR | | 2nd PCR | |
|-------|--------------------|----------------|----------------|----------------|----------------|----------------|----------------|
| | | Forward primer | Reverse primer | Forward primer | Reverse primer | Forward primer | Reverse primer |
| mRNA1 | mDNA1 | Primer-49 | Primer-50 | Primer-3 | Primer-51 | - | - |
| mRNA2 | mDNA2 | Primer-52 | Primer-53 | Primer-49 | Primer-54 | Primer-3 | Primer-51 |
| mRNA3 | mDNA3 | Primer-55 | Primer-56 | Primer-49 | Primer-54 | Primer-3 | Primer-51 |

Table 7.

4. 5. 3 Preparation of AA-tRNA by flexizyme

Aminoacylation reaction was carried out following section 2. 6. 2.

4. 5. 4 In vitro translation

The *in vitro* translation was carried out following section 2. 6. 3, with an additional 3 mM Mg(OAc)₂. (final concentration: 15 mM).

MALDI-TOF MS was carried out after the FLAG purification. After the reaction, the mixture was diluted with the same volume of FLAG-purification buffer [100 mM Tris-HCl (pH 7.6), 300 mM NaCl]. The expressed peptide was immobilized on anti-FLAG M2 agarose beads (Sigma) by

incubating at 25°C for 1 hour. After washing the beads with 25 µL of wash buffer [50 mM Tris-HCl (pH 7.6), 150 mM NaCl], the immobilized peptides were eluted with 15 µL of 0.2% TFA.

For the quantification analysis, the translation reaction was performed in the presence of 50 µM [¹⁴C]-Asp instead of 200 µM cold Asp. The translation product was analyzed by 15% tricine-SDS-PAGE and autoradiography using a Typhoon FLA 7000 (GE Healthcare) without FLAG purification. The expression level of peptide products was quantified based on the relative band intensity of the peptide product to the sum intensities present in the lane, *i.e.*, the sum intensities of unreacted free Asp and peptide products.

Chapter 5.

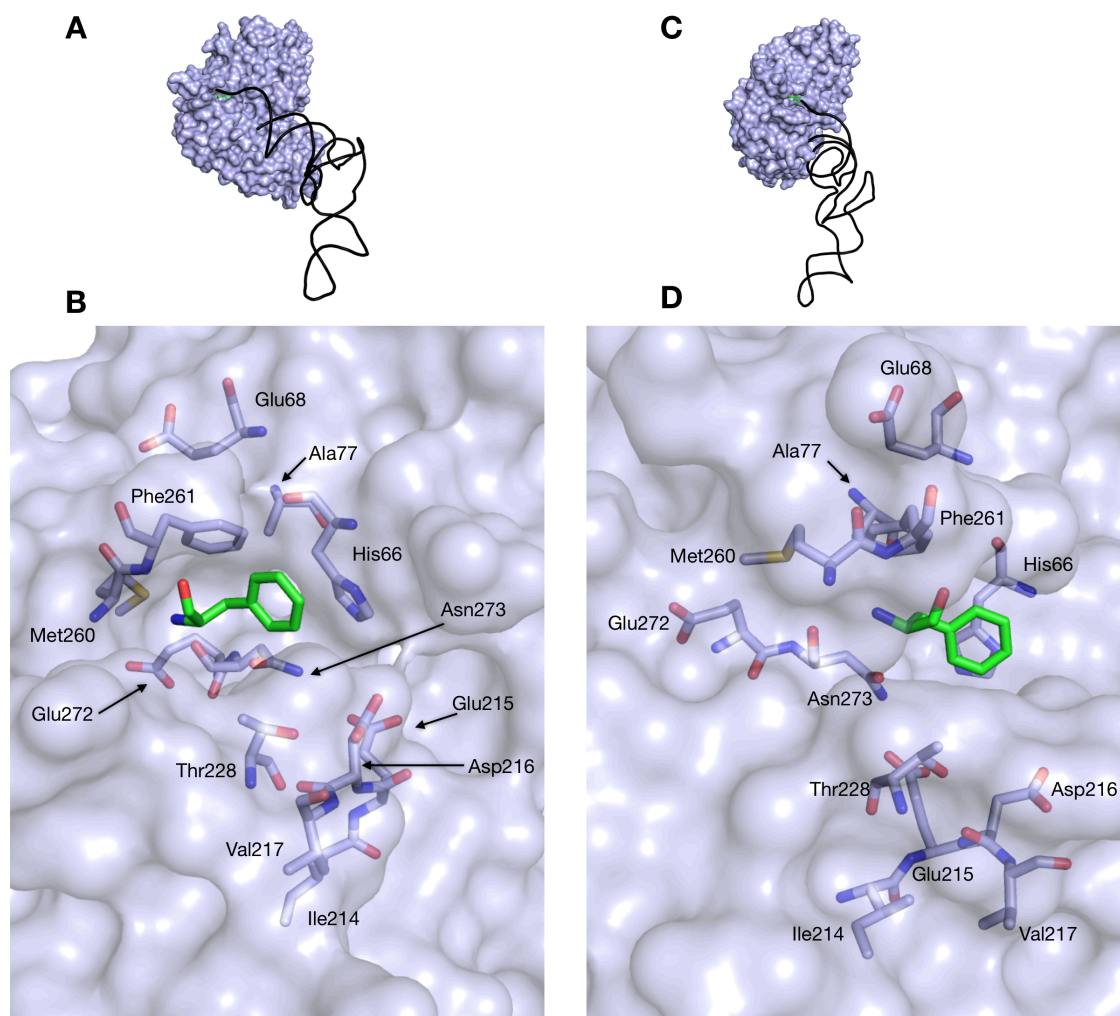
Analysis of affinity between aminoacyl-tRNA and EF-Tu with a mutated binding pocket

5. 1. Introduction

In the prokaryotic translation system, elongation factor thermo-unstable (EF-Tu) deliver all proteinogenic aminoacyl-tRNA (pAA-tRNA) to the ribosome. EF-Tu binds to pAA-tRNA in near-uniform affinities in order that nascent polypeptide chains can be elongated with twenty various proteinogenic amino acids (1, 103). EF-Tu recognizes two distinct regions of AA-tRNAs: the amino acid moiety and the T-stem region of the tRNA (91–93, 104). The overall binding affinities between EF-Tu and AA-tRNAs are determined as the sum of these two interactions, and they are in a compensatory relationship between the two binding regions in order to achieve uniform affinities.

In Chapter 4, the affinity between EF-Tu and AA-tRNAs mediated by the tRNA T-stem has been engineered. Alternatively, to intensive research on tRNA T-stem regions, the binding pocket of EF-Tu has been modified. Doi *et al.* had introduced E215A, D216A, and the double mutant of them (E215A and D216A) to EF-Tu. These substitutions enlarged the binding pocket of EF-Tu, allowing the sufficient affinity for bulky npAA-tRNA, such as pyrenylated alanine (65). Park *et al.*, has reported that an EF-Tu variant, EF-Sep, originated from a directed evolution in *E. coli*, enables the efficient incorporation of phosphoserine (66). In EF-Sep, six residues have been substituted (H66R, E215N, D216G, F218Y, T228S, and N273W), resulting in the enhanced affinity for the negatively charged phosphoserine. By expressing EF-Sep in *E. coli*, phosphoserine was successfully incorporated into a protein.

Collectively, these reports demonstrate that the affinity between AA-tRNA and EF-Tu is an important factor determining translation efficiency. However, compared to the tRNA T-stem cases, the affinity profile of the EF-Tu binding pocket was poorly understood. Since there remains some npAAs as the stumbling blocks in the translation system, further understanding of affinities between EF-Tu and AA-tRNAs is required. In this study, I aimed to investigate the structure-affinity relationship between EF-Tu mutants and npAA-tRNAs. I prepared 35 kinds of EF-Tu mutants, whose binding pocket for the amino acid was mutated, and then a comprehensive binding assay was conducted to reveal the critical residues.



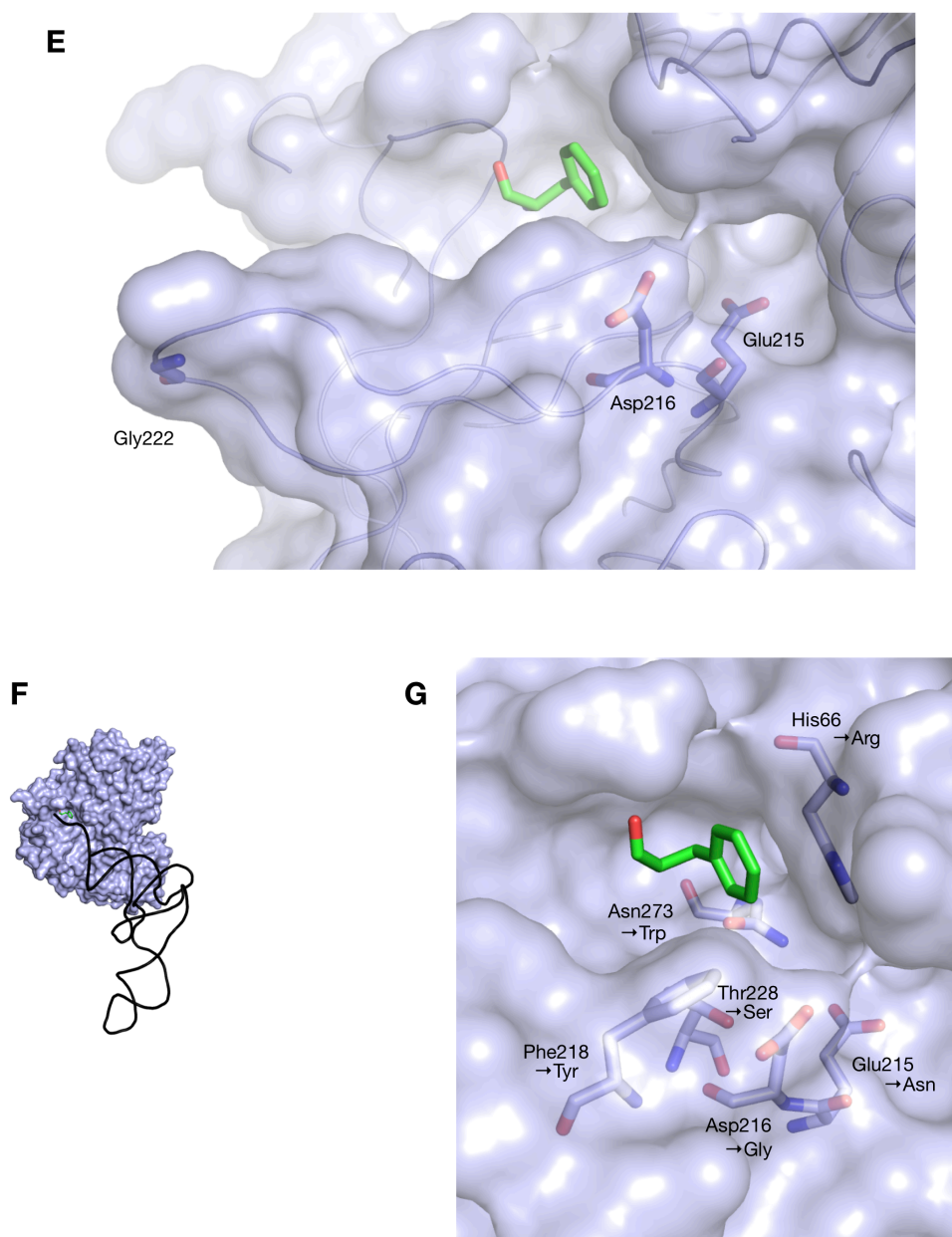


Figure 60 The positions mutated in this study. (A–D) the whole view of the ternary complex (A, C) and the magnified view of the binding pocket (B, C). (A and B) or (C and D) showed the view from the same angle respectively. (E) The position of loop G222. (F, G) The whole view and magnified view of EF-Sep. These figures were created by using PDB ID: 5AFI.

5. 2. Results and discussion

5. 2. 1 Design and preparation of EF-Tu variants.

To investigate how the EF-Tu binding pocket recognizes the substrate AA-tRNA, I decided to prepare various kinds of EF-Tu variants with a single amino acid substitution locating around the binding pocket. The substitution positions were selected based on the cryo-EM structure of EF-Tu and Phe-tRNA^{Phe} (PDB ID: 5AFI) (105). The design concept of the EF-Tu variants is as follows. At first, H66, E68, I214, E215, D216, V217, T228, M260, F261, E272, and N273 residues were selected as the neighboring residues of the esterified amino acid on tRNA and substituted with Ala to enlarge the cavity space shaped by the binding pocket (Figure 60). Among these Ala substitution variants, reported variants in previous research from Doi *et al.*, are included ((8)E215A, (11)D216A) (65). Some of these residues were substituted with a different amino acid to alter the property of the pocket. For example, (3)H66F and (4)H66W were designed to modify the size of the side chain while they keep an aromatic side chain. I have also designed oppositely charged variants (such as (10)E215R, (13)D216K) to drastically affect the property of the pocket. In contrast, since the residue of A77, which is close to the pocket, has been already Ala residue, this residue was substituted with Val in order to decrease the size of the pocket ((6)A77V). In addition to these point-mutation variants focusing on the neighboring residues, I have also prepared four variants with different concepts. The residue Gly222 locates at the loop position, which seems not to directly interact with the amino acid esterified on tRNA, but it is connected to the important residues (E215 and D216). I expected that the modification of this loop structure may have a large impact on the pocket by moving neighboring residue at once, I have designed (16)G222Δ (*i.e.*, G222 residue has been deleted) and (17)G222GG (*i.e.*, an additional Gly residue has been inserted into G222 position resulting in the consecutive Gly residues) (Figure 60E). Furthermore, a reported mutant with double mutation ((35)E215A/D216A, listed as “Double”) has been prepared (65). Finally, EF-Sep, a reported EF-Tu variant that had been originated from a directed evolution (66), has also been included as a test variant (Figure 60F, G). In total, 35 kinds of EF-Tu variants were designed as shown in Figure 62. These EF-Tu variants were expressed in *E. coli* BL21(DE3) *pLysS* cell line transformed with pET21a-*tufA*, in which a residue(s) had been mutated by inverse PCR. The expressed EF-Tu variants were purified by His-tag affinity spin column and dialysis. In the case of (35)double variant, a carryover of endogenous AA-tRNA has been observed. To avoid this, RNase A (Sigma) was added during cell lysis (see the supplementary result 5. 4.).

Since the purified EF-Tu variants may be in a GDP-form (which cannot bind to AA-tRNAs), I reconstituted it to a GTP-form (which binds to AA-tRNAs) by incubating EF-Tu variants in a

reconstitution buffer (see 5. 5. 6. for the experimental detail) in before the formation of the ternary complex.

5. 2. 2 Evaluation of ternary complex formation with *pAA-tRNAs*

The binding affinities between EF-Tu variants and AA-tRNAs of interest were evaluated by gel mobility shift assay (65, 83, 106). In this assay, AA-tRNA and EF-Tu (GTP form) were incubated in a 1-to-1 ratio to form the ternary complex (TC; EF-Tu·GTP·AA-tRNA). The incubated solution was then loaded onto a native polyacrylamide gel and run electrophoresis at 4 °C to maintain the bound complex. The EF-Tu protein itself runs slowly in the native gel, while the TC runs faster because the TC contains the tRNA with a highly negatively charged phosphate backbone (Figure 61).

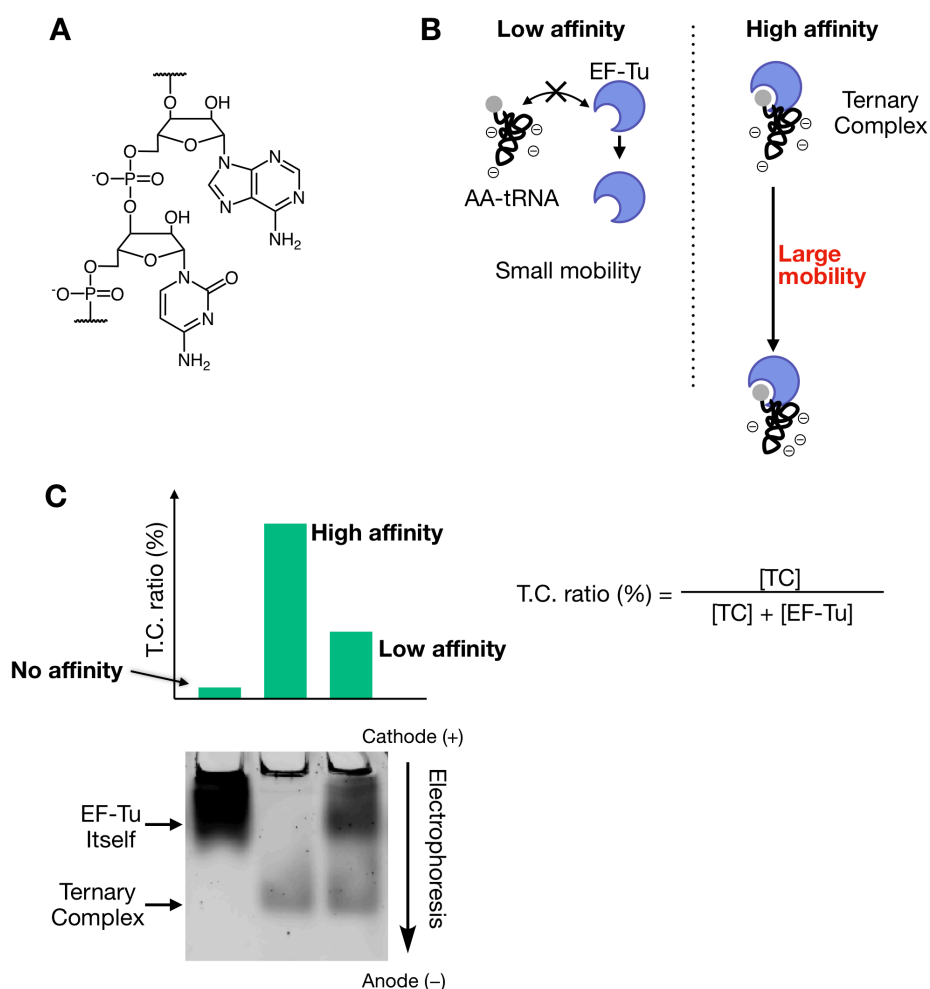


Figure 61 The schematic illustrations of the gel mobility shift assay. (A) the backbone structure of RNA, which are negatively charged. (B) The difference of the mobility depending on whether the ternary complex is formed or not. (C) The quantification of the affinity by mobility shift.

I prepared 13 kinds of proteinogenic AA-tRNA^{Pro1E2#3_{CGG}} (L-Asp, Gly, L-Lys, L-Met, L-Phe, L-Pro, L-Thr, L-Ile, L-Ser, L-Tyr, L-Cys, L-Trp, and L-Gln), incubated them with GTP-reconstituted EF-Tu variants, and analyzed by a native PAGE. The gel was stained with SYPRO Red by following the manufacturer's instructions. Figure 62. shows one of the gels as an example, where L-Pro-tRNA^{Pro1E2#3_{CGG}} and 36 EF-Tu variants were incubated together to form the TC. To evaluate the affinity of EF-Tu variants, an index called TC ratio was defined as $(100 \times [TC])/([EF-Tu] + [TC])$ (%), where the intensity of EF-Tu itself (unbound EF-Tu) and TC (bound EF-Tu) was denoted as [EF-Tu] and [TC]. This index indicates that what percentage of EF-Tu is involved in the TC. The TC ratio between L-Pro-tRNA^{Pro1E2#3_{CGG}} and 36 EF-Tu variants are shown in Figure 62B. In addition to this TC ratio, the relative TC index was defined as $\log_2(\text{TC ratio of interest}/\text{TC ratio of WT})$. The positive TC ratio indicates that the focused variant showed a higher TC ratio than the WT and vice versa. The calculated TC ratio and index for all 13 kinds of proteinogenic AA-tRNA^{Pro1E2#3_{CGG}} are summarized in Figure 63.

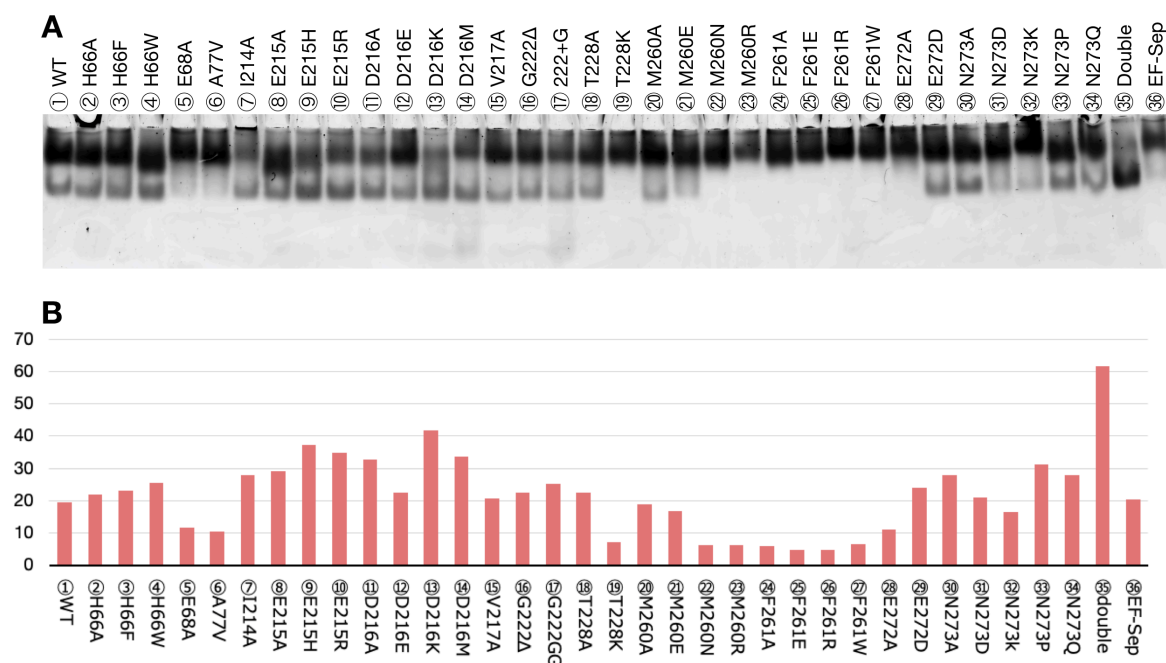


Figure 62 The example of the evaluation of the TC formation. (A) The raw gel image showing the native-PAGE of the TC between EF-Tu variants and L-Pro-tRNA. The gel was stained by SYPRO-Red. (B) The quantified TC ratio between EF-Tu variants and L-Pro-tRNA.

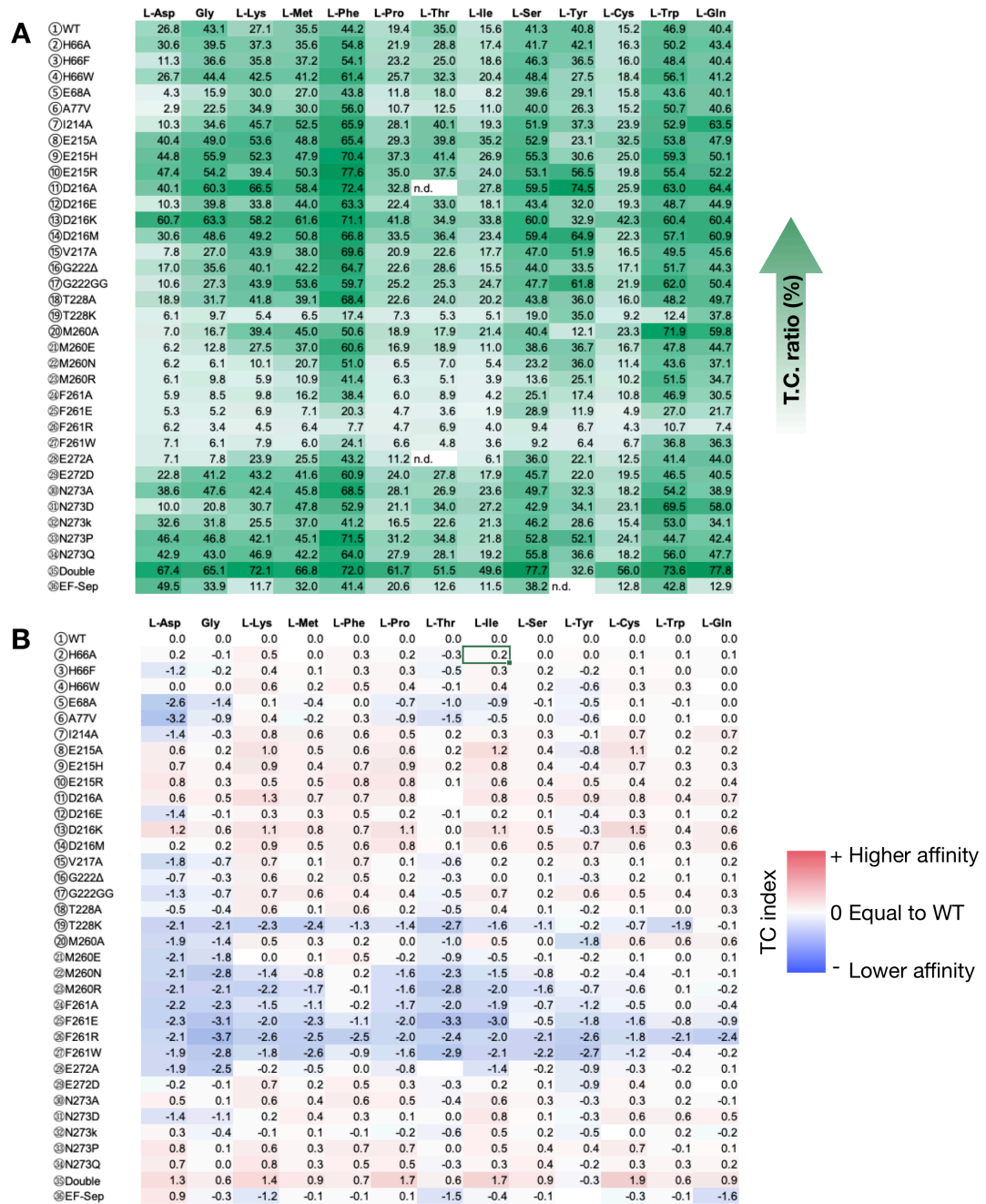


Figure 63 The summary of TC ratio (A) and TC index (B) using pAA-tRNAs.

The binding pocket of EF-Tu recognizes the esterified amino acid itself and its affinity for the amino acid highly depends on the species of amino acids (6). In Figure 63, the esterified amino acids are placed in the order of their affinity according to the literature (6). Even though I used common proteinogenic L-amino acids, the WT EF-Tu showed only 15–45% of the TC ratio (Figure 63A), regardless of the species of AA-tRNA^{Pro1E2#3_{CGG}} in this analysis. This indicates that the full conversion to the TC is not necessary for the translation. In the cases of tested EF-Tu variants, the TC ratios varied greatly depending on the substitution. At first, variant ⑦–⑭ (except for ⑫D216E variant, which has only one carbon elongation) almost always showed positive TC indexes (Figure 63B) indicating that the affinities for AA-tRNAs were improved compared to the WT.

By focusing variant ⑳–㉓, a faint trend was observed, in which the TC ratio dropped to less than 10% only when amino acids with relatively weak EF-Tu affinities were used (L-Asp, Gly, L-Lys, and L-Met). When the amino acid had relatively strong affinities (L-Ser, L-Tyr, L-Cys, L-Trp, and L-Gln), these variant ⑳–㉓ recovered the TC ratio comparable with other EF-Tu variants. In variant ⑳–㉓, the residue M260 or F261 was substituted, indicating that these residues play a moderately important role in the amino acid recognition, even though their importance is relatively smaller than E215 and D216. Notably, ㉓F261R variant always showed a very low TC ratio even when L-Gln was tested. This is probably because the large cationic guanidino group of Arg may disrupt the folding of the structure of EF-Tu, resulting in the complete loss of its affinity for AA-tRNAs. In addition, These M260 and F261 residues are well conserved over various organisms, suggesting that their critical role (Figure 64). The FASTA sequence data was cited from the NCBI protein database.

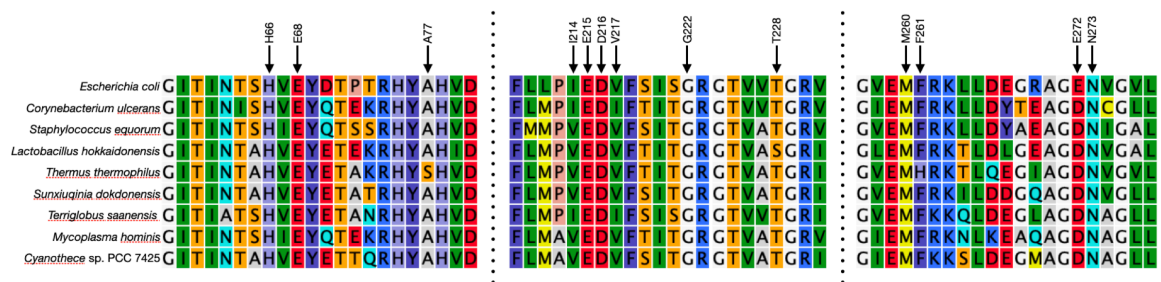


Figure 64 The conserved sequence at M260 and F261. The top sequence (pdb4Q7J) denotes the *E. coli* K-12 strain EF-Tu.

In the case of EF-Sep, the situation was much different. EF-Sep showed the relatively high TC ratio when L-Asp was charged on tRNA, even though the EF-Tu affinity of L-Asp is the lowest among the tested proteinogenic L-amino acids (6). This can be explained by the property of EF-Sep, which was discovered as the variant enabling the efficient delivery of phosphorylated serine (Sep). This improved affinity for the negatively charged amino acid has been achieved by substituting pocket with positively charged residues, i.e., H66R (weakly basic to strongly basic), E215N (acidic to neutral), and D216G (acidic to neutral). This positively charged binding pocket had an electrostatic interaction with L-Asp-tRNA, resulting in a relatively high TC ratio. This electrostatic interaction model is also consistent with the relatively low TC ratio between EF-Sep and L-Lys-tRNA (positively charged amino acid).

H66 residue was reported to interact with an aromatic ring of esterified Phe via a π - π stacking manner (107), but the H66A variant maintained the affinities for L-Phe-, L-Tyr-, and L-Trp-tRNA. This is probably because the tRNA^{Pro1E2#3}_{CGG} itself has enough affinity for EF-Tu (108) regardless of π - π stacking. To examine this, I evaluated the effect of the T-stem substitution. Previously used tRNA^{Pro1E2#3}_{CGG} has the #3 T-stem with the second strongest affinity among four designer sequences reported in the previous research (108). To decrease the affinity mediated by T-stem, I used tRNA^{Pro1E2#2}_{GUG}, which has #2 T-stem (the third strongest affinity) in comparison with tRNA^{Pro1E2#3}_{CGG}, while fixing the esterified amino acid to L-Tyr.

The quantified TC values are shown in Figure 65. The substitution with T-stem #3 to #2 caused the general decrease of affinities as expected with a couple of exceptions (⑧E215A, ⑬D216K, and ③⑥EF-Sep). Among these variants, ②H66A also dropped the affinity for Tyr-tRNA. This result indicates that the H66 residue may interact with aromatic AA-tRNAs secondarily, but the interaction may not be essential for the recognition.

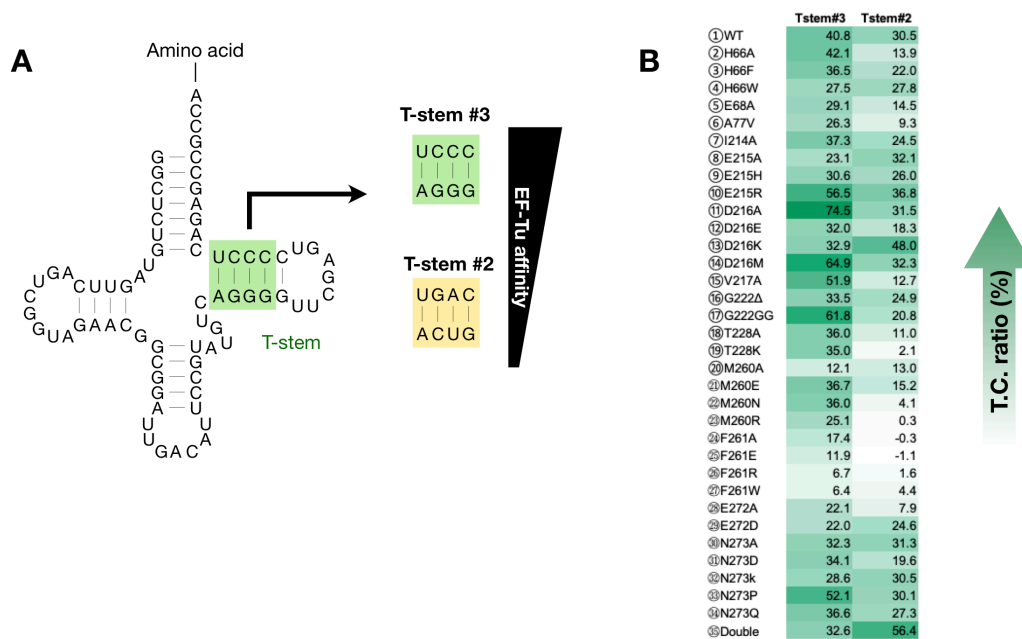


Figure 65 The contribution of the T-stem substitution. (A) The sequences of tRNA with T-stem #3 and #2. (B) The TC ratios between EF-Tu variants and L-Tyr-tRNA^{Asn#3} or L-Tyr-tRNA^{Asn#2}.

5. 2. 3 Evaluation of ternary complex formation with npAA-tRNAs

Next, I tested the binding assay with npAA-tRNA similarly to the pAA-tRNAs. The TC ratio and index are shown in Figure 66. The trend is almost same as the pAA-tRNAs cases. The substitution with E215 or D216 resulted in enhanced affinities for various npAA-tRNAs. Since the ①WT EF-Tu showed relatively lower affinities for various npAA-tRNAs, the reinforcement by substitution was larger than those of pAA-tRNAs cases. In addition to them, N273 substitutions also showed enhanced affinities. The affinities were almost completely lost by M260 and F261 substitutions again.

Among these variants, I focused on E215 and D216 residues. As previously introduced, E215A and D216A mutants have been reported to have enhanced affinity for bulky npAA-tRNAs (65). The authors attributed this enhancement to the enlarged binding pocket by shortening the side chains. However, ⑧E215A, ⑪D216A, and ⑳double variants tested in this study showed enhanced affinities for almost all kinds of pAA-tRNAs and npAA-tRNAs, independently from the size of amino acid esterified on the tRNA. Especially, ⑩E215R or ⑬D216K substitutions should not change the size of the residue drastically, or rather relatively have bigger than its original residues, but the trend of affinity enhancement appeared similarly. This may suggest that not the residue sizes

but other factors, such as the negative charge of E215 or D216, would play a more important role to control the AA-tRNA affinity. Further experiments such as X-ray crystallography or cryo-electron microscopy will be required to examine how these substitutions change the structure of EF-Tu; however, the above results have collectively provided insights into the significance of the binding pocket residues.

| A | | D-Ala | D-Lys | D-Phe | D-Ser | D-Tyr | D-Trp | D-Phe | D-Gln |
|---------|--|-------|-------|-------|-------|-------|-------|-------|-------|
| ①WT | | 29.4 | 22.0 | 1.8 | 34.3 | 15.8 | 30.3 | 5.5 | 1.2 |
| ②H66A | | 25.7 | 14.0 | 0.7 | 28.4 | 26.6 | 6.5 | 2.6 | 0.9 |
| ③H66F | | 19.6 | 10.0 | 0.9 | 27.2 | 18.2 | 18.3 | 3.7 | 1.8 |
| ④H66W | | 42.3 | 18.8 | 3.2 | 41.1 | 34.5 | 32.2 | 15.3 | 3.0 |
| ⑤E68A | | 12.0 | 5.7 | 1.6 | 14.6 | 22.5 | 7.5 | 5.6 | 2.3 |
| ⑥A77V | | 10.6 | 15.2 | 2.5 | 22.1 | 17.5 | 15.1 | 4.4 | 2.4 |
| ⑦I214A | | 25.2 | 11.6 | 7.8 | 28.1 | 23.9 | 18.6 | 9.3 | 6.3 |
| ⑧E215A | | 61.5 | 42.3 | 25.1 | 52.9 | 56.7 | 42.7 | 46.6 | 6.8 |
| ⑨E215H | | 57.5 | 35.4 | 13.9 | 48.6 | 48.6 | 41.8 | 44.3 | 3.9 |
| ⑩E215R | | 47.5 | 8.9 | 7.2 | 47.5 | 41.5 | 43.5 | 28.3 | 0.5 |
| ⑪D216A | | 43.7 | 34.6 | 4.7 | 49.2 | 34.5 | 38.4 | 29.9 | 4.6 |
| ⑫D216E | | 19.5 | 15.0 | 2.3 | 32.8 | 20.3 | 10.3 | 2.7 | 0.6 |
| ⑬D216K | | 67.6 | 37.7 | 10.6 | 56.8 | 53.3 | 50.5 | 36.7 | 13.0 |
| ⑭D216M | | 24.0 | 21.5 | 4.3 | 38.4 | 28.3 | 30.6 | 7.3 | 2.7 |
| ⑮V217A | | 4.3 | 10.0 | 2.8 | 15.9 | 11.4 | 6.8 | 1.7 | 0.4 |
| ⑯G222Δ | | 7.1 | 17.8 | 8.4 | 31.6 | 14.7 | 6.7 | 7.9 | 0.4 |
| ⑰G222GG | | 6.1 | 11.3 | 4.0 | 18.8 | 7.7 | 18.8 | 3.7 | 2.8 |
| ⑱T228A | | 2.3 | 13.9 | 4.2 | 28.2 | 7.6 | 2.1 | 1.4 | 2.8 |
| ⑲T228K | | -1.1 | 6.9 | 2.6 | 8.8 | 5.2 | 0.7 | 1.7 | 0.3 |
| ⑳M260A | | 1.3 | 7.8 | 3.4 | 19.0 | 5.7 | 5.7 | 2.8 | 2.2 |
| ㉑M260E | | 1.8 | 8.6 | 2.9 | 22.1 | 4.3 | 8.4 | 2.0 | 3.9 |
| ㉒M260N | | 0.0 | 6.6 | 1.9 | 11.0 | 4.9 | 0.9 | 2.0 | 1.5 |
| ㉓M260R | | 5.0 | 5.7 | 2.8 | 5.8 | 7.3 | -0.2 | 2.9 | 2.0 |
| ㉔F261A | | 0.0 | 6.1 | 2.4 | 8.8 | 7.8 | -0.6 | 2.2 | 1.3 |
| ㉕F261E | | -0.1 | 4.6 | 2.1 | 5.5 | 5.9 | 0.9 | 1.8 | 0.6 |
| ㉖F261R | | 4.9 | 7.9 | 1.8 | 5.6 | 6.8 | -1.9 | 2.1 | 1.6 |
| ㉗F261W | | 10.8 | 7.8 | 4.8 | 7.0 | 8.7 | -1.4 | 4.8 | 2.0 |
| ㉘E272A | | 8.4 | 7.0 | 3.1 | 8.6 | 5.4 | 1.7 | 4.5 | 4.7 |
| ㉙E272D | | 18.8 | 23.3 | 1.8 | 33.8 | 7.7 | 21.7 | 5.8 | 2.6 |
| ㉚N273A | | 39.7 | 34.2 | 12.2 | 34.9 | 39.9 | 35.9 | 39.7 | 2.3 |
| ㉛N273D | | 5.3 | 7.9 | 2.0 | 16.2 | 4.8 | -0.8 | 4.8 | 0.2 |
| ㉜N273K | | 17.1 | 8.4 | 1.7 | 18.0 | 7.6 | 8.0 | 10.9 | 2.4 |
| ㉝N273P | | 27.7 | 37.0 | 9.0 | 39.4 | 41.8 | 36.7 | 28.1 | 5.1 |
| ㉞N273Q | | 18.5 | 28.3 | 1.2 | 30.6 | 23.1 | 34.1 | 9.0 | 3.4 |
| ㉟Double | | 55.8 | 65.7 | 46.9 | 61.9 | 64.8 | 73.2 | 62.1 | 45.1 |
| ㊱EF-Sep | | 10.4 | 4.8 | 0.6 | 4.7 | 3.8 | 3.9 | 4.5 | 7.2 |

| B | | D-Ala | D-Lys | D-Phe | D-Ser | D-Tyr | D-Trp | D-Phe | D-Gln |
|---------|-----|-------|-------|-------|-------|-------|-------|-------|-------|
| ①WT | | 0.0 | 0.0 | 0.0 | 0.0 | 0.0 | 0.0 | 0.0 | 0.0 |
| ②H66A | | -0.2 | -0.6 | -1.4 | -0.3 | 0.7 | -2.2 | -1.1 | -0.5 |
| ③H66F | | -0.6 | -1.1 | -1.0 | -0.3 | 0.2 | -0.7 | -0.6 | 0.5 |
| ④H66W | | 0.5 | -0.2 | 0.9 | 0.3 | 1.1 | 0.1 | 1.5 | 1.3 |
| ⑤E68A | | -1.3 | -2.0 | -0.2 | -1.2 | 0.5 | -2.0 | 0.0 | 0.9 |
| ⑥A77V | | -1.5 | -0.5 | 0.5 | -0.6 | 0.1 | -1.0 | -0.3 | 1.0 |
| ⑦I214A | | -0.2 | -0.9 | 2.1 | -0.3 | 0.6 | -0.7 | 0.8 | 2.4 |
| ⑧E215A | | 1.1 | 0.9 | 3.8 | 0.6 | 1.8 | 0.5 | 3.1 | 2.5 |
| ⑨E215H | | 1.0 | 0.7 | 3.0 | 0.5 | 1.6 | 0.5 | 3.0 | 1.7 |
| ⑩E215R | | 0.7 | -1.3 | 2.0 | 0.5 | 1.4 | 0.5 | 2.4 | -1.3 |
| ⑪D216A | | 0.6 | 0.6 | 1.4 | 0.5 | 1.1 | 0.3 | 2.4 | 1.9 |
| ⑫D216E | | -0.6 | -0.6 | 0.4 | -0.1 | 0.4 | -1.6 | -1.0 | -1.0 |
| ⑬D216K | | 1.2 | 0.8 | 2.6 | 0.7 | 1.8 | 0.7 | 2.7 | 3.4 |
| ⑭D216M | | -0.3 | 0.0 | 1.3 | 0.2 | 0.8 | 0.0 | 0.4 | 1.2 |
| ⑮V217A | | -2.8 | -1.1 | 0.6 | -1.1 | -0.5 | -2.1 | -1.7 | -1.6 |
| ⑯G222Δ | | -2.1 | -0.3 | 2.3 | -0.1 | -0.1 | -2.2 | 0.5 | -1.6 |
| ⑰G222GG | | -2.3 | -1.0 | 1.2 | -0.9 | -1.0 | -0.7 | -0.6 | 1.2 |
| ⑱T228A | | -3.7 | -0.7 | 1.2 | -0.3 | -1.1 | -3.8 | -2.0 | 1.2 |
| ⑲T228K | *** | -1.7 | 0.5 | -2.0 | -1.6 | -5.4 | -1.7 | -1.9 | |
| ⑳M260A | | -4.5 | -1.5 | 0.9 | -0.9 | -1.5 | -2.4 | -1.0 | 0.8 |
| ㉑M260E | | -4.1 | -1.3 | 0.7 | -0.6 | -1.9 | -1.8 | -1.5 | 1.7 |
| ㉒M260N | *** | -1.7 | 0.1 | -1.6 | -1.7 | -5.0 | -1.5 | 0.3 | |
| ㉓M260R | | -2.6 | -2.0 | 0.6 | -2.6 | -1.1 | *** | -0.9 | 0.7 |
| ㉔F261A | *** | -1.8 | 0.4 | -2.0 | -1.0 | *** | -1.3 | 0.0 | |
| ㉕F261E | *** | -2.3 | 0.3 | -2.6 | -1.4 | -5.1 | -1.6 | -1.0 | |
| ㉖F261R | | -2.6 | -1.5 | 0.0 | -2.6 | -1.2 | *** | -1.4 | 0.4 |
| ㉗F261W | | -1.4 | -1.5 | 1.4 | -2.3 | -0.9 | *** | -0.2 | 0.7 |
| ㉘E272A | | -1.8 | -1.7 | 0.8 | -2.0 | -1.6 | -4.1 | -0.3 | 2.0 |
| ㉙E272D | | -0.6 | 0.1 | 0.0 | 0.0 | -1.0 | -0.5 | 0.1 | 1.1 |
| ㉚N273A | | 0.4 | 0.6 | 2.8 | 0.0 | 1.3 | 0.2 | 2.8 | 0.9 |
| ㉛N273D | | -2.5 | -1.5 | 0.2 | -1.1 | -1.7 | *** | -0.2 | -2.9 |
| ㉜N273K | | -0.8 | -1.4 | -0.1 | -0.9 | -1.1 | -1.9 | 1.0 | 1.0 |
| ㉝N273P | | -0.1 | 0.7 | 2.3 | 0.2 | 1.4 | 0.3 | 2.3 | 2.1 |
| ㉞N273Q | | -0.7 | 0.4 | -0.5 | -0.2 | 0.5 | 0.2 | 0.7 | 1.5 |
| ㉟Double | | 0.9 | 1.6 | 4.7 | 0.9 | 2.0 | 1.3 | 3.5 | 5.2 |
| ㊱EF-Sep | | -1.5 | -2.2 | -1.5 | -2.9 | -2.1 | -3.0 | -0.3 | 2.6 |

Figure 66 The summary of TC ratio (A) and TC index (B) using npAA-tRNAs.

5. 2. 4. Translation using EF-Tu variants

To evaluate the effect of the binding affinities on translation efficiencies, I conducted the *in vitro* translation using some EF-Tu variants. I selected ⑧E215A, ⑪D216A, ③⑤double, and ③⑥ EF-Sep for the testing factors, and I also selected D-Asp and D-Pro as the incorporating amino acids.

The EF-Tu affinities were measured by gel mobility shift assay as previously explained. The WT EF-Tu① showed a very small mobility shift with D-Asp-tRNA^{EnAsn}, indicating that the affinity between D-Asp-tRNA^{EnAsn} and the WT EF-Tu is not enough for maintaining the TC during the electrophoresis (Figure 67A). On the other hand, tested four variants ⑧E215A, ⑪D216A, ③⑤double, and ③⑥ EF-Sep showed significant affinities. The ③⑥ EF-Sep variant was originally discovered as the good binder for phosphoseryl-tRNA and thus the reinforced affinity with EF-Sep is also consistent with the charge contribution. For the translation reaction, the above-mentioned EF-Tu variants were additionally supplemented to the FIT system, which already has the WT EF-Tu. This is because the model peptide Pep61 consists of not only D-Asp but also standard pAAs, and the coexistence of the WT EF-Tu and another variant could be effective for the translation of such peptides.

In the case WT EF-Tu, D-Asp could be incorporated into the Pep61 determined by MALDI-TOF MS. This indicates that a very small fraction of the TC could be enough for the translation, even though the affinity was not so strong. By supplementing ⑧E215A, ⑪D216A, or ③⑤double also generated the Pep61 containing D-Asp, but the significant enhancement was not observed. However, in the case of ③⑥EF-Sep, Pep61 with D-Asp was cleanly synthesized in the FIT system.

In the case of D-Pro, the mobility shift was hardly observed with the WT EF-Tu (Figure 68A). Unlike D-Asp, ⑪D216A and ③⑥EF-Sep showed the almost same mobility shift with the WT. On the other hand, ⑧E215A and ③⑤double showed the improved mobility shift. Then I focused on ⑧E215A and the WT EF-Tu and tested the D-Pro incorporation experiment with the model peptide Pep172 (Figure 68B). The WT EF-Tu again showed the incorporation of D-Pro into Pep172, but accompanying byproducts were also observed. Note that the isotopic pattern of the main peak corresponding to Pep172 with D-Pro was not matched with the calculation, clearly indicating that this peak is not the sole product Pep172 with D-Pro. Judging from the isotopic pattern, the Thr-misincorporation could occur. On the other hand, the ⑧E215A variant can synthesize the Pep172 with D-Pro with less byproducts. Even though the ③⑤double variant showed the enhanced TC formation, the translation did not proceed.

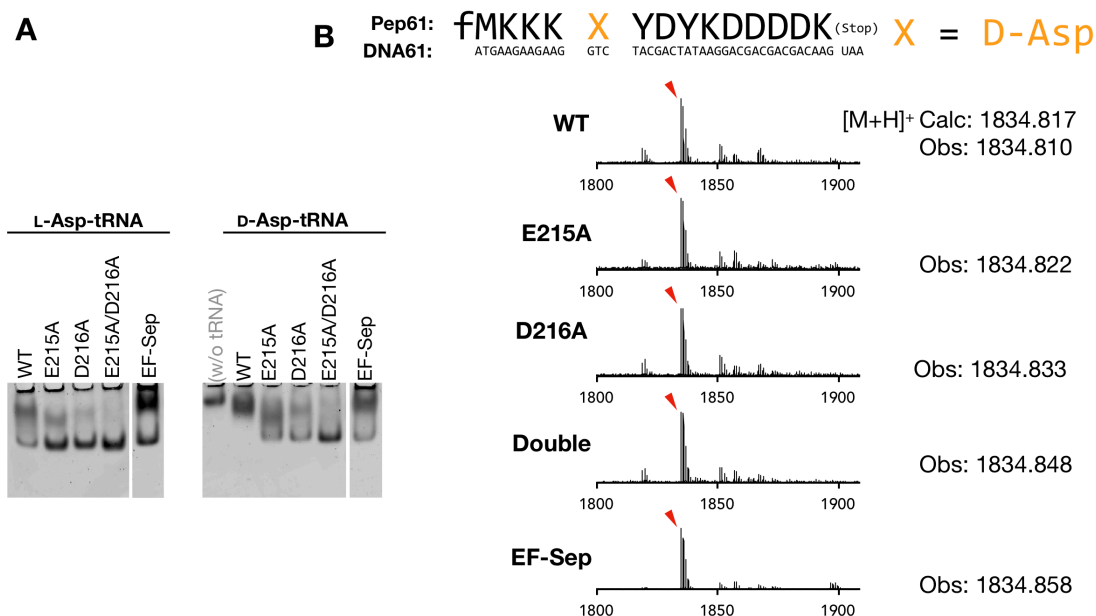


Figure 67 The translation experiment using D-Asp. (A) The gel image of the TC between EF-Tu variants and L- or D-Asp-tRNA. (B) The MALDI-TOF mass spectra of translation experiments.

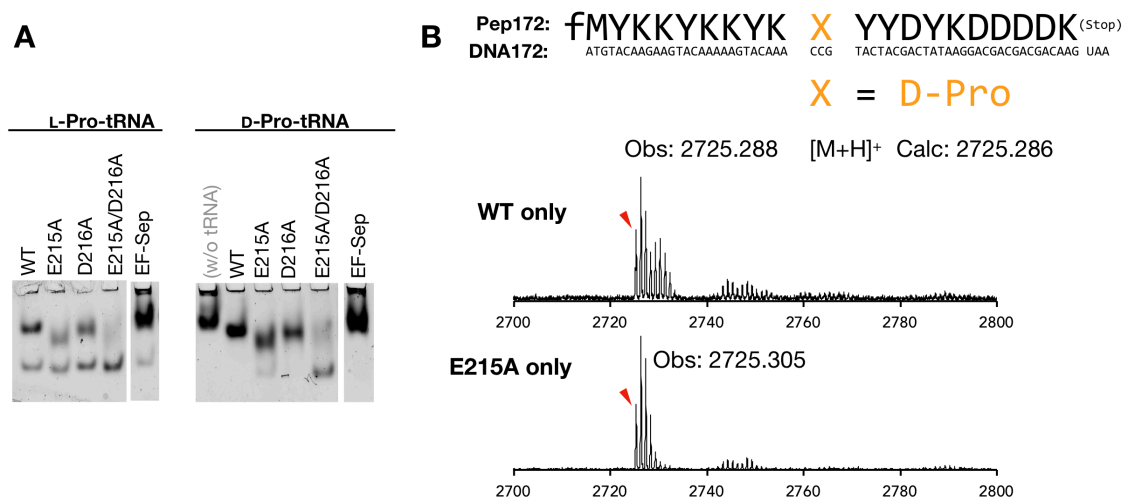


Figure 68 The translation experiment using D-Pro. (A) The gel image of the TC between EF-Tu variants and L- or D-Pro-tRNA. (B) The MALDI-TOF mass spectra of translation experiments.

Overall, these translation experiments have provided two insights. First, the binding affinities between EF-Tu and npAA-tRNAs have the effect on the incorporation of npAAs similarly to much of previous research (65, 108). Especially, some D-AAs (D-Ala, D-Ser, D-Phe, and D-Cys) have been efficiently incorporated into peptides by modifying tRNAs in previous research (62, 109); here, in this research, the incorporation of D-Pro and D-Asp was also enhanced by modifying the EF-Tu binding pocket, which has not been reported. This indicates that the EF-Tu structure must be one of the important factors determining translation efficiency. On the other hand, however, the second point raised by this research is that the strong affinity does not always lead to improved incorporation efficiency. Especially ③⑤double mutant showed almost always the highest affinities even with D-Asp and D-Pro, but the incorporation efficiency of these D-AAs was not improved by using ③⑤double mutant. There are reports that too strong affinities between EF-Tu and AA-tRNA prevent the efficient release of AA-tRNA to the ribosome, resulting in the inefficient translation (100, 108, 110); however, the gel mobility shift assay did not show such a too strong affinity. Therefore, other factors must be present in the translation system, which determines the translation efficiency. Hecht *et al.* has reported that the evolution of the ribosome to improve the incorporation efficiencies of npAAs (111–113). Combining such engineered ribosomes with engineered EF-Tu could be effective for the translation incorporating difficult npAAs.

5. 3. Conclusion

Here I investigated the binding affinities between 36 kinds of EF-Tu variants and 13 kinds of AA-tRNAs by gel mobility shift assay. Through this assay, substitution at E215 and D216 residues of EF-Tu drastically improved the AA-tRNA affinities, regardless of the species of amino acid esterified on the tRNA. Previously, it had been reported that these E215A and D216 are important in recognizing the size of npAAs (65), but the result presented in this study showed that the negative charges of these residues may have more importance rather than their sizes. In addition, M260 and F261 residues are newly discovered as the critical residues to maintain the structure and/or function of EF-Tu. Further structural investigations, such as X-ray crystallography or cryo-electron microscopy will be required to examine how these substitutions change the structure of EF-Tu.

I also conducted translation experiments using some EF-Tu variants. I have revealed that EF-Sep and E215A variants showed an enhanced affinity for D-Asp-tRNA and D-Pro-tRNA respectively, improving the efficiency in incorporating D-Asp and D-Pro. These results suggest that the engineering of the EF-Tu binding pocket would be effective in incorporating npAAs. It should be noted that the other EF-Tu variants also showed an enhanced affinity for these D-AA-tRNAs, but a significant improvement in the translation was not observed. This suggests that other limitations existing in the translation system should be engineered.

In summary, I have investigated the structure-affinity relationship between EF-Tu mutants and AA-tRNAs. The findings that improved affinities and enhanced translation efficiency would lead to the further engineering of EF-Tu.

5. 4. Supplementary results

It has been reported that the ③⑤double variant possesses a higher affinity for AA-tRNAs than the WT EF-Tu, and a carryover of endogenous AA-tRNA from *E. coli* seems to occur during the purification of EF-Tu. I have checked this carryover prior to the purification of all EF-Tu variants.

I purified the three EF-Tu variants ⑧E215A, ⑪D216A, and ③⑤double (E215A/D216A) from *E. coli* cells following the procedure (see section 3. 5. 3. for the experimental detail) except for the supplement of RNase A and measured the UV absorbance. As shown in Figure 69, the ③⑤double variant showed a large absorbance at A_{260} , which can be attributed to the tRNA.

To avoid the contamination of RNA, RNase A was supplemented during the cell lysis as shown in section 5. 5. 2. Then, the UV absorbance at A_{260} was removed.

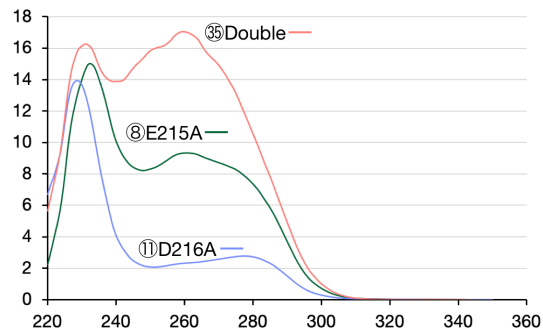


Figure 69 The UV-spectra of EF-Tu variants without RNaseA

5. 5. Experimental details

5. 5. 1. Introduction of point-mutations by inverse PCR

All inverse-PCR reaction for mutagenesis was carried by KOD FX Neo (TOYOBO, Japan), following the manufacturer protocol. The typical reaction mix (15 μ L for one variant) is composed of 5 μ L 2 \times Buffer for KOD FX Neo, dNTP mix (final concentration 0.2 mM each), 0.2 unit of KOD FX Neo, 1.8 ng of the pET21a-*tufA*. The primers used in the mutagenesis inverse-PCR are summarized in Table 8, and the combinations of primers are listed in Table 9. The inverse-PCR reaction was conducted in three types of thermal cycles. 2 steps cycle: initial denaturing (94 °C for 2 min), then 20 cycles of denaturing (98 °C for 10 sec) and extending (68 °C for 4 min). 3 steps cycle: initial denaturing (94 °C for 2 min), then 20 cycles of denaturing (98 °C for 10 sec), annealing (55 °C for 30 sec), and extending (68 °C for 4 min). Step-down cycle: initial denaturing (94 °C for 2 min), then 5 cycles of denaturing (98 °C for 10 sec) and extending (74 °C for 4 min), 5 cycles of denaturing (98 °C for 10 sec) and extending (74 °C for 4 min), 5 cycles of denaturing (98 °C for 10 sec) and extending (72 °C for 4 min), 5 cycles of denaturing (98 °C for 10 sec) and extending (70 °C for 4 min), and 5 cycles of denaturing (98 °C for 10 sec) and extending (68 °C for 4 min). After the inverse-PCR reaction, 2 μ L of the reaction solution was mixed with 2 \times DNA loading buffer and analyzed by 0.8% (w/v) agarose gel electrophoresis (135 V for 20 min.) to confirm the amplification. The gel was pre-stained by ethidium bromide and visualized in a UV transilluminator.

10 μ L of the inverse-PCR solution was subjected to mixed with 10 units of *DpnI* and 1 μ L of T buffer (TAKARA, Japan), and incubated at 37 °C overnight. After the digestion of the PCR template plasmid, 5 μ L of reaction mix was transformed into *E. coli* DH5 α competent cell by the standard heat shock protocol. Transformed DH5 α strains were spread onto LB-agar plates containing 10 mg/mL Amp and incubated at 37 °C overnight. Several colonies of DH5 α were picked and inoculated into 10 mL of liquid LB medium (Amp) and incubated at 37 °C overnight. The culture was subjected to plasmid extraction by means of FastGene Plasmid Mini Kit (Nippon Genetics, Japan) following the manufacturer's standard protocol.

| Primer | Sequence (5' → 3') |
|----------|--|
| 02H66A | GGTATCACCATCAACACTTCTGCGGTTGAATACGACACC |
| 03H66F | GGTATCACCATCAACACTTCTTTTGTGAATACGACACC |
| 04H66W | GGTATCACCATCAACACTTCTTGGGTTGAATACGACACC |
| H66rev | AGAAGTGTGATGGTGATACCACGAGCTTT |
| 05E68A | ACCATCAACACTTCTCACGTTGCGTACGACACCCCGACC |
| E68rev | AACGTGAGAAGTGTGATGGTGATACCAG |
| 06A77V | GACACCCCGACCCGTCACGTACGTGCACGTAGACTGCCCG |
| A77rev | GTAGTGACGGGTCGGGGTGTGCTATTCAAC |
| 07I214A | GACAAGCCGTTCTGCTGCCGGCGGAAGACGTATTCTCC |
| I214rev | CGGCAGCAGGAACGGCTTGTCAATCGCACG |
| 08E215A | AAGCCGTTCTGCTGCCGATCGCGGACGTATTCTCCATC |
| 09E215H | AAGCCGTTCTGCTGCCGATCCACGACGTATTCTCCATC |
| 10E215R | AAGCCGTTCTGCTGCCGATCCGTGACGTATTCTCCATC |
| E215rev | GATCGGCAGCAGGAACGGCTTGTCAATCGC |
| 11D216A | CCGTTCTGCTGCCGATCGAAGCGGTATTCTCCATCTCC |
| 12D216E | CCGTTCTGCTGCCGATCGAAGAAGTATTCTCCATCTCC |
| 13D216K | CCGTTCTGCTGCCGATCGAAAAAGTATTCTCCATCTCC |
| 14D216M | CCGTTCTGCTGCCGATCGAAATGGTATTCTCCATCTCC |
| D216rev | TTCGATCGGCAGCAGGAACGGCTTGTCAAT |
| 15V217A | TTCTGCTGCCGATCGAAGACGCGTTCTCCATCTCCGGT |
| V217rev | GTCTTCGATCGGCAGCAGGAACGGCTTGTGTC |
| 16G222Δ | GAAGACGTATTCTCCATCTCCGTTGGTACCGTTGTT |
| 17G222GG | GAAGACGTATTCTCCATCTCCGTTGGCGGTGGTACCGTTGTT |
| G222rev | GGAGATGGAGAATACGCTTTCGATCGGCAG |
| 18T228A | CCGGTCGTGGTACCGTTGTTGCCGGTCGTGAGAACG |
| 19T228K | TCCGGTCGTGGTACCGTTGTTAAAGGTCGTGAGAACGC |
| T228rev | AACAACGGTACCACGACCGGAGATGGAGAA |
| 20M260A | TCTACCTGTACTGGCGTTGAAGCGTTCCGCAAACTGCTG |
| 21M260E | TCTACCTGTACTGGCGTTGAAGAATTCGCAAACTGCTG |
| 22M260N | TCTACCTGTACTGGCGTTGAAAACCTCCGCAAACTGCTG |
| 23M260R | TCTACCTGTACTGGCGTTGAACGTTTCCGCAAACTGCTG |
| M260rev | TTCAACGCCAGTACAGGTAGACTTCTGAGT |
| 24F261A | ACCTGTACTGGCGTTGAAATGGCGCGCAAACTGCTGGAC |
| 25F261E | ACCTGTACTGGCGTTGAAATGGAACGCAAACTGCTGGAC |
| 26F261R | ACCTGTACTGGCGTTGAAATGCGTCGCAAACTGCTGGAC |
| 27F261W | ACCTGTACTGGCGTTGAAATGTGGCGCAAACTGCTGGAC |
| F261rev | CATTTCAACGCCAGTACAGGTAGACTTCTG |
| 28E272A | CTGGACGAAGGCCGTGCTGGTGCGAACGTAGGTGTTCTG |
| 29E272D | CTGGACGAAGGCCGTGCTGGTGATAACGTAGGTGTTCTG |
| E272rev | ACCAGCACGGCCTTCGTCCAGCAGTTTGGC |
| 30N273A | GACGAAGGCCGTGCTGGTGAGGCGGTAGGTGTTCTGCTG |
| 31N273D | GACGAAGGCCGTGCTGGTGAGGATGTAGGTGTTCTGCTG |
| 32N273K | GACGAAGGCCGTGCTGGTGAGAAAGTAGGTGTTCTGCTG |
| 33N273P | GACGAAGGCCGTGCTGGTGAGCCGGTAGGTGTTCTGCTG |
| 34N273Q | GACGAAGGCCGTGCTGGTGAGCAGGTAGGTGTTCTGCTG |
| N273rev | CTACCCAGCACGGCCTTCGTCCAGCAGTTT |
| 35double | AAGCCGTTCTGCTGCCGATCGCGCGGTATTCTCCATCTCC |
| pET21F | GGGAATTGTGAGCGGATAAC |
| pET21R | CTAGTTATTGCTCAGCGGTG |

Table 8 The list of primers used in this study.

| Variant | Forward | Reverse |
|---------|----------|---------|
| ②H66A | 02H66A | H66rev |
| ③H66F | 03H66F | H66rev |
| ④H66W | 04H66W | H66rev |
| ⑤E68A | 05E68A | E68rev |
| ⑥A77V | 06A77V | A77rev |
| ⑦I214A | 07I214A | I214rev |
| ⑧E215A | 08E215A | E215rev |
| ⑨E215H | 09E215H | E215rev |
| ⑩E215R | 10E215R | E215rev |
| ⑪D216A | 11D216A | D216rev |
| ⑫D216E | 12D216E | D216rev |
| ⑬D216K | 13D216K | D216rev |
| ⑭D216M | 14D216M | D216rev |
| ⑮V217A | 15V217A | V217rev |
| ⑯G222Δ | 16G222Δ | G222rev |
| ⑰G222GG | 17G222GG | G222rev |
| ⑱T228A | 18T228A | T228rev |
| ⑲T228K | 19T228K | T228rev |
| ⑳M260A | 20M260A | M260rev |
| ㉑M260E | 21M260E | M260rev |
| ㉒M260N | 22M260N | M260rev |
| ㉓M260R | 23M260R | M260rev |
| ㉔F261A | 24F261A | F261rev |
| ㉕F261E | 25F261E | F261rev |
| ㉖F261R | 26F261R | F261rev |
| ㉗F261W | 27F261W | F261rev |
| ㉘E272A | 28E272A | E272rev |
| ㉙E272D | 29E272D | E272rev |
| ㉚N273A | 30N273A | N273rev |
| ㉛N273D | 31N273D | N273rev |
| ㉜N273k | 32N273K | N273rev |
| ㉝N273P | 33N273P | N273rev |
| ㉞N273Q | 34N273Q | N273rev |
| ㉟double | 35double | E215rev |

Table 9 The combinations of primers used for the inverse-PCR.

5. 5. 2. The sequence of pET-21a-tufA

The sequence of the recovered plasmids was confirmed by Fasmac DNA sequencing service (Japan), using pET21F primer and pET21R primer (Table 8). The sequence of WT used in this study is shown in Table 10. The accompanying boxes are corresponding the open reading frame of the *tufA* gene (EF-Tu) derived from *Escherichia coli*. and the sequences without boxes are flanking sequences of pET21a plasmid. The residue number starts from -3 because the first three residues (Met-2, Ala-1, and Ser0) are originated from the restriction enzyme recognition site of pET21a. The pink-colored regions, which is prior or posterior to the *tufA* gene, are pET21F and pET21R primers used for sequencing. The yellow-colored residues are mutated in this research.

5. 5. 3. Purification of EF-Tu

0.5 µg of pET21a-*tufA* variant plasmids (20~40 ng/ml) were transformed into 50 µL of *E. coli* BL21(DE3)pLysS competent cell by the standard heat shock protocol. After the heat shock, 500 µL of SOC medium was added to the competent cells and incubated for 1 h at 37 °C as the cell recovery step. The media was centrifuged to reduce the volume and the cells were resuspended in SOC media. The cells were spread onto the LB-agar plates (100 mg/mL Amp, 20 mg/mL Cm, and 1% (w/v) glucose) and incubated at 37 °C overnight. Several colonies of BL21(DE3)pLysS were picked up, inoculated into 10 mL of liquid LB (Amp/Cm/glucose) and incubated at 37 °C overnight. 800 µL of the medium was mixed with 200 µL of 80% glycerol for glycerol stock. 6 mL of media was inoculated into 600 mL of liquid LB (Amp/Cm/glucose) and incubated at 37 °C, monitoring the optical density at 600 nm (OD600). After OD 600 reaches 0.4~0.6, 600 µL of 0.5 M IPTG was added and incubated at 15 °C for 24 hr. The cells were collected by centrifugation (5,000 × g, 4 °C, 15 min) and stored at -80 °C until the protein purification.

The pellet of BL21(DE3)pLysS was resuspended in Lysis buffer (20 mM Tris-HCl (pH 7.6), 20 mM imidazole (pH 7.6), 300 mM NaCl, 10 µM GTP, 1 mM DTT) and 5 µL of 100 mg/mL RNase A (Sigma-Aldrich, R6513) was added to the suspension. The cells were disrupted by sonication (Branson, Sonifier SFX 150, equipped with the microtip, 40% amplitude, pulse mode with 1 sec on and 2 sec off, and the total sonication time is 1 min). The cell lysate was centrifuged (15,000 × g, 4 °C, 15 min) twice, and the supernatant was recovered. The supernatant was subjected to His SpinTrap (GE Healthcare) following the manufacturer's standard protocol (Binding buffer: 20 mM Tris-HCl (pH 7.6), 20 mM imidazole (pH 7.6), 300 mM NaCl, 10 µM GTP, 1 mM DTT, Elution buffer: 20 mM Tris-HCl (pH 7.6), 500 mM imidazole (pH 7.6), 300 mM NaCl, 10 µM GTP, 1 mM DTT).

Table 10 The sequence of pET-21a-tufA

The eluent containing the EF-Tu variant was injected to Slide-A-Lyzer G2 Dialysis Cassette (Thermo Fisher, 3.5 K molecular weight cut off, 0.5 mL scale) and dialyzed in 2 L of Dialysis buffer (10 mM Tris-HCl (pH 7.6), 50 mM KCl, 10 μ M GTP, 1 mM DTT) at 4 °C twice. The EF-Tu variants collected from the dialysis cassette were centrifuged to get rid of a small portion of precipitation. The concentration of EF-Tu variants was measured by Qubit Fluorometer (Thermo Fischer) and the quality of protein was analyzed by 10% Glycine-SDS PAGE (180 V, 40 min, SYPRO Red stain).

5. 5. 4. Preparation of nucleotides (DNA template, tRNA, flexizyme)

DNA templates, tRNAs, eFx, and dFx were prepared following section 2. 6. 1.

5. 5. 5. Preparation of aminoacyl-tRNAs

The aminoacylation by means of flexizyme was carried out following section 2. 5. 3. For the following gel shift assay, the AA-tRNA pellet was dissolved in 10 mM of NaOAc (pH 5.2). The concentration of AA-tRNA was adjusted to 50 μ M by measuring A_{260} , considering the following two points. (A) The RNA pellet contains not only tRNA but also flexizyme in a 1:1 ratio, and (B) the aminoacylation efficiencies vary depending on the species of the substrate activated amino acids. The aminoacylation efficiency was reported in the previous research (108). The concentration of AA-tRNA was adjusted 50 μ M by adding an appropriate volume of 10 mM AcONa.

5. 5. 6. Reconstitution of EF-Tu/GTP/AA-tRNA

Purified EF-Tu variants were a mixture of GDP-form and GTP forms. To reconstitute EF-Tu·GTP, the reconstitution mix containing 10 μ M of EF-Tu, 70 mM HEPES -KOH (pH 7.6), 52 mM NH_4OAc , 8 mM $\text{Mg}(\text{OAc})_2$, 30 mM KCl, 6% glycerol, 1 mM GTP, 1 mM DTT, 10 mM phosphoenolpyruvate, and 0.08 U/ μ L (final concentration) of pyruvate kinase (Sigma Aldrich, P7768) was incubated at 37 °C for 15 min. The resulting reaction mix (5 μ L, 25 pmol of EF-Tu) was mixed with 2 μ L of Ternary Complex Buffer [150 mM HEPES-KOH (pH 7.6), 195 mM NH_4OAc , and 30 mM $\text{Mg}(\text{OAc})_2$] and 2 μ L of water, and 1 μ L of AA-tRNA. To reconstitute the ternary complex, this reaction mix was incubated at 37 °C for 10 min.

The ternary complex mix was supplemented with 1 μ L of 50% glycerol/BPB. The mixture was loaded on a native gel (8% acrylamide (19:1), 50 mM Tris-HCl (pH 6.8), 65 mM NH_4OAc , 10 mM $\text{Mg}(\text{OAc})_2$), and ran with 50 V, 120 min at 4 °C. The native gel was stained by SYPRO Red (Lonza) following the manufacturer's standard protocol. The gel was visualized by a gel scanner Typhoon FLA 7000 (GE Healthcare).

5. 5. 7. Preparation of DNA, tRNA, and flexizyme

The preparation of DNA, tRNA, and flexizyme was carried out following section 2. 6. 2. The primers are listed in Table 11, and the combinations of primers are shown in Table 12.

| Primer | Sequence (5' → 3') |
|---------------------|--|
| T7ex5.F22 | GGCGTAATACGACTCACTATAG |
| T7eSD6M.F46 | TAATACGACTCACTATAGGGTTAACTTTAACAAGGAGAAAAACATG |
| 172R | CGAAGCTTACTTGTCGTCGTCCTTGATGTCGTACGGGTGTTTGTACTTTTGTACTTCTTGTA |
| flaguaa.R33 | CGAAGCTTACTTGTCGTCGTCCTTGATGTC |
| flaguaa.R18 | CGAAGCTTACTTGTCGTC |
| Fx5'.F36 | GTAATACGACTCACTATAGGATCGAAAGATTTCCGC |
| dFx.R46 | ACCTAACGCCATGTACCCCTTCGGGGATGCGGAAATCTTTCGATCC |
| dFx.R19 | ACCTAACGCCATGTACCCCT |
| eFx.R45 | ACCTAACGCTAATCCCTTCGGGGCCGCGGAAATCTTTCGATCC |
| eFx.R18 | ACCTAACGCTAATCCCT |
| Pro1E.F50 | GTAATACGACTCACTATAGGGTGATTGGCGAGCCTGGTAGCGCACTTCG |
| Pro1E2#3CGG_Pro.R62 | TGGCGGGTGATAGGGGATTGGAACCCCTGACCCCTTCGTCCCGAACGAAGTGCCTACCAAG |
| Pro1E2#3-OMe.R20 | TG(M)GCGGGTGATAGGGGATTC |
| Pro1E2#5gug_His.R62 | TGGCGGGTGATACTGGATTGGAACCAAGTGACCCCTTCGTTACAACGAAGTGCCTACCAAG |
| Pro1E2#5-OMe.R20 | TG(M)GCGGGTGATACTGGATTC |

Table 11 The primers used for the preparation of DNA, tRNA, and flexizyme.

| | Primer extension | Primer extension | PCR | PCR |
|--|------------------|---------------------|-----------|------------------|
| Sequence | Forward | Reverse | Forward | Reverse |
| dfx | Fx5'.F36 | dFx.R46 | T7ex5.F22 | dFx.R19 |
| efx | Fx5'.F36 | eFx.R45 | T7ex5.F22 | eFx.R18 |
| tRNA ^{Pro1E2#3_{CGG}} | Pro1E.F50 | Pro1E2#3CGG_Pro.R62 | T7ex5.F22 | Pro1E2#3-OMe.R20 |
| tRNA ^{Pro1E2#3_{GUG}} | Pro1E.F50 | Pro1E2#5gug_His.R62 | T7ex5.F22 | Pro1E2#5-OMe.R20 |

| | Primer extension | Primer extension | 1st PCR | 1st PCR | 2nd PCR |
|----------|------------------|------------------|-----------|-------------|-----------|
| Sequence | Forward | Reverse | Forward | Reverse | Forward |
| 172 | T7eSD6M.F46 | 172R | T7ex5.F22 | flaguaa.R33 | T7ex5.F22 |

Table 12 The combinations of primers.

5. 5. 8. In vitro translation

The *in vitro* translation was carried out following section 2. 6. 3.

Chapter 6.

General conclusion

The translation system is a powerful tool to synthesize peptides and proteins. It has also a great potential to synthesize useful peptidic compounds, but the accessible substrates had been previously limited to kinds of twenty proteinogenic L-amino acids in the natural translation system. Recently, the genetic code reprogramming technologies, such as the FIT system, have been established to install various kinds of non-proteinogenic amino acids, allowing expansion of the chemical space of the translated peptides; however, there still remains a hurdle to synthesize peptides containing stumbling blocks, such as a thiazole and β -amino acids. To overcome this hurdle, creative solutions during the nascent peptide synthesis and after the translation are required.

In chapter 2, I and Dr. Maini demonstrated that thioamide can be installed into the peptides translated in the FIT system. The ribosomal formation of thioamide had been reported nearly 50 years ago, but identification of the product was not sufficient in the previous research; here we directly observed the peptide products containing thioamide by MALDI-TOF MS. I also observed that thioamide-containing peptide was accompanied by the oxoamide-counterpart. Even though a certain amount of S-to-O exchange is unavoidable in this method, the ribosomal formation of thioamide would have advantages over the SPPS method in the aspect of the application in mRNA-display screening, mutagenesis analysis, and longer peptide synthesis.

In chapter 3, I have developed a post-translational modification reaction mediated by a thioamide. This reaction proceeds spontaneously without any catalyst under aquatic conditions, and thus this reaction is fairly compatible with the translation system. In addition, by combining this heterocyclization with an enzymatic dehydrogenation by GodE, the chemoenzymatic formation of thiazole-containing peptides have been demonstrated in the translation system. This method has also been applied to the conventional macrocyclization closed by a thioether linkage, enabling the ribosomal synthesis of macrocyclic peptides containing a thiazole. Taking advantage of the thioamide-mediated heterocyclization, I have also investigated the substrate scope of GodE and revealed that GodE has promiscuity during the dehydrogenation other than its native substrate.

In chapter 4, I and Dr. Iwane developed a method to incorporate multiple ^{Me}AAs into peptides by substituting the tRNA T-stem sequence. Dr. Iwane demonstrated that the designed T-stem sequences can alter the EF-Tu affinity as expected and the reinforced affinity can enhance the incorporation efficiency of ^{Me}AAs. Taking advantage of this T-stem engineering technology, I demonstrated that the appropriate combination, in which EF-Tu affinity is tuned to uniform level, dramatically improved the translation efficiency of *N*-methyl peptides in both a linear and a macrocyclic scaffold.

In chapter 5, I have prepared 35 EF-Tu variants to test the affinities for various AA-tRNAs by

gel mobility shift assay. I have revealed that M260 and F261 residues play an important role to recognize the amino acid esterified on the tRNA. In addition, previously D215 and E216 residues have been reported to have steric hindrance against the side chain of the esterified amino acid due to their longer side chain, but the result presented in this study indicates that not the sizes but the negative charges of them are more critical in the amino acid recognition. Also, by using EF-Sep and E215A variants the incorporation efficiencies of D-Asp and D-Pro were improved.

In conclusion, I have further expanded the chemical space of the translated peptides. The application of these methodologies to mRNA display systems, such as the RaPID system, would facilitate the *de novo* discovery of the bioactive peptides containing thiazoles in the near future. Besides, I have revealed the critical residues in EF-Tu for recognizing the amino acid esterified on the tRNA. This finding would enable the further engineering of EF-Tu or other translational factors, such as the ribosome. Overall, a step forward in the practical engineering of the translation system and its understanding has been made. This study would promote the research on the translation system.

References

1. Schmeing, T.M. and Ramakrishnan, V. (2009) What recent ribosome structures have revealed about the mechanism of translation. *Nature*, **461**, 1234–1242.
2. Parker, J. (1989) Errors and alternatives in reading the universal genetic code. *Microbiol. Rev.*, **53**, 273–298.
3. Yamane, T., Miller, D.L. and Hopfield, J.J. (1981) Discrimination between d- and l-tyrosyl Transfer Ribonucleic Acids in Peptide Chain Elongation. *Biochemistry*, **20**, 7059–7064.
4. Fukai, S., Nureki, O., Sekine, S. ichi, Shimada, A., Tao, J., Vassilyev, D.G. and Yokoyama, S. (2000) Structural basis for double-sieve discrimination of L-valine from L-isoleucine and L-threonine by the complex of tRNA(Val) and valyl-tRNA synthetase. *Cell*, **103**, 793–803.
5. Rodnina, M. V., Gromadski, K.B., Kothe, U. and Wieden, H.J. (2005) Recognition and selection of tRNA in translation. *FEBS Lett.*, **579**, 938–942.
6. Uhlenbeck, O.C. and Schrader, J.M. (2018) Evolutionary tuning impacts the design of bacterial tRNAs for the incorporation of unnatural amino acids by ribosomes. *Curr. Opin. Chem. Biol.*, **46**, 138–145.
7. Wilcox, M. and Nirenberg, M. (1968) Transfer RNA as a cofactor coupling amino acid synthesis with that of protein. *Proc. Natl. Acad. Sci. U. S. A.*, **61**, 229–36.
8. Stanzel, M., Schön, A. and Sprinzl, M. (1994) Discrimination against misacylated tRNA by chloroplast elongation factor Tu. *Eur. J. Biochem.*, **219**, 435–439.
9. Inoue, M., Shinohara, N., Tanabe, S., Takahashi, T., Okura, K., Itoh, H., Mizoguchi, Y., Iida, M., Lee, N. and Matsuoka, S. (2010) Total synthesis of the large non-ribosomal peptide polytheonamide B. *Nat. Chem.*, **2**, 280–285.
10. Lee, D.H., Granja, J.R., Martinez, J.A., Severin, K. and Ghadiri, M.R. (1996) A self-replicating peptide. *Nature*, **382**, 525–528.
11. Hamada, T., Matsunaga, S., Fujiwara, M., Fujita, K., Hirota, H., Schmucki, R., Güntert, P. and Fusetani, N. (2010) Solution structure of polytheonamide B, a highly cytotoxic nonribosomal polypeptide from marine sponge. *J. Am. Chem. Soc.*, **132**, 12941–12945.
12. Wu, X., Stockdill, J.L., Wang, P. and Danishefsky, S.J. (2010) Total synthesis of cyclosporine: Access to N-methylated peptides via Isonitrile coupling reactions. *J. Am. Chem. Soc.*, **132**, 4098–4100.
13. Van Der Velden, N.S., Kälin, N., Helf, M.J., Piel, J., Freeman, M.F. and Künzler, M. (2017) Autocatalytic backbone N-methylation in a family of ribosomal peptide natural products. *Nat. Chem. Biol.*, **13**, 833–835.
14. Conradi, R.A., Hilgers, A.R., Ho, N.F.H. and Burton, P.S. (1992) The Influence of Peptide Structure on Transport Across Caco-2 Cells. II. Peptide Bond Modification Which Results in Improved Permeability. *Pharm. Res.*, **9**, 435–439.
15. Haviv, F., Fitzpatrick, T.D., Swenson, R.E., Nichols, C.J., Mort, N.A., Bush, E.N., Diaz, G.,

- Bammert,G., Nguyen,A., Rhutasel,N.S., *et al.* (1993) Effect of *N*-Methyl Substitution of the Peptide Bonds in Luteinizing Hormone-Releasing Hormone Agonists. *J. Med. Chem.*, **36**, 363–369.
16. Chikhale,E.G., Ng,K.Y., Burton,P.S. and Borchardt,R.T. (1994) Hydrogen Bonding Potential as a Determinant of the *in Vitro* and *in Situ* Blood–Brain Barrier Permeability of Peptides. *Pharm. Res.*, **11**, 412–419.
 17. Bockus,A.T., Schwochert,J.A., Pye,C.R., Townsend,C.E., Sok,V., Bednarek,M.A. and Lokey,R.S. (2015) Going Out on a Limb: Delineating the Effects of β -Branching, *N*-Methylation, and Side Chain Size on the Passive Permeability, Solubility, and Flexibility of Sanguinamide A Analogues. *J. Med. Chem.*, **58**, 7409–7418.
 18. Nielsen,D.S., Shepherd,N.E., Xu,W., Lucke,A.J., Stoermer,M.J. and Fairlie,D.P. (2017) Orally Absorbed Cyclic Peptides. *Chem. Rev.*, **117**, 8094–8128.
 19. Hayakawa,Y., Sasaki,K., Adachi,H., Furihata,K., Nagai,K. and Shin-Ya,K. (2006) Thioviridamide, a novel apoptosis inducer in transformed cells from *Streptomyces olivoviridis*. *J. Antibiot. (Tokyo)*, **59**, 1–5.
 20. Mahanta,N., Szantai-Kis,D.M., Petersson,E.J. and Mitchell,D.A. (2019) Biosynthesis and Chemical Applications of Thioamides. *ACS Chem. Biol.*, **14**, 142–163.
 21. Comba,P., Dovalil,N., Gahan,L.R., Hanson,G.R. and Westphal,M. (2014) Cyclic peptide marine metabolites and Cu^{II}. *Dalt. Trans.*, **43**, 1935–1956.
 22. Kim,M.Y., Vankayalapati,H., Shin-Ya,K., Wierzba,K. and Hurley,L.H. (2002) Telomestatin, a potent telomerase inhibitor that interacts quite specifically with the human telomeric intramolecular G-quadruplex. *J. Am. Chem. Soc.*, **124**, 2098–2099.
 23. Shen,X., Mustafa,M., Chen,Y., Cao,Y. and Gao,J. (2019) Natural thiopeptides as a privileged scaffold for drug discovery and therapeutic development. *Med. Chem. Res.*, **28**, 1063–1098.
 24. Bowers,A.A., Acker,M.G., Koglin,A. and Walsh,C.T. (2010) Manipulation of thiocillin variants by prepeptide gene replacement: Structure, conformation, and activity of heterocycle substitution mutants. *J. Am. Chem. Soc.*, **132**, 7519–7527.
 25. Schwalen,C.J., Hudson,G.A., Kosol,S., Mahanta,N., Challis,G.L. and Mitchell,D.A. (2017) In Vitro Biosynthetic Studies of Bottromycin Expand the Enzymatic Capabilities of the YcaO Superfamily. *J. Am. Chem. Soc.*, **139**, 18154–18157.
 26. Freeman,M.F., Gurgui,C., Helf,M.J., Morinaka,B.I., Uria,A.R., Oldham,N.J., Sahl,H.-G., Matsunaga,S. and Piel,J. (2012) Metagenome Mining Reveals Polytheonamides as Posttranslationally Modified Ribosomal Peptides. *Science*, **338**, 387–390.
 27. Dunbar,K.L., Melby,J.O. and Mitchell,D.A. (2012) YcaO domains use ATP to activate amide backbones during peptide cyclodehydrations. *Nat. Chem. Biol.*, **8**, 569–575.
 28. L. Dunbar,K., H. Scharf,D., Litomska,A. and Hertweck,C. (2017) Enzymatic Carbon–Sulfur Bond Formation in Natural Product Biosynthesis. *Chem. Rev.*, **117**, 5521–5577.
 29. Duerfahrt,T., Eppelmann,K., Müller,R. and Marahiel,M.A. (2004) Rational Design of a

- Bimodular Model System for the Investigation of Heterocyclization in Nonribosomal Peptide Biosynthesis. *Chem. Biol.*, **11**, 261–271.
30. Schneider, T.L., Shen, B. and Walsh, C.T. (2003) Oxidase domains in epothilone and bleomycin biosynthesis: Thiazoline to thiazole oxidation during chain elongation. *Biochemistry*, **42**, 9722–9730.
 31. Ozaki, T., Yamashita, K., Goto, Y., Shimomura, M., Hayashi, S., Asamizu, S., Sugai, Y., Ikeda, H., Suga, H. and Onaka, H. (2017) Dissection of goadsporin biosynthesis by *in vitro* reconstitution leading to designer analogues expressed *in vivo*. *Nat. Commun.*, **8**, 14207.
 32. Fraaije, M.W. and Mattevi, A. (2000) Flavoenzymes: Diverse catalysts with recurrent features. *Trends Biochem. Sci.*, **25**, 126–132.
 33. Umhau, S., Pollegioni, L., Molla, G., Diederichs, K., Welte, W., Pilone, M.S. and Ghisla, S. (2000) The x-ray structure of D-amino acid oxidase at very high resolution identifies the chemical mechanism of flavin-dependent substrate dehydrogenation. *Proc. Natl. Acad. Sci. U. S. A.*, **97**, 12463–12468.
 34. Hirose, H., Tsiamantas, C., Katoh, T. and Suga, H. (2019) *In vitro* expression of genetically encoded non-standard peptides consisting of exotic amino acid building blocks. *Curr. Opin. Biotechnol.*, **58**, 28–36.
 35. de la Torre, D. and Chin, J.W. (2021) Reprogramming the genetic code. *Nat. Rev. Genet.*, **22**, 169–184.
 36. Xiao, H. and Schultz, P.G. (2016) At the Interface of Chemical and Biological Synthesis: An Expanded Genetic Code. *Cold Spring Harb. Perspect. Biol.*, **8**, a023945.
 37. Dumas, A., Lercher, L., Spicer, C.D. and Davis, B.G. (2015) Designing logical codon reassignment – Expanding the chemistry in biology. *Chem. Sci.*, **6**, 50–69.
 38. Wang, L. and Schultz, P.G. (2005) Expanding the Genetic Code. *Angew. Chem., Int. Ed.*, **44**, 34–66.
 39. Wang, L., Brock, A., Herberich, B. and Schultz, P.G. (2001) Expanding the Genetic Code of *Escherichia coli*. *Science*, **292**, 498–500.
 40. Reddington, S.C., Baldwin, A.J., Thompson, R., Brancale, A., Tippmann, E.M. and Jones, D.D. (2015) Directed evolution of GFP with non-natural amino acids identifies residues for augmenting and photoswitching fluorescence. *Chem. Sci.*, **6**, 1159–1166.
 41. Mukai, T., Hoshi, H., Ohtake, K., Takahashi, M., Yamaguchi, A., Hayashi, A., Yokoyama, S. and Sakamoto, K. (2015) Highly reproductive *Escherichia coli* cells with no specific assignment to the UAG codon. *Sci. Rep.*, **5**, 9699.
 42. Shimizu, Y., Inoue, A., Tomari, Y., Suzuki, T., Yokogawa, T., Nishikawa, K. and Ueda, T. (2001) Cell-free translation reconstituted with purified components. *Nat. Biotechnol.*, **19**, 751–755.
 43. Hecht, S.M., Alford, B.L., Kuroda, Y. and Kitano, S. (1978) “Chemical aminoacylation” of tRNA’s. *J. Biol. Chem.*, **253**, 4517–4520.
 44. Tan, Z., Forster, A.C., Blacklow, S.C. and Cornish, V.W. (2004) Amino Acid Backbone

- Specificity of the Escherichia coli Translation Machinery. *J. Am. Chem. Soc.*, **126**, 12752–12753.
45. Josephson, K., Hartman, M.C.T. and Szostak, J.W. (2005) Ribosomal Synthesis of Unnatural Peptides. *J. Am. Chem. Soc.*, **127**, 11727–11735.
 46. Iqbal, E.S., Dods, K.K. and Hartman, M.C.T. (2018) Ribosomal incorporation of backbone modified amino acids via an editing-deficient aminoacyl-tRNA synthetase. *Org. Biomol. Chem.*, **16**, 1073–1078.
 47. Goto, Y., Katoh, T. and Suga, H. (2011) Flexizymes for genetic code reprogramming. *Nat. Protoc.*, **6**, 779–790.
 48. Murakami, H., Saito, H. and Suga, H. (2003) A Versatile tRNA Aminoacylation Catalyst Based on RNA. *Chem. Biol.*, **10**, 655–662.
 49. Xiao, H., Murakami, H., Suga, H. and Ferré-D'Amaré, A.R. (2008) Structural basis of specific tRNA aminoacylation by a small *in vitro* selected ribozyme. *Nature*, **454**, 358–361.
 50. Ohta, A., Murakami, H., Higashimura, E. and Suga, H. (2007) Synthesis of Polyester by Means of Genetic Code Reprogramming. *Chem. Biol.*, **14**, 1315–1322.
 51. Takatsuji, R., Shinbara, K., Katoh, T., Goto, Y., Passioura, T., Yajima, R., Komatsu, Y. and Suga, H. (2019) Ribosomal Synthesis of Backbone-Cyclic Peptides Compatible with In Vitro Display. *J. Am. Chem. Soc.*, **141**, 2279–2287.
 52. Kawakami, T., Murakami, H. and Suga, H. (2008) Messenger RNA-Programmed Incorporation of Multiple N-Methyl-Amino Acids into Linear and Cyclic Peptides. *Chem. Biol.*, **15**, 32–42.
 53. Kawakami, T., Murakami, H. and Suga, H. (2008) Ribosomal Synthesis of Polypeptoids and Peptoid–Peptide Hybrids. *J. Am. Chem. Soc.*, **130**, 16861–16863.
 54. Katoh, T. and Suga, H. (2018) Ribosomal Incorporation of Consecutive β -Amino Acids. *J. Am. Chem. Soc.*, **140**, 12159–12167.
 55. Katoh, T. and Suga, H. (2020) Ribosomal Elongation of Cyclic γ -Amino Acids using a Reprogrammed Genetic Code. *J. Am. Chem. Soc.*, **142**, 4965–4969.
 56. Katoh, T. and Suga, H. (2020) Ribosomal Elongation of Aminobenzoic Acid Derivatives. *J. Am. Chem. Soc.*, **142**, 16518–16522.
 57. Katoh, T., Sengoku, T., Hirata, K., Ogata, K. and Suga, H. (2020) Ribosomal synthesis and de novo discovery of bioactive foldamer peptides containing cyclic β -amino acids. *Nat. Chem.*, **12**, 1081–1088.
 58. Nemoto, N., Miyamoto-Sato, E., Husimi, Y. and Yanagawa, H. (1997) In vitro virus: Bonding of mRNA bearing puromycin at the 3'-terminal end to the C-terminal end of its encoded protein on the ribosome in vitro. *FEBS Lett.*, **414**, 405–408.
 59. Rogers, J.M., Passioura, T. and Suga, H. (2018) Nonproteinogenic deep mutational scanning of linear and cyclic peptides. *Proc. Natl. Acad. Sci.*, **115**, 10959–10964.
 60. Fujino, T., Goto, Y., Suga, H. and Murakami, H. (2013) Reevaluation of the D-Amino Acid

- Compatibility with the Elongation Event in Translation. *J. Am. Chem. Soc.*, **135**, 1830–1837.
61. Achenbach, J., Jahnz, M., Bethge, L., Paal, K., Jung, M., Schuster, M., Albrecht, R., Jarosch, F., Nierhaus, K.H. and Klusmann, S. (2015) Outwitting EF-Tu and the ribosome: translation with d-amino acids. *Nucleic Acids Res.*, **43**, 5687–5698.
 62. Katoh, T., Iwane, Y. and Suga, H. (2017) Logical engineering of D-arm and T-stem of tRNA that enhances D-amino acid incorporation. *Nucleic Acids Res.*, **45**, 12601–12610.
 63. Katoh, T., Wohlgemuth, I., Nagano, M., Rodnina, M. V. and Suga, H. (2016) Essential structural elements in tRNA^{Pro} for EF-P-mediated alleviation of translation stalling. *Nat. Commun.*, **7**, 11657.
 64. Guo, J., Melançon, C.E., Lee, H.S., Groff, D. and Schultz, P.G. (2009) Evolution of Amber Suppressor tRNAs for Efficient Bacterial Production of Proteins Containing Nonnatural Amino Acids. *Angew. Chem., Int. Ed.*, **48**, 9148–9151.
 65. Doi, Y., Ohtsuki, T., Shimizu, Y., Ueda, T. and Sisido, M. (2007) Elongation Factor Tu Mutants Expand Amino Acid Tolerance of Protein Biosynthesis System. *J. Am. Chem. Soc.*, **129**, 14458–14462.
 66. Park, H.-S., Hohn, M.J., Umehara, T., Guo, L.-T., Osborne, E.M., Benner, J., Noren, C.J., Rinehart, J. and Söll, D. (2011) Expanding the Genetic Code of *Escherichia coli* with Phosphoserine. *Science*, **333**, 1151–1154.
 67. A. Patani, G. and J. LaVoie, E. (1996) Bioisosterism: A Rational Approach in Drug Design. *Chem. Rev.*, **96**, 3147–3176.
 68. Reiner, A., Wildemann, D., Fischer, G. and Kiefhaber, T. (2008) Effect of Thiopeptide Bonds on α -Helix Structure and Stability. *J. Am. Chem. Soc.*, **130**, 8079–8084.
 69. Walters, C.R., Szantai-Kis, D.M., Zhang, Y., Reinert, Z.E., Horne, W.S., Chenoweth, D.M. and Petersson, E.J. (2017) The effects of thioamide backbone substitution on protein stability: a study in α -helical, β -sheet, and polyproline II helical contexts. *Chem. Sci.*, **8**, 2868–2877.
 70. Chen, X., Mietlicki-Baase, E.G., Barrett, T.M., McGrath, L.E., Koch-Laskowski, K., Ferrie, J.J., Hayes, M.R. and Petersson, E.J. (2017) Thioamide Substitution Selectively Modulates Proteolysis and Receptor Activity of Therapeutic Peptide Hormones. *J. Am. Chem. Soc.*, **139**, 16688–16695.
 71. Verma, H., Khatri, B., Chakraborti, S. and Chatterjee, J. (2018) Increasing the bioactive space of peptide macrocycles by thioamide substitution. *Chem. Sci.*, **9**, 2443–2451.
 72. Goldberg, J.M., Batjargal, S. and Petersson, E.J. (2010) Thioamides as Fluorescence Quenching Probes: Minimalist Chromophores To Monitor Protein Dynamics. *J. Am. Chem. Soc.*, **132**, 14718–14720.
 73. F. Wissner, R., Batjargal, S., M. Fadzen, C. and James Petersson, E. (2013) Labeling Proteins with Fluorophore/Thioamide Förster Resonant Energy Transfer Pairs by Combining Unnatural Amino Acid Mutagenesis and Native Chemical Ligation. *J. Am. Chem. Soc.*, **135**, 6529–6540.

74. Zacharie,B., Lagraoui,M., Dimarco,M., L. Penney,C., Gagnon,L., Penney,C.L. and Gagnon,L. (1999) Thioamides: Synthesis, Stability, and Immunological Activities of Thioanalogues of Imreg. Preparation of New Thioacylating Agents Using Fluorobenzimidazolone Derivatives. *J. Med. Chem.*, **42**, 2046–2052.
75. Zhang,W., Li,J., Liu,L.-W., Wang,K.-R., Song,J.-J., Yan,J.-X., Li,Z.-Y., Zhang,B.-Z. and Wang,R. (2010) A novel analog of antimicrobial peptide Polybia-MPI, with thioamide bond substitution, exhibits increased therapeutic efficacy against cancer and diminished toxicity in mice. *Peptides*, **31**, 1832–1838.
76. Nayak,D.D., Mahanta,N., Mitchell,D.A. and Metcalf,W.W. (2017) Post-translational thioamidation of methyl-coenzyme M reductase, a key enzyme in methanogenic and methanotrophic archaea. *Elife*, **6**, 1–18.
77. Dunbar,K.L., Büttner,H., Molloy,E.M., Dell,M., Kumpfmüller,J. and Hertweck,C. (2018) Genome Editing Reveals Novel Thiotemplated Assembly of Polythioamide Antibiotics in Anaerobic Bacteria. *Angew. Chem., Int. Ed.*, **57**, 14080–14084.
78. Mahanta,N., Liu,A., Dong,S., Nair,S.K. and Mitchell,D.A. (2018) Enzymatic reconstitution of ribosomal peptide backbone thioamidation. *Proc. Natl. Acad. Sci. U. S. A.*, **115**, 3030–3035.
79. Mukherjee,S., Verma,H. and Chatterjee,J. (2015) Efficient Site-Specific Incorporation of Thioamides into Peptides on a Solid Support. *Org. Lett.*, **17**, 3150–3153.
80. Batjargal,S., Wang,Y.J., Goldberg,J.M., Wissner,R.F. and Petersson,E.J. (2012) Native Chemical Ligation of Thioamide-Containing Peptides: Development and Application to the Synthesis of Labeled α -Synuclein for Misfolding Studies. *J. Am. Chem. Soc.*, **134**, 9172–9182.
81. Victorova,L.S., Kotusov,V.V., Azhaev,A.V., Krayevsky,A.A., Kukhanova,M.K. and Gottikh,B.P. (1976) Synthesis of thioamide bond catalyzed by E. coli ribosomes. *FEBS Lett.*, **68**, 215–218.
82. Maini,R., Kimura,H., Takatsuji,R., Katoh,T., Goto,Y. and Suga,H. (2019) Ribosomal Formation of Thioamide Bonds in Polypeptide Synthesis. *J. Am. Chem. Soc.*, **141**, 20004–20008.
83. Terasaka,N., Hayashi,G., Katoh,T. and Suga,H. (2014) An orthogonal ribosome-tRNA pair via engineering of the peptidyl transferase center. *Nat. Chem. Biol.*, **10**, 555–557.
84. Taiji,M., Yokoyama,S. and Miyazawa,T. (1983) Transacylation rates of aminoacyladenine moiety at the 3'-terminus of aminoacyl-transfer ribonucleic acid. *Biochemistry*, **22**, 3220–3225.
85. Vinogradov,A.A., Yin,Y. and Suga,H. (2019) Macrocyclic Peptides as Drug Candidates: Recent Progress and Remaining Challenges. *J. Am. Chem. Soc.*, **141**, 4167–4181.
86. Yamagishi,Y., Shoji,I., Miyagawa,S., Kawakami,T., Katoh,T., Goto,Y. and Suga,H. (2011) Natural Product-Like Macrocyclic N-Methyl-Peptide Inhibitors against a Ubiquitin Ligase Uncovered from a Ribosome-Expressed De Novo Library. *Chem. Biol.*, **18**, 1562–1570.

87. Ellman, J.A., Mendel, D. and Schultz, P.G. (1992) Site-Specific Incorporation of Novel Backbone Structures into Proteins. *Science*, **255**, 197–200.
88. Subtelny, A.O., Hartman, M.C.T. and Szostak, J.W. (2008) Ribosomal Synthesis of *N*-Methyl Peptides. *J. Am. Chem. Soc.*, **130**, 6131–6136.
89. Furano, A. V. (1975) Content of elongation factor Tu in *Escherichia coli*. *Proc. Natl. Acad. Sci.*, **72**, 4780–4784.
90. LaRiviere, F.J., Wolfson, A.D. and Uhlenbeck, O.C. (2001) Uniform Binding of Aminoacyl-tRNAs to Elongation Factor Tu by Thermodynamic Compensation. *Science*, **294**, 165–168.
91. Nissen, P., Kjeldgaard, M., Thirup, S., Polekhina, G., Reshetnikova, L., Clark, B.F.C. and Nyborg, J. (1995) Crystal Structure of the Ternary Complex of Phe-tRNA^{Phe}, EF-Tu, and a GTP Analog. *Science*, **270**, 1464–1472.
92. Asahara, H. and Uhlenbeck, O.C. (2002) The tRNA Specificity of *Thermus thermophilus* EF-Tu. *Proc. Natl. Acad. Sci. U. S. A.*, **99**, 3499–3504.
93. Sanderson, L.E. and Uhlenbeck, O.C. (2007) Directed Mutagenesis Identifies Amino Acid Residues Involved in Elongation Factor Tu Binding to yeast Phe-tRNA^{Phe}. *J. Mol. Biol.*, **368**, 119–130.
94. Jeong, K. W., Pavlov, M. Y., Kwiatkowski, M., Ehrenberg, M. and Forster, A.C. (2014) A tRNA body with high affinity for EF-Tu hastens ribosomal incorporation of unnatural amino acids. *RNA*, **20**, 632–643.
95. Gan, R., Perez, J.G., Carlson, E.D., Ntai, I., Isaacs, F.J., Kelleher, N.L. and Jewett, M.C. (2017) Translation System Engineering in *Escherichia coli* Enhances Non-Canonical Amino Acid Incorporation into Proteins. *Biotechnol. Bioeng.*, **114**, 1074–1086.
96. Katoh, T., Iwane, Y. and Suga, H. (2018) tRNA engineering for manipulating genetic code. *RNA Biol.*, **15**, 453–460.
97. Pleiss, J.A. and Uhlenbeck, O.C. (2001) Identification of Thermodynamically Relevant Interactions between EF-Tu and Backbone Elements of tRNA. *J. Mol. Biol.*, **308**, 895–905.
98. Schrader, J.M., Chapman, S.J. and Uhlenbeck, O.C. (2009) Understanding the Sequence Specificity of tRNA Binding to Elongation Factor Tu using tRNA Mutagenesis. *J. Mol. Biol.*, **386**, 1255–1264.
99. Iwane, Y., Hitomi, A., Murakami, H., Katoh, T., Goto, Y. and Suga, H. (2016) Expanding the amino acid repertoire of ribosomal polypeptide synthesis via the artificial division of codon boxes. *Nat. Chem.*, **8**, 317–325.
100. Schrader, J.M., Chapman, S.J. and Uhlenbeck, O.C. (2011) Tuning the affinity of aminoacyl-tRNA to elongation factor Tu for optimal decoding. *Proc. Natl. Acad. Sci. U. S. A.*, **108**, 5215–5220.
101. Goto, Y., Ohta, A., Sako, Y., Yamagishi, Y., Murakami, H. and Suga, H. (2008) Reprogramming the Translation Initiation for the Synthesis of Physiologically Stable Cyclic Peptides. *ACS Chem. Biol.*, **3**, 120–129.

102. Ohtsuki,T., Manabe,T. and Sisido,M. (2005) Multiple incorporation of non-natural amino acids into a single protein using tRNAs with non-standard structures. *FEBS Lett.*, **579**, 6769–6774.
103. Pape,T., Wintermeyer,W. and Rodnina,M. (1999) Induced fit in initial selection and proofreading of aminoacyl-tRNA on the ribosome. *EMBO J.*, **18**, 3800–3807.
104. Asahara,H. and Uhlenbeck,O.C. (2005) Predicting the Binding Affinities of Misacylated tRNAs for *Thermus thermophilus* EF-Tu·GTP. *Biochemistry*, **44**, 11254–11261.
105. Fischer,N., Neumann,P., Konevega,A.L., Bock,L. V., Ficner,R., Rodnina,M. V. and Stark,H. (2015) Structure of the E. coli ribosome-EF-Tu complex at <3 Å resolution by Cs-corrected cryo-EM. *Nature*, **520**, 567–570.
106. Katoh,T. and Suga,H. (2019) Flexizyme-catalyzed synthesis of 3'-aminoacyl-NH-tRNAs. *Nucleic Acids Res.*, **47**, e54.
107. Chapman,S.J., Schrader,J.M. and Uhlenbeck,O.C. (2012) Histidine 66 in *Escherichia coli* Elongation Factor Tu Selectively Stabilizes Aminoacyl-tRNAs. *J. Biol. Chem.*, **287**, 1229–1234.
108. Iwane,Y., Kimura,H., Katoh,T. and Suga,H. (2021) Uniform affinity-tuning of N -methyl-aminoacyl-tRNAs to EF-Tu enhances their multiple incorporation . *Nucleic Acids Res.*, 10.1093/nar/gkab288.
109. Katoh,T., Tajima,K. and Suga,H. (2017) Consecutive Elongation of D-Amino Acids in Translation. *Cell Chem. Biol.*, **24**, 46–54.
110. Mittelstaet,J., Konevega,A.L. and Rodnina,M. V. (2013) A Kinetic Safety Gate Controlling the Delivery of Unnatural Amino Acids to the Ribosome. *J. Am. Chem. Soc.*, **135**, 17031–17038.
111. Dedkova,L.M., Fahmi,N.E., Golovine,S.Y. and Hecht,S.M. (2006) Construction of modified ribosomes for incorporation of D-amino acids into proteins. *Biochemistry*, **45**, 15541–51.
112. Maini,R., Dedkova,L.M., Paul,R., Madathil,M.M., Chowdhury,S.R., Chen,S. and Hecht,S.M. (2015) Ribosome-Mediated Incorporation of Dipeptides and Dipeptide Analogues into Proteins in Vitro. *J. Am. Chem. Soc.*, **137**, 11206–11209.
113. Maini,R., Chowdhury,S.R., Dedkova,L.M., Roy,B., Daskalova,S.M., Paul,R., Chen,S. and Hecht,S.M. (2015) Protein Synthesis with Ribosomes Selected for the Incorporation of β-Amino Acids. *Biochemistry*, **54**, 3694–3706.

List of achievements

【Publication related to the thesis】

1. Maini,R., Kimura,H., Takatsuji,R., Katoh,T., Goto,Y., and Suga,H. (2019) Ribosomal Formation of Thioamide Bond in Polypeptide Synthesis. *J. Am. Chem. Soc.* **141**, 20004–20008
2. Iwane,Y., Kimura,H., Katoh,T., and Suga,H., (2021) Uniform affinity-tuning of *N*-methyl-aminoacyl-tRNAs to EF-Tu enhances their multiple incorporation. *Nucleic Acids Res.* <https://doi.org/10.1093/nar/gkab288> (advanced online publication)

【Publication not related to the thesis】

1. 木村寛之, 加藤敬行, 菅裕明 (2018) 「遺伝暗号リプログラミングを用いた特殊ペプチド翻訳合成と高速探索技術」『中分子創薬に資するペプチド・核酸・糖鎖の合成技術』第II編, 第8章, シーエムシー出版, 2018年
2. Tsutsumi,H., Kuroda,T., Kimura,H., Goto,Y., and Suga,H. (2021) Posttranslational chemical installation of azoles into translated peptides. *Nat. Commun.* **12**, 696.
3. Kimura,H. and Suga,H. (2021) Incorporation of backbone modifications in mRNA-displayable peptides. *Methods Enzymol.* **656**, 521–544

【Poster presentation】

1. Kimura,H., Katoh,T., and Suga,H.
Incorporation of D-amino acids in the translation system using EF-Tu variants.
4th International Conference on Circular Proteins and Peptides, 2018, Tokyo, Japan

【Oral presentation】

1. Kimura,H., Maini,R., Goto,Y., and Suga,H.
Chemoenzymatic Formation of Thiazole-Containing Peptides via Thioamide.
ETH-Todai Virtual Symposium 2020, 2020, Online

謝辞

この研究を取りまとめるにあたり、多くの方々に多大なご迷惑をおかけしたことをお詫びするとともに、これまでに頂いた数え切れない助言と力添えに感謝いたします。

まず指導教官である菅裕明先生に最大限の感謝と謝意を表します。私のわがままであった休学と復学を許可してくださったこと、私が研究方針を模索していた際に適切な助言で道を示してくださったこと、そして博士論文執筆の際に熱意をもって叱咤激励してくださったことはどれだけ感謝しても感謝しきれません。本当にありがとうございました。

続いて加藤敬行先生、後藤佑樹先生、寺坂尚紘先生、Alexander A. Vinogradov 先生、また既に研究室を離れておられる狩野直和先生、Toby J. Passioura 先生のご指導に深く感謝いたします。先生がたの熱く細かなご指導のおかげで実りある研究活動ができました。

発展性のある研究テーマを立案された岩根由彦博士、高辻諒博士、Rumit Maini 博士研究員にも感謝を表します。先輩方と共同で研究テーマに携わることで得難い経験ができ、さらに共同研究を通して私自身の研究テーマを立案することもできました。

また尾仲宏康 東京大学大学院農学系研究科教授から、先生が発見された脱水素酵素 GodE のプラスミドを提供して頂きました。本酵素なくして本研究は成り立たなかったと思っております。使用許可をくださった尾仲先生のご厚意に深く感謝いたします。続いて GodE の精製を行ってくれた村岡くん、寺北くんにも感謝します。さらに脱水環化酵素 PatD を提供してくださった加藤保治博士、EF-Tu、EF-Sep を提供してくださった林勇樹博士研究員にも感謝いたします。

最後に、楽しいときにも辛いときにも一緒に過ごしてくださった菅研究室の先輩、同期、後輩、研究員、そして秘書の全員に深く感謝いたします。私一人では本研究をまとめることはできなかったと確信しています。皆様の全てのお力添えのおかげで今の私がいることを感謝いたします。